UNIVERSITAT DE BARCELONA

Bioimpedance & dielectrophoresis instrumentation equipments for living cells manipulation and monitoring

Beatriz del Moral Zamora

![Universitat de Barcelona logo]

Bioimpedance & Dielectrophoresis instrumentation equipments for living cells manipulation and monitoring

Beatriz del Moral Zamora
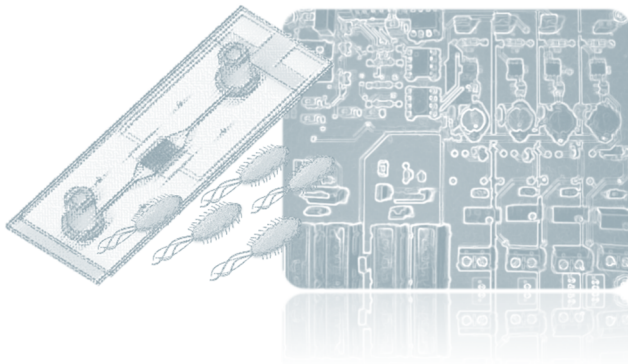
Thesis directed by: Pere Ll. Miribel-Català and Antoni Homs-Corbera
Tutor: Pere Ll. Miribel-Català

Al motor de mi vida:
mi familia y amigos

INDEX

INDEX OF FIGURES

INDEX OF TABLES

CHAPTER 1. INTRODUCTION

This chapter describes the aim and objectives of the thesis. It also introduces the concepts, technologies and methods, while reviewing their state-of-the-art, which have been used in order to achieve these objectives.

.

1.1 Objectives and Scope

Since the first microfluidic device was developed in the early 1950s, when the basics for today's inkjet technology were set, thousands of publications have appeared related to the topic [1]. Important milestones on the development of this technology include the realization for the first miniaturized gas chromatograph (GC) [2], using Silicon technology, in the 70s, and the proof of concept of the first miniaturized high-pressure liquid chromatograph (HPLC) in the 90s. This later work from Manz *et al.*[3] is considered today to be the true fosterer of the field which was, at that time, mainly focused to improve analytical chemistry procedures.

The increasing interest on these technologies is caused by its ability to be scaled and its rapid development, which allows manipulating and detecting small quantities of analites even at the cellular scale [4]. The integration of microfluidic technologies with specific sensors and actuators at minute scales in order to achieve a set of automated laboratory operations and perform a particular solution for a specific application, generally on the life sciences and chemistry fields, was defined as Lab-on-a-chip (LoC)[5]. LoC devices have the potential to become a powerful technology for some fields, such as health, food security or environmental control. Their low cost and portability make them also suitable to improve medical diagnosis and research in developing countries [6]. Moreover, these systems permit also to explore new methods for manipulation and characterization of cells by means of electrical cell properties, by using techniques such as dielectrophoresis (DEP) or impedance spectroscopy (IS). In fact, the dielectrophoretic force allows manipulating cells, taking advantage of their electrical properties, by applying an electric field. Likewise, impedance allows measuring electrical properties of materials and, used wisely, inform about characteristics such as presence, composition or size of cells or other biological materials.

This work aims, in its final stage, to exploit the combined potential of both techniques, DEP and IS, in a compact system for bioanalytical bench-top applications. The creation of the complete device has been a long

procedure alternating theoretical calculations and experimental tests. It has included different steps such as the design of the need electronic equipment stages, the study of different microfluidic designs, an accurate bacteria concentration and manipulation protocol definition, and the study of the viability of the bacteria populations recovered with our device. These studies have made possible to finally obtain an automated bacteria concentrator for microbiology, food, water and environmental control applications while performing impedance cell analysis to monitor bacteria accumulation during the process. The system has been adjusted and proved for the real case of *Escherichia Coli* (*E. coli*) concentration and analysis. *E. coli* presents pathogenic variants that cause morbidity and mortality worldwide [7] being therefore a topic of interest. *E. coli* is one of the main antimicrobials resistant pathogens in healthcare-associated infections reported to the National Healthcare Safety Network [8], being the primary cause of widespread pathologies such as significant diarrheal and extra-intestinal diseases [7] or urinary tract infections [9]. Furthermore, *E. coli* can be found as a bacterial food contamination [10] and causes avian coli-bacillosis, one of the major bacterial diseases in the poultry industry and the most common avian disease communicable to humans [11]. Currently, bacterium presence detection involve long time culture processes [12], [13] only to obtain a valid sample which could be properly detected. DEP concentration is a strong selective manipulation method which allows reducing sample preparation time. Moreover, by taking profit of IS, *E. coli* could be rapidly detected in the same equipment. For that reason, it is thought the proposed devices will be a useful tool for some current microbiology laboratories.

Hence the mainly aims of the present thesis are: (I) to prove the feasibility of custom DEP generator for controlling bacteria and find the best signal to accomplish this, (II) to look for the best microfluidic chip option for bacteria preconcentration purposes on bioanalytical applications, (III) to test the feasibility of a custom IS device and (IV) to use the previous studies to design a complete electronic equipment, taken profit of combination of both

techniques to have an autonomous system (V) To demonstrate the proof of concept of the full device with the real case of *E. coli* concentration.

1.2 From microfluidics strengths to Lab-on-a-chip devices.

Microfluidics is a research field exploiting the behavior of fluids at the microscale to perform complex chemical or biological operations in a miniaturized environment [14], [15]. At first, microfluidics were used to conceive analytical devices with improved performance, which were early referred as uTAS (Micro Total analysis Systems) [3]. These took advantage of the particular characteristics of fluids inside microfluidic channels, such as laminar and turbulent flow regimes, as well as the possibility of using small sample volumes.

Microfluidic technologies could be considered to start with the gas-phase chromatography (GPC) system [10] developed to manipulate fluids at high precision by Standfort University. A big step forward was done due to the creation of the inkjet printers. In the 1950s first commercial printer was developed by Siemens and in the 1970s IBM licensed the continuous inkjet technology [16]. These were, in fact, the first microfluidic devices. Then, the microfluidics field grew considerably through the program of U.S military defense (called bio-defense) aimed to detect chemical and biological attacks [17]. Later, genomics boosted this technique [18], which provided higher resolution and sensitivity.

Finally, microelectronics gave the final impulse to microfluidics, This was by means of the microfabrication techniques developed for microelectromechanical systems (MEMS) [19], which improved microfluidic systems fabrication methods such as those involved in photolithographic techniques. However, the most significant improvement in microfluidic systems development appeared with the use of poly (dimethylsiloxane) (PDMS) elastomer [20]. Until then, silicon and Silica were widely used to fabricate miniaturized fluidic devices, but PDMS offered different interesting

14

properties. These included optical transparency, smoothness, mechanical stability, rapid development and biocompatibility. The combination of PDMS and soft-lithography techniques allowed to obtain rapid prototyping of microfluidic devices [20]. This was seen as a potential breakthrough to facilitate the use of disposable microfluidic chips for handheld diagnostic and point-of-care devices [21]. From the integration of different devices and technologies emerged the term uTAS, which enclosed the operations required by an analytical laboratory inside a small chip [22]. Later these devices were also termed Lab-on-a-Chip as a more broader term [1], since these devices integrated other disciplines, such as fluid dynamics, sample pre-treatment, sample separation and signal detection within a single device. Due to its potentiality and benefits LOCs are being used in many applications[4], [6], [23], [24], including diseases diagnostic, genomic and proteomic research, analytical chemistry and environmental control.

1.3 Cell manipulation techniques in LOC devices

Cell manipulation is the action performed on a biological cell which produces a change in its normal cell behavior. This change could have different results such as a cell movement, a cell shape or even a new condition, such as dead or poration. Cell manipulation is nowadays key in many biological studies, including diagnosis, pathogen detection, cell trapping and separation, cell treatment or cell analysis.

Before microfluidic chips were introduced, many manipulation techniques have been proposed and performed. These methods started back in the 1900s, when manipulation and identification of cells was done using fluorescence techniques. One of these techniques exploited the fluorescence difference between excitation and emission spectra, the Stoke shift, to identify antigens in cells and tissue [25], [26]. Also, in the same years, it was achieved to label antibodies with fluorescein isothiocyanate (FITC) [27], which became a revolution in the cell visualization field.

In mid-1900's the interest move to physical particle manipulation, where a first optical trapping technique was reported [28]. After, microscopic particles were captured by a laser beam [29]. Also, a first cytometer based on a photoelectric device was presented [30]. Also these optical forces were explored to manipulate particles as tweezers (named in fact optical tweezers). In 1970s, Ashkin demonstrated that these forces could displace dielectric micro-particles in water and air [28]. These studies were extended by using optical tweezers to manipulate neutral atoms, live bacteria and viruses, obtaining a high force sensitivity [29]. Additionally, atomic force microscope (AFM) created in 1986 by Binnig et al [31] opened also new options in this field, since it allowed to modify the surface and manipulate individual molecules. Also, in 1999, Schnelle et al [32] conclude that it was viable to attract yeast cells to a unique gold wire, which opens the possibility to use metals as tweezers for real manually cell manipulation. Soon after tweezers were improved by taking profit of DEP effect, as Matsue et al reported [33].Then, appeared the manipulation based on hydrodynamic forces [34] and DEP was discovered [35], although it wasn't then applied for cell manipulation.

Also, magnetic techniques were used for manipulating purposes, by using active on chip micromagnets. This was first introduced by Kolm in 1971 [36], which extracted magnetic monopoles from massive quantities of deep sea sediment, and later adapted to microfluidics [37].These techniques currently have evolved. In fact, in 2005, Smistrup et al. [38] created a homogenous magnetic field inside a microfluidic channel where a fluorescent particle was trapped, by using permanent magnets based on magnetized Permalloy.

Notwithstanding these important contributions, DEP techniques were also improved for manipulation, taking advantage of the advancements in microfluidics and lab-on-a-chip devices. DEP rose up a great number of microfluidic designs so as to get benefited from DEP forces [39]–[41].

1.3.1 Theory of Dielectrophoresis

Dielectrophoresis [35] or DEP is the term that describes the electrical force resulting from particle polarization inside a non-uniform electric field. Although DEP has been used for many years, interest on the use of this phenomenon to manipulate or characterize biological material on lab-on-a-chip (LoC) devices has been increasing recently [6], [23], [39], [42], because of its versatility to miniaturize several analytical operations [4], [18]. DEP effect-based techniques enable the controlled and efficient manipulation of biomolecules and cells.

DEP is based on the effect of dielectric particles inside electric fields. When a particle is subjected to a non-uniform field particle, it is polarized and the formation of the dipole moment creates the dielectrophoretic force. Thus, cells can be reduced as complex dielectric particles suspended in a medium. The dielectrophoretic effect is commonly expressed as the time averaged DEP force acting on a particle suspended in a dielectric medium [43]

$$\langle F_{DEP} \rangle = \frac{1}{2} V \bullet Re[\alpha^*(\omega)] \bullet \nabla |E_{rms}|^2 \qquad \text{(Eq. 1)}$$

Where $Re[\alpha^*(\omega)]$ is the real part of a factor, the effective polarizability, which is dependent on the relation between εp^* and εm^*, that are the complex permittivity's of the particle and the medium. These permittivity's have a real and an imaginary part, such as $\varepsilon^* = \varepsilon - \sigma / j2\pi f$, where f corresponds to the applied electric field frequency and σ the conductivity. On the other hand, εp^* is related to the shape and dielectric properties of all the parts of the cell such as its membranes and internal media. Moreover, V is the volume of the particle, and E_{rms} is the root mean square electric field.

Furthermore, $Re[\alpha^*(\omega)]$ has a dependence with the electric field frequency due to its complex nature. Hence, the sign of this factor will indicate the particle movement inside the microfluidic chip, towards a maximum or a minimum of the field (which was named positive DEP or negative DEP). Then, for a cell with given dielectric properties, the sign of this force will

depend on the electrical properties of the medium and the applied electric field frequency (Fig.1.1.)

nDEP

$$\varepsilon_p > \varepsilon_m$$

pDEP

$$\varepsilon_p < \varepsilon_m$$
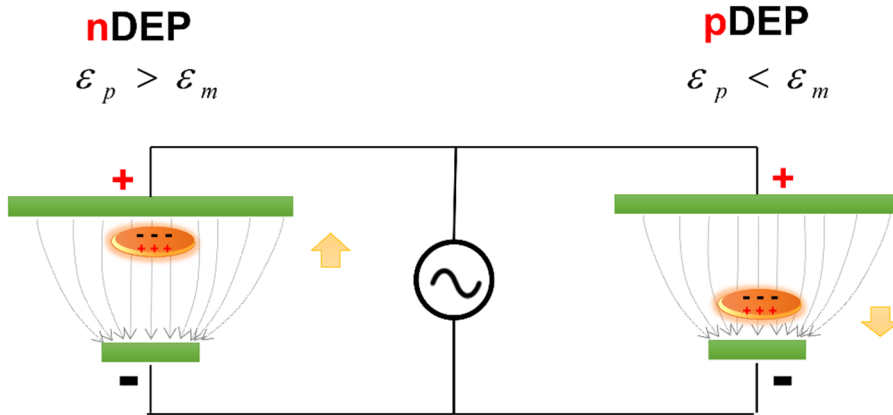
Fig.1. 1. Graphical view of DEP effect depending on the permittivities relation.

Since the DEP force is highly associated with the intrinsic electrical properties of a particle, the medium, and the applied electrical field, it can be tuned and it is used in many applications [41] including concentrators [44], [45], sorters [46]–[48], of biological material. One of the most common DEP application was sample pre-treatment by means of DEP concentration. The application of a concentrating procedure for a biological target is part of the sample preparation protocol in a number of analytical techniques. In biomedical, food-control or environmental analyses where a small amount of target-cells are found in a large sample volume, this operation is critical. In these cases, the analytical equipment needs a minimum concentration of the analyte to obtain a reliable measure. However, current procedures for sample pre-concentration involve long time processes, such as culture methods [12], [13] or electrophoresis [49], which are difficult to further integrate on bench-top complex analytical instruments. Moreover, they lack efficiency for relatively small samples.

Thus, on these occasions, the use of an efficient continuous-flow DEP-based LoC device becomes a practical option due to its swiftness and selectivity.

A device based on a large number of interdigitated metal electrodes placed in a microfluidic channel was used for this purpose in a number of publications [50], [51]. One example of such works is the study by Chun-Ping Jen et al. [52], in which HeLa cells were concentrated with 63% efficiency using DEP interdigitated chrome-gold curvy electrodes. Also, R. Hamada e t al. [53] reported the use of interdigitated chrome electrodes to concentrate *E. coli* before measuring its impedance. Other relevant work was that of M. R. Bown et al. [54] who used titanium-gold electrodes to pre-concentrate λ- phage DNA with an average 8-fold factor.

However, these devices have the limitation of generating DEP forces near the bottom of the LoC devices limiting their capabilities to trap the overall sample of interest at high flows [19-20]. Thus, new advances appearing from the inclusion of dielectric structures to DEP devices, which allow manipulating bigger cell quantities or to work at higher flow rates. Some works based on using conductive columns to enhance the trapping capabilities were reported [57]–[59]. However, these techniques imply rather complex chip fabrication and replication techniques.

On the other hand, the use of insulating structures to generate electrical field non-uniformities as an alternative, or a complement, to patterned metal electrodes could solve these issues. This well-known technique can be referred to as insulator-based dielectrophoresis (iDEP)[51] and it allows to generate convenient electric field gradients without the need of integrating complex and more numerous electrodes. B.H. Lapizco-Encinas et al.[60] concentrated and separated *E. coli* and several Bacillus species in water using isolated circular posts with a diameter of 150 μm. Similarly, W.A.Braff et al. [61] used poly (methyl methacrylate) (PMMA) structures to trap *E. coli* and Bacillus cereus at a range of dc potentials.

1.4 Cell characterization on a chip

Different methods have been discovered for measurement and characterization of cells. As has been stated before, flow cytometry was an innovative technique for counting and identifying cells [62]. Also, other methods were used for this purpose in case of small sample volumes. Lab on a chip technology was also a big impulse for these experiments [6], [63], taking profit of cell manipulation abilities as before explained.

Moreover, cells were also identified by using electrical techniques. These could be possible due to cells dielectric properties. In fact, from these properties emerged AC electrokinetic techniques as DEP and electrorotation, but also characterization methods as impedance spectroscopy, named bio-impedance due to the applied field.

Bioimpedance is the ability of tissues and cells to oppose the electric current flow [64]. It permits to measure membrane capacitance, resistance, cytoplasmic conductivity and also permittivity. In fact, first bio-impedance measurement was made in 1910 by Höber [65]. In there, internal conductivity of erythrocytes was successfully measured. Later, in 1925, Fricke [66] made the first assessment of the cell membrane thickness and by measuring capacitance, although first single cell measurement occurred when Curtis and Cole in 1937, by two electrodes placed in a groove, achieved to characterize a Nitella cell [67]. However, it wasn't until 2009 that impedance was used in a microfluidic chip. It was Holmes et al who achieved to construct a microfluidic cytometer base on impedance measurements [68]

1.4.1   Theory of Impedance spectroscopy

Electrical impedance spectroscopy measures in fact the AC electrical properties of cells, which are directly related to its dielectric properties. The impedance of a single particle could be measured by injecting an AC voltage inside a microfluidic channel thought electrodes. Usually one of these three electrode configurations is used:

1. The two-electrode-system or bipolar method (Fig. 1. 2 .A) Consists of introducing a constant current (I0) by means of two electrodes and reading the cell bioimpedance on the same electrodes. In here, electrode impedance must be accomplished the condition of being higher than the biological measured impedance.
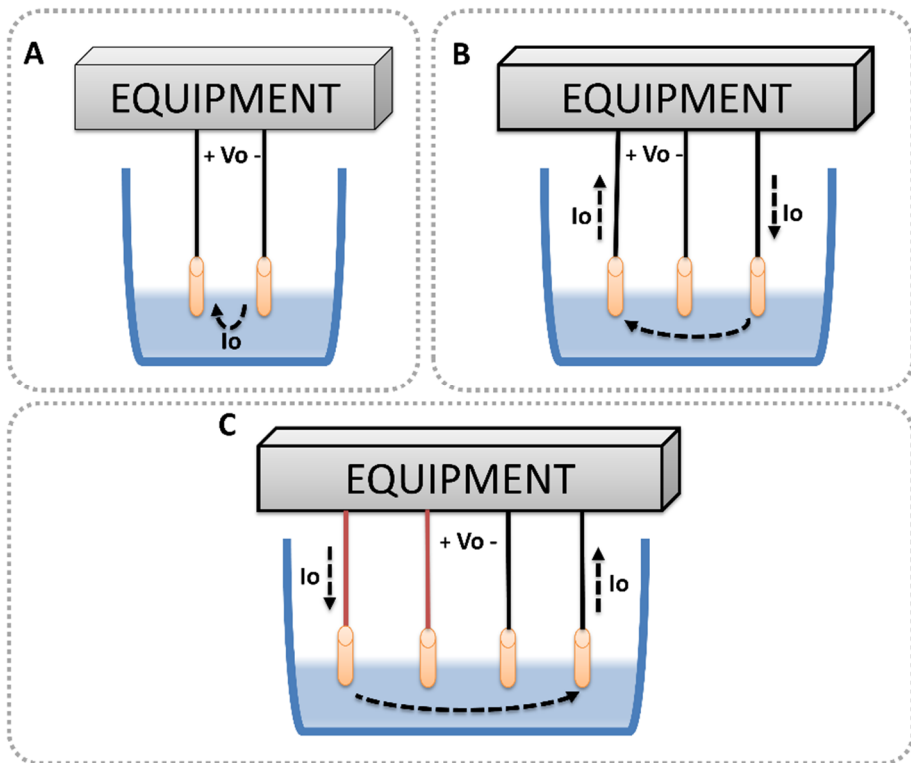
Fig.1. 2. Available methods for bioimpedance measurement. A. 2-electrode methos B. 3-electrode method C. 4-electrode method.

2. The 3 electrode system (Fig.1. 2. B), where current is applied through two electrodes, considering one as a reference and another as the injector electrode. Then, bioimpedance is measured between the reference and the third electrode. The main advantage of this method is the reading electrode (Ze''), which doesn't transport current. Thus, no voltage is introduced into the cell.

3. The 4 electrode method (Fig.1. 2. C) is based on two current injection electrodes and two voltage reading electrodes, where the obtained differential voltage is related to the cell impedance by Ohm's law. Then, electrode impedance is cancelled.

The obtained bioimpedance in these methods were previously described by Maxwell Equations [64]:

$$D = \varepsilon_0 E + P \tag{Eq. 2}$$

Which, if component magnetic is avoided, (1) is reduced to:

$$\frac{\partial D}{\partial t} = -J \tag{Eq. 3}$$

Considering the interface between electrodes and biomaterial as a capacitor with metal area A and dielectric thickness L, which material is homogeneous and isotropic, in which a voltage v is applied, then,

$$\frac{\partial D}{\partial t} = \frac{j\omega v \varepsilon}{L} = J \tag{Eq. 4}$$

$$i = \frac{j\omega v \varepsilon A}{L} = v j \omega C \tag{Eq. 5}$$

Where i is the current. The bioimpedance in admittance terms is in fact (consider G as conductance ($G = \sigma' A/L$)),

$$Y = \frac{i}{v} = G + jwC \tag{Eq. 6}$$

Nevertheless, Foster and Schwan [69], complete the bioimpedance model in 1989 for cells in suspending medium, by approaching its physical properties to a complete electric circuit.

The particle was modelled as a resistor Ri and a capacitor Ci in series, which was equivalent to the cytoplasm. Also, the membrane was modelled as a resistor Rmem and a capacitor Cmem in parallel, as it is detailed below.

22
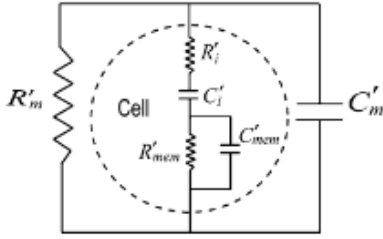
Fig.1. 3 Electrical model of a cell.

$$R'm = \frac{1}{\sigma_0.Gf} \qquad \text{(Eq. 7)}$$

$$C'm = \varepsilon_\infty \cdot Gf \qquad \text{(Eq. 8)}$$

$$R'i = \frac{1}{(k2 + k3)Gf} \qquad \text{(Eq. 9)}$$

$$C'i = (\Delta\varepsilon_1 + \Delta\varepsilon_2)Gf \qquad \text{(Eq. 10)}$$

Complete cell:

$$R'mem = \frac{1}{Gf}\left[\frac{\tau_1 + \tau_2}{\Delta\varepsilon_1 + \Delta\varepsilon_2} - \frac{1}{k2 + k3} - \frac{\tau_1\tau_2(k2 + k3)}{(\Delta\varepsilon_1 + \Delta\varepsilon_2)^2}\right] \qquad \text{(Eq. 11)}$$

$$C'mem = \frac{\tau_1\tau_2(k2 + k3)}{(\Delta\varepsilon_1 + \Delta\varepsilon_2)R'mem} \qquad \text{(Eq. 12)}$$

1.5   Combining DEP and IS for a specific solution: bacteria pre-treatment and detection.

As commented before, DEP concentration is a selective method which allows reductions in sample preparation time [70], [71]. Since it is dependent on the electrical properties of particles, it is a convenient handling method that has been applied in many biological fields and especially in lab-on-a-chip (LoC) devices [4], [6], [18]. In case of bacterium manipulation, DEP was previously shown to be an effective solution [61], [72] as previously introduced. In this thesis, DEP was applied to pre-concentrate *E. coli* so as to prepare the sample for the subsequent detection. In fact, many publications have used this method to concentrate bacterium. In Table 1.1 a summary of recent publications related to this topic is shown.

23

Table 1.1. Summary of recent publications on bacteria trapping and concentration by means of DEP procedures.

Concentrated bacteria	Device used	DEP signal applied	DEP Generator	Ref
Escherichia coli (ATCC 25927)	Microfluidic device with parallel gold electrodes	20 Vpp at 100 kHz	Function generator 33120A, Agilent	[73]
Escherichia coli (type not specified)	ITO electrodes separated by an V-shape narrow gap of 60°	1 Vpp at 1 kHz	Function generator (no Brand specified)	[74]
Staphylococcus aureus and Pseudomonas aeruginosa	Quadruple electrode in droplet form. The trapping region is in the middle.	15 Vpp, 100 kHz to 1.2 MHz	Multi-output function generator (FLUKE 284)	[75]
E. coli (ATCC] 11775)	Pore-type iDEP chip coated with ITO. Hexagon shape	128 V/mm at 300 kHz	Function generator (Agilent, 33120A)	[76]
E. coli (strain Top10)	iDEP device - insulating structures- and external platinum wire electrodes to apply the electric field.	600 V/cm	High-voltage sequencer model HVS448 (LabSmith)	[77]
E. coli ATCC 8739	Inclined (45°) interdigitated electrodes	4 Vpp at 100 kHz	No specified	[78]
Bacillus atrophaeus	Gold interdigitated electrodes	10 kHz to 60 MHz	DEPtech 3 DEP dielectrophoresis analyser (Labtech)	[79]

Otherwise, frequency dependence of impedance, related to the electrical conductivity and permittivity properties of the material, was reported as an effective solution to the characterization of cells and their behaviour [80], also in LoC devices [81]. In fact, some publications have reported the use of IA technique to control bacterial growth or to detect its presence and especially in case of *E. coli* detection. In Table 1.2, a summary of the last publications related to *E. coli* detection or characterization by means of impedance is represented. In these publications, impedance is used to

24

quantify or characterize *E. coli* by means of electrochemical custom sensors or wired based commercial sensor. In this thesis we will approach this technique in combination with microfluidics and electrokinetics, as it will be later detailed.

Table 1.2. Summary of recent publications on bacteria characterization by means of IS.

Measured *E. coli*	Sensor	Applied signal	Used device	Ref
E. coli O157:H7	Gold sensor chips (GWC technologies Inc.)	100 kHz to 1 Hz, at 10 mVp	VMP2 multipotentiostat (Princeton Applied Research)	[82]
E. coli O157:H7	Custom interdigitated electrode (chromium and gold)	100 Hz to 10 MHz, at 500 mVp	Agilent 4294A Impedance analyzer	[83]
E. coli ORN 178	Gold electrodes modified with mixed SAMs	0.05 Hz to 1000 kHz, at 5 mVp	Echem Analyst from Gamry	[84]
E. coli ATCC 873	To board-printed paralled electrodes	10 kHz at 5 Vpp	Lock-in-amp, HF2LI, Zurich Instruments	[78]
E. coli K12 and *E. coli* O157:H7	Gold interdigitated microelectrodes	1 Hz to 1 MHz, at 10mV	ZAHNER chemical station	[85]
E. coli O157:H7 and *E. coli* DH 5	Graphene oxide paper based electrode	0.1 to 100 kHz, at 5mV	Impedance-Gain-Phase Analyser 1260 in combination Electrochemical Interface 1287 (Solartron)	[86]
E. coli O157:H7	Platinum wires inserted in a PDMS microfluidic chip	1 Hz to 100 kHz, at 50mVpp	Electrochemical analyser VersaSTAT3 (METEK)	[87]

By combining bioimpedance with the DEP entrapping and concentrating procedure, we will demonstrate the viability of rapid bacteria concentration and large samples monitoring, using a compact equipment together with a

specially designed micro-fluidic chip. The combination of these techniques is currently an emerging field of application to point-of-use devices and only a few publications about this topic are available. In fact, during the last stages of this thesis a number of publications appeared from R. Hamada group (R&D of Panasonic Healthcare) related to the combination of both techniques in a microfluidic chip [88], [89]. This device was used for some applications of bacteria detection in saliva: for general quantification [88] and for the detection of *Tannerella forsythia*, to diagnose chronic periodontitis [89].

On the other side, as it can be observed in Tables 1.1 and 1.2, the vast majority of these publications use commercial devices to achieve the necessary electrical signals for the experimental. Commercial equipment's are of large dimensions, and although they have so many features these are, in many cases, not necessary for the application. In this thesis we will look for the best option to solve the necessities in each case study without giving up important features. As a result, we will be able to increase the portability of the system while reducing the cost of the prototypes and final devices.

1.6 Using custom electronics to improve laboratory procedures.

As stated before, commercial devices have been used to explore the related methods. However, in only a few of these publications, custom electronics are shown as a good alternative (Table 1.3). This is key in order to achieve full integration and miniaturization of these techniques in order to use them on biological laboratories or point-of-care setups.

In here, custom electronics offer their versatility and its low cost for specific solutions. Moreover, in some cases, it allows to miniaturize systems to make it more portable, which clearly benefits point-of-use devices.Generally, in the related publications a combination of analogic and digital electronics is used. These make custom electronic platforms more user-friendly. Also, the whole system is usually adapted to the designed

26

sensor or the microfluidic chip. In here, we will look to gather all this tips. We would like to obtain a portable a lost cost device, but also specific for the application and with the availability to make it accessible, giving results in real time.

Table 1.3. Published works on custom electronics for IC and DEP studies.

Aim of the work	Method	Basis of the custom device	Voltage range	Frequency range	Ref
Improve chemical and biological experiments	DEP	CMOS IC microfluidic device + board to adapt to computer interface	5 Vpp	Dc to 11 MHZ	[90]
Improve individual manipulation, maintaining cell properties	DEP	Two-dimensional array of microsites activated by transistors + bias generator block +readout circuit	3.3 to 6.6Vpp	DC to 10M Hz	[91]
Enrich rare cells	DEP	Relays activated by a microcontroller	16 V	600 kHz	[92]
To manipulate particles without making connections to the microfluidic chip	DEP	Microwell array activated by an RFID + signal adapter circuit + activator	$6V_{DC}$	DC	[93]
Detection of *E. coli* in Blood	IS	uController + adapting module + Sensor	50 mV-1V	100 Hz-1 MHz	[94]
E. coli and S.Typhimurim detection	IS	uController + Adapting stage + Sensor	4 - 63,55V	100Hz-80kHz	[95]

1.7 Objectives and roadmap

The scope of this thesis is to design, develop, test, and combine, different electronic modules to manipulate and characterize cells by means of DEP and IS. The combination of these two techniques has many life sciences applications to facilitate current benchtop standard procedures but also to generate novel portable miniaturized sample preparation and analytical devices. This should be directed to medical and food control field, not forgetting to improve current diagnostic and detection techniques.

Chapter 2. The dielectrophoretic effect. Introduction and preliminary studies. In this chapter, an electronic device was specially designed and tested as a module to generate DEP forces in benchtop setups for microfluidic disposables. As a proof of concept, the dielectrophoretic effect is exploited for a given bacteria concentration application, and results are analyzed in terms of trapping efficiency. A classical microfluidic chip with interdigitated electrodes configuration was designed, fabricated and tested, obtaining exhaustive statistics for different DEP configurations.

Chapter 3. Improving the concentrating cell methods. Insulated poles benefits in DEP devices. In this chapter, the classical microfluidic chip was modified and improved by generating further electric field inhomogeneity's in the medium through insulating poles. By including the poles higher trapping efficiencies are obtained and test could be done at higher flow rates. The device was completely characterized by a cytometer analysis and fluorescence performances.

Chapter 4. Bioimpedance as a method for biological material characterization. In this chapter, a miniaturized impedance measuring device was designed and validated for biological material characterization. The proposed and developed electronic device was capable of measuring the impedance by the 4-electrode method in order to improve the bioimpedance measurements. Different materials were measured by this method, so as to characterize a tissue sensor for in-vivo testing.

Chapter 5. Combining manipulating methods with electric measures. Using DEP and Bioimpedance together for a rapid detection of *E. coli* in the water. In this chapter the whole system is characterized for water contamination detection and microbes analysis. The strengths of DEP and bioimpednace are combined and exploited to detect small amounts of *E. coli* in large sample volumes.

Chapter 6. Concluding remarks and future prospects. The objectives of the presented thesis are revised to retake and frame the different issues that have been solved and the achievements accomplished through the thesis. Additionally, some future directions are exposed which are related to this work.

References

[1]   D. Mark, S. Haeberle, G. Roth, F. von Stetten, and R. Zengerle, "Microfluidic lab-on-a-chip platforms: requirements, characteristics and applications.," *Chem. Soc. Rev.*, vol. 39, no. 3, pp. 1153–82, Mar. 2010.

[2]   S. C. Terry, J. H. Jerman, and J. B. Angell, "A gas chromatographic air analyzer fabricated on a silicon wafer," *IEEE Trans. Electron Devices*, vol. 26, no. 12, pp. 1880–1886, Dec. 1979.

[3]   A. Manz, N. Graber, and H. M. Widmer, "Miniaturized total chemical analysis systems: A novel concept for chemical sensing," *Sensors Actuators B Chem.*, vol. 1, no. 1–6, pp. 244–248, Jan. 1990.

[4]   H. A. Stone, A. D. Stroock, and A. Ajdari, "Engineering flows in small devices: Microfluidics toward a lab-on-a-chip," *Annu. Mech.*, vol. 36, pp. 381–411, 2004.

[5]   M. A. Burns, "An Integrated Nanoliter DNA Analysis Device," *Science (80-.)*., vol. 282, no. 5388, pp. 484–487, Oct. 1998.

[6]   C. D. Chin, V. Linder, and S. K. Sia, "Lab-on-a-chip devices for global health: Past studies and future opportunities," *Lab Chip*, vol. 7, no. 1, pp. 41–57, 2007.

[7]   M. A. Croxen, R. J. Law, R. Scholz, K. M. Keeney, M. Wlodarska, and B. B. Finlay, "Recent advances in understanding enteric pathogenic Escherichia coli.," *Clin Microbiol Rev*, vol. 26, no. 4, pp. 822–880, Oct. 2013.

[8]   D. M. Sievert, P. Ricks, J. R. Edwards, A. Schneider, J. Patel, A. Srinivasan, A. Kallen, B. Limbago, and S. Fridkin, "Antimicrobial-resistant pathogens associated with healthcare-associated infections: summary of data reported to the National Healthcare Safety Network at the Centers for Disease Control and Prevention, 2009-2010.," *Infect. Control Hosp. Epidemiol.*, vol. 34, no. 1, pp. 1–14, Jan. 2013.

30

[9]   G. C. Ulett, M. Totsika, K. Schaale, A. J. Carey, M. J. Sweet, and M. A. Schembri, "Uropathogenic Escherichia coli virulence and innate immune responses during urinary tract infection.," *Curr Opin Microbiol*, vol. 16, no. 1, pp. 100–107, Feb. 2013.

[10]   M. D. Zordan, M. M. G. Grafton, G. Acharya, L. M. Reece, C. L. Cooper, A. I. Aronson, K. Park, and J. F. Leary, "Detection of pathogenic E. coli O157:H7 by a hybrid microfluidic SPR and molecular imaging cytometry device.," *Cytom. A*, vol. 75, no. 2, pp. 155–162, Feb. 2009.

[11]   K. Dhama, S. Chakraborty, R. Tiwari, A. K. Verma, M. Saminathan, Y. S. M. Amarpal, Z. Nikousefat, M. Javdani, and R. U. Khan, "RESEARCH OPINIONS IN ANIMAL & VETERINARY SCIENCES."

[12]   P. T. Feldsine, M. T. Falbo-Nelson, and D. L. Hustead, "ColiComplete® substrate-supporting disc method for confirmed detection of total coliforms and Escherichia coli in all foods: comparative study," *J. AOAC Int.*, vol. 77, no. 1, pp. 58–63, 1994.

[13]   F. Pouch Downes and K. Ito, *Compendium of Methods for the Microbiological Examination of Foods*, 4th ed. American Public Health Association, 2001.

[14]   P. Tabeling, "Introduction to Microfluidics: Paperback: Patrick Tabeling - Oxford University Press," *Introduction to microfluidics*, 2010. [Online]. Available: http://ukcatalogue.oup.com/product/9780199588169.do. [Accessed: 27-Jun-2015].

[15]   N.-T. Nguyen and S. T. Wereley, *Fundamentals and Applications of Microfluidics*. Artech House, 2002.

[16]   E. Bassous, H. H. Taub, and L. Kuhn, "Ink jet printing nozzle arrays etched in silicon," *Appl. Phys. Lett.*, vol. 31, no. 2, p. 135, Aug. 1977.

[17]   P. Yager, T. Edwards, E. Fu, K. Helton, K. Nelson, M. R. Tam, and

B. H. Weigl, "Microfluidic diagnostic technologies for global public health.," *Nature*, vol. 442, no. 7101, pp. 412–8, Jul. 2006.

[18]   D. Figeys and D. Pinto, "Lab-on-a-chip: a revolution in biological and medical sciences.," *Anal. Chem.*, vol. 72, no. 9, p. 330 A–335 A, 2000.

[19]   E. Verpoorte and N. F. De Rooij, "Microfluidics meets MEMS," *Proc. IEEE*, vol. 91, no. 6, pp. 930–953, Jun. 2003.

[20]   D. C. Duffy, J. C. McDonald, O. J. A. Schueller, and G. M. Whitesides, "Rapid Prototyping of Microfluidic Systems in Poly(dimethylsiloxane)," *Anal. Chem.*, vol. 70, no. 23, pp. 4974–4984, Dec. 1998.

[21]   L. Gervais, N. de Rooij, and E. Delamarche, "Microfluidic chips for point-of-care immunodiagnostics.," *Adv. Mater.*, vol. 23, no. 24, pp. H151–76, Jun. 2011.

[22]   H. Andersson and A. Van den Berg, "Microfluidic devices for cellomics: A review," *Sensors Actuators, B Chem.*, vol. 92, no. 3, pp. 315–325, 2003.

[23]   G. T. Vladisavljević, N. Khalid, M. A. Neves, T. Kuroiwa, M. Nakajima, K. Uemura, S. Ichikawa, and I. Kobayashi, "Industrial lab-on-a-chip: design, applications and scale-up for drug discovery and delivery.," *Adv. Drug Deliv. Rev.*, vol. 65, no. 11–12, pp. 1626–63, Nov. 2013.

[24]   G. Medoro, N. Manaresi, A. Leonardi, L. Altomare, M. Tartagni, and R. Guerrieri, "A lab-on-a-chip for cell detection and manipulation," in *Sensors, 2002. Proceedings of IEEE*, 2002, vol. 1, pp. 472–477.

[25]   A. H. Coons, "Labelled antigens and antibodies.," *Annu. Rev. Microbiol.*, vol. 8, pp. 333–52, Jan. 1954.

[26]   A. H. Coons, "Studies on antibody production: i. a method for the histochemical demonstration of specific antibody and its application

to a study of the hyperimmune rabbit.," *J. Exp. Med.*, vol. 102, no. 1, pp. 49–60, Jul. 1955.

[27]   A. H. Coons, "The beginnings of immunofluorescence.," *J. Immunol.*, vol. 87, no. 5, pp. 499–503, Nov. 1961.

[28]   A. Ashkin, "Acceleration and Trapping of Particles by Radiation Pressure," *Phys. Rev. Lett.*, vol. 24, no. 4, pp. 156–159, Jan. 1970.

[29]   A. Ashkin and J. Dziedzic, "Optical trapping and manipulation of viruses and bacteria," *Science (80-.).*, vol. 235, no. 4795, pp. 1517–1520, Mar. 1987.

[30]   A. Moldavan, "Photo-electric technique for the counting of microscopical cells.," *Science*, vol. 80, no. 2069, pp. 188–9, Aug. 1934.

[31]   G. Binnig and C. F. Quate, "Atomic Force Microscope," *Phys. Rev. Lett.*, vol. 56, no. 9, pp. 930–933, Mar. 1986.

[32]   T. Schnelle, T. Müller, R. Hagedorn, A. Voigt, and G. Fuhr, "Single micro electrode dielectrophoretic tweezers for manipulation of suspended cells and particles," *Biochim. Biophys. Acta - Gen. Subj.*, vol. 1428, no. 1, pp. 99–105, Jun. 1999.

[33]   T. Matsue, N. Matsumoto, S. Koike, and I. Uchida, "Microring-ring electrode for manipulation of a single cell," *Biochim. Biophys. Acta - Gen. Subj.*, vol. 1157, no. 2, pp. 332–335, Jun. 1993.

[34]   L. Herzenberg and R. Sweet, "Fluorescence-activated Cell Sorting," *Fluorescence-activated cell sorting*, 1976. .

[35]   H. A. Pohl, "The Motion and Precipitation of Suspensoids in Divergent Electric Fields," *J. Appl. Phys.*, vol. 22, no. 7, p. 869, 1951.

[36]   H. H. Kolm, F. Villa, and A. Odian, "Search for Magnetic

Monopoles," *Phys. Rev. D*, vol. 4, no. 5, pp. 1285–1296, Sep. 1971.

[37]   C. H. Ahn, M. G. Allen, W. Trimmer, Y.-N. Jun, and S. Erramilli, "A fully integrated micromachined magnetic particle separator," *J. Microelectromechanical Syst.*, vol. 5, no. 3, pp. 151–158, 1996.

[38]   K. Smistrup, T. Lund-Olesen, M. F. Hansen, and P. T. Tang, "Microfluidic magnetic separator using an array of soft magnetic elements," *J. Appl. Phys.*, vol. 99, no. 8, p. 08P102, Apr. 2006.

[39]   R. Pethig, "Review Article—Dielectrophoresis: Status of the theory, technology, and applications," *Biomicrofluidics*, vol. 4, p. 22811, 2010.

[40]   K. Khoshmanesh, S. Nahavandi, S. Baratchi, A. Mitchell, and K. Kalantar-zadeh, "Dielectrophoretic platforms for bio-microfluidic systems.," *Biosens. Bioelectron.*, vol. 26, no. 5, pp. 1800–14, Jan. 2011.

[41]   Y. Demircan, E. Özgür, and H. Külah, "Dielectrophoresis: Applications and future outlook in point of care," *Electrophoresis*, vol. 34, no. 7, pp. 1008–1027, 2013.

[42]   A. M. Foudeh, T. Fatanat Didar, T. Veres, and M. Tabrizian, "Microfluidic designs and techniques using lab-on-a-chip devices for pathogen detection for point-of-care diagnostics.," *Lab Chip*, vol. 12, no. 18, pp. 3249–66, Sep. 2012.

[43]   H. A. Pohl and J. S. Crane, "Dielectrophoresis of cells," *Biophys. J.*, vol. 11, no. 9, pp. 711–727, 1971.

[44]   S. V. Puttaswamy, C.-H. Lin, S. Sivashankar, Y.-S. Yang, and C.-H. Liu, "Electrodeless dielectrophoretic concentrator for analyte pre-concentration on poly-silicon nanowire field effect transistor," *Sensors Actuators B Chem.*, vol. 178, pp. 547–554, 2013.

[45]   M. Li, S. Li, W. Cao, W. Li, W. Wen, and G. Alici, "Improved concentration and separation of particles in a 3D dielectrophoretic

chip integrating focusing, aligning and trapping," *Microfluid. Nanofluidics*, vol. 14, no. 3–4, pp. 527–539, 2013.

[46]   M. Viefhues, S. Wegener, A. Rischmüller, M. Schleef, and D. Anselmetti, "Dielectrophoresis based continuous-flow nano sorter: fast quality control of gene vaccines," *Lab Chip*, 2013.

[47]   M. Alshareef, N. Metrakos, E. J. Perez, F. Azer, F. Yang, X. Yang, and G. Wang, "Separation of tumor cells with dielectrophoresis-based microfluidic chip," *Biomicrofluidics*, vol. 7, p. 11803, 2013.

[48]   T. Kodama, T. Osaki, R. Kawano, K. Kamiya, N. Miki, and S. Takeuchi, "Round-Tip Dielectrophoresis-Based Tweezers for Single Micro-Object Manipulation," *Biosens. Bioelectron.*, 2013.

[49]   C. R. Cabrera and P. Yager, "Continuous concentration of bacteria in a microfluidic flow cell using electrokinetic techniques.," *Electrophoresis*, vol. 22, no. 2, pp. 355–62, Jan. 2001.

[50]   K. Khoshmanesh, S. Nahavandi, S. Baratchi, A. Mitchell, and K. Kalantar-zadeh, "Dielectrophoretic platforms for bio-microfluidic systems," *Biosens. Bioelectron.*, vol. 26, no. 5, pp. 1800–1814, 2011.

[51]   R. Martinez-Duarte, "Microfabrication technologies in dielectrophoresis applications?A review," *Electrophoresis*, vol. 33, no. 21, pp. 3110–3132, 2012.

[52]   C.-P. Jen, C.-T. Huang, and H.-H. Chang, "A cellular preconcentrator utilizing dielectrophoresis generated by curvy electrodes in stepping electric fields," *Microelectron. Eng.*, vol. 88, no. 8, pp. 1764–1767, 2011.

[53]   R. Hamada, H. Takayama, Y. Shonishi, L. Mao, M. Nakano, and J. Suehiro, "A rapid bacteria detection technique utilizing impedance measurement combined with positive and negative dielectrophoresis," *Sensors Actuators B Chem.*, 2013.

[54]   M. R. Bown and C. D. Meinhart, "AC electroosmotic flow in a DNA concentrator," *Microfluid. Nanofluidics*, vol. 2, no. 6, pp. 513–523, 2006.

[55]   M. Nayak, D. Singh, H. Singh, R. Kant, A. Gupta, S. S. Pandey, S. Mandal, G. Ramanathan, and S. Bhattacharya, "Integrated sorting, concentration and real time PCR based detection system for sensitive detection of microorganisms.," *Sci. Rep.*, vol. 3, p. 3266, Jan. 2013.

[56]   L. Rozitsky, A. Fine, D. Dado, S. Nussbaum-Ben-Shaul, S. Levenberg, and G. Yossifon, "Quantifying continuous-flow dielectrophoretic trapping of cells and micro-particles on micro-electrode array.," *Biomed. Microdevices*, vol. 15, no. 5, pp. 859–65, Oct. 2013.

[57]   R. Martinez-Duarte, F. Camacho-Alanis, P. Renaud, and A. Ros, "Dielectrophoresis of lambda-DNA using 3D carbon electrodes.," *Electrophoresis*, vol. 34, no. 7, pp. 1113–22, Apr. 2013.

[58]   M. D. C. Jaramillo, R. Martínez-Duarte, M. Hüttener, P. Renaud, E. Torrents, and A. Juárez, "Increasing PCR sensitivity by removal of polymerase inhibitors in environmental samples by using dielectrophoresis.," *Biosens. Bioelectron.*, vol. 43, pp. 297–303, May 2013.

[59]   M. Elitas, R. Martinez-Duarte, N. Dhar, J. D. McKinney, and P. Renaud, "Dielectrophoresis-based purification of antibiotic-treated bacterial subpopulations.," *Lab Chip*, vol. 14, no. 11, pp. 1850–7, Jun. 2014.

[60]   B. H. Lapizco-Encinas, B. A. Simmons, E. B. Cummings, and Y. Fintschenko, "Insulator-based dielectrophoresis for the selective concentration and separation of live bacteria in water," *Electrophoresis*, vol. 25, no. 10-11, pp. 1695–1704, 2004.

[61]   W. A. Braff, A. Pignier, and C. R. Buie, "High sensitivity three-dimensional insulator-based dielectrophoresis," *Lab Chip*, vol. 12, no. 7, pp. 1327–1331, 2012.

36

[62]   H. M. Shapiro, "The evolution of cytometers," *Cytometry*, vol. 58A, no. 1, pp. 13–20, Mar. 2004.

[63]   Y. Zheng, J. Nguyen, Y. Wei, and Y. Sun, "Recent advances in microfluidic techniques for single-cell biophysical characterization.," *Lab Chip*, vol. 13, no. 13, pp. 2464–83, Jul. 2013.

[64]   O. G. Martinsen and S. Grimnes, *Bioimpedance and Bioelectricity Basics.* 2011.

[65]   R. Höber, "Eine Methode, die elektrische Leitfähigkeit im Innern von Zellen zu messen," *Pflüger's Arch. für die Gesammte Physiol. des Menschen und der Tiere*, vol. 133, no. 4–6, pp. 237–253, Jul. 1910.

[66]   H. Fricke, "THE ELECTRIC CAPACITY OF SUSPENSIONS WITH SPECIAL REFERENCE TO BLOOD," *J. Gen. Physiol.*, vol. 9, no. 2, pp. 137–152, Nov. 1925.

[67]   H. J. Curtis and K. S. Cole, "TRANSVERSE ELECTRIC IMPEDANCE OF NITELLA.," *J. Gen. Physiol.*, vol. 21, no. 2, pp. 189–201, Nov. 1937.

[68]   D. Holmes, D. Pettigrew, C. H. Reccius, J. D. Gwyer, C. van Berkel, J. Holloway, D. E. Davies, and H. Morgan, "Leukocyte analysis and differentiation using high speed microfluidic single cell impedance cytometry.," *Lab Chip*, vol. 9, no. 20, pp. 2881–9, Oct. 2009.

[69]   K. R. Foster and H. P. Schwan, "Dielectric properties of tissues and biological materials: a critical review.," *Crit. Rev. Biomed. Eng.*, vol. 17, no. 1, pp. 25–104, Jan. 1989.

[70]   H. Morgan and N. G. Green, *AC electrokinetics: colloids and nanoparticles*, no. 2. Research Studies Press, 2003.

[71]   H. A. Pohl and I. Hawk, "Separation of living and dead cells by dielectrophoresis," *Science (80-.).*, vol. 152, no. 3722, p. 647, 1966.

[72]   B. H. Lapizco-Encinas, B. A. Simmons, E. B. Cummings, and Y. Fintschenko, "Dielectrophoretic concentration and separation of live and dead bacteria in an array of insulators," *Anal. Chem.*, vol. 76, no. 6, pp. 1571–1579, 2004.

[73]   S. Park, Y. Zhang, T.-H. Wang, and S. Yang, "Continuous dielectrophoretic bacterial separation and concentration from physiological media of high conductivity.," *Lab Chip*, vol. 11, no. 17, pp. 2893–2900, Sep. 2011.

[74]   Y. Inoue, R. Obara, M. Nakano, and J. Suehiro, "Concentration of bacteria in high conductive medium using negative dielectrophoresis," in *2015 IEEE International Conference on Industrial Technology (ICIT)*, 2015, pp. 3336–3340.

[75]   I.-F. Cheng, T.-Y. Chen, R.-J. Lu, and H.-W. Wu, "Rapid identification of bacteria utilizing amplified dielectrophoretic force-assisted nanoparticle-induced surface-enhanced Raman spectroscopy.," *Nanoscale Res. Lett.*, vol. 9, no. 1, p. 324, Jan. 2014.

[76]   Y.-K. Cho, S. Kim, K. Lee, C. Park, J.-G. Lee, and C. Ko, "Bacteria concentration using a membrane type insulator-based dielectrophoresis in a plastic chip.," *Electrophoresis*, vol. 30, no. 18, pp. 3153–9, Sep. 2009.

[77]   H. Moncada-Hernández and B. H. Lapizco-Encinas, "Simultaneous concentration and separation of microorganisms: insulator-based dielectrophoretic approach," *Anal. Bioanal. Chem.*, vol. 396, no. 5, pp. 1805–1816, 2010.

[78]   M. Kim, T. Jung, Y. Kim, C. Lee, K. Woo, J. H. Seol, and S. Yang, "A microfluidic device for label-free detection of Escherichia coli in drinking water using positive dielectrophoretic focusing, capturing, and impedance measurement.," *Biosens. Bioelectron.*, vol. 74, pp. 1011–1015, Jul. 2015.

[79]   H. O. Fatoyinbo, M. C. McDonnell, and M. P. Hughes, "Dielectrophoretic sample preparation for environmental monitoring of microorganisms: Soil particle removal.," *Biomicrofluidics*, vol. 8,

no. 4, p. 044115, Jul. 2014.

[80]   L. Yang and R. Bashir, "Electrical/electrochemical impedance for rapid detection of foodborne pathogenic bacteria.," *Biotechnol. Adv.*, vol. 26, no. 2, pp. 135–50, Jan. 2008.

[81]   A. M. Foudeh, T. Fatanat Didar, T. Veres, and M. Tabrizian, "Microfluidic designs and techniques using lab-on-a-chip devices for pathogen detection for point-of-care diagnostics.," *Lab Chip*, vol. 12, no. 18, pp. 3249–66, Sep. 2012.

[82]   M. Barreiros dos Santos, J. P. Agusil, B. Prieto-Simón, C. Sporer, V. Teixeira, and J. Samitier, "Highly sensitive detection of pathogen Escherichia coli O157:H7 by electrochemical impedance spectroscopy.," *Biosens. Bioelectron.*, vol. 45, pp. 174–80, Jul. 2013.

[83]   M. Dweik, R. C. Stringer, S. G. Dastider, Y. Wu, M. Almasri, and S. Barizuddin, "Specific and targeted detection of viable Escherichia coli O157:H7 using a sensitive and reusable impedance biosensor with dose and time response studies," *Talanta*, vol. 94, pp. 84–89, 2012.

[84]   X. Guo, A. Kulkarni, A. Doepke, H. B. Halsall, S. Iyer, and W. R. Heineman, "Carbohydrate-based label-free detection of Escherichia coli ORN 178 using electrochemical impedance spectroscopy.," *Anal. Chem.*, vol. 84, no. 1, pp. 241–6, Jan. 2012.

[85]   Z. Li, Y. Fu, W. Fang, and Y. Li, "Electrochemical Impedance Immunosensor Based on Self-Assembled Monolayers for Rapid Detection of Escherichia coli O157:H7 with Signal Amplification Using Lectin.," *Sensors (Basel).*, vol. 15, no. 8, pp. 19212–24, Jan. 2015.

[86]   Y. Wang, J. Ping, Z. Ye, J. Wu, and Y. Ying, "Impedimetric immunosensor based on gold nanoparticles modified graphene paper for label-free detection of Escherichia coli O157:H7.," *Biosens. Bioelectron.*, vol. 49, pp. 492–8, Nov. 2013.

[87]   F. Tan, P. H. M. Leung, Z. Liu, Y. Zhang, L. Xiao, W. Ye, X. Zhang, L. Yi, and M. Yang, "A PDMS microfluidic impedance immunosensor for E. coli O157:H7 and Staphylococcus aureus detection via antibody-immobilized nanoporous membrane," *Sensors Actuators B Chem.*, vol. 159, no. 1, pp. 328–335, Nov. 2011.

[88]   K. HIROTA, S. INAGAKI, R. HAMADA, K. ISHIHARA, and Y. MIYAKE, "Evaluation of a Rapid Oral Bacteria Quantification System Using Dielectrophoresis and the Impedance Measurement," *Biocontrol Sci.*, vol. 19, no. 1, pp. 45–49, Mar. 2014.

[89]   Y. Ishii, K. Imamura, Y. Kikuchi, S. Miyagawa, R. Hamada, J. Sekino, H. Sugito, K. Ishihara, and A. Saito, "Point-of-care detection of Tannerella forsythia using an antigen-antibody assisted dielectrophoretic impedance measurement method.," *Microb. Pathog.*, vol. 82, pp. 37–42, May 2015.

[90]   D. Issadore, T. Franke, K. A. Brown, and R. M. Westervelt, "A microfluidic microprocessor: controlling biomimetic containers and cells using hybrid integrated circuit/microfluidic chips," *Lab Chip*, vol. 10, no. 21, pp. 2937–2943, 2010.

[91]   N. Manaresi, A. Romani, G. Medoro, L. Altomare, A. Leonardi, M. Tartagni, and R. Guerrieri, "A CMOS chip for individual cell manipulation and detection," *Solid-State Circuits, IEEE J.*, vol. 38, no. 12, pp. 2297–2305, 2003.

[92]   C. P. Jen and H. H. Chang, "Handheld device for the enrichment of rare cells utilising dielectrophoresis in stepping electric fields," *Micro Nano Lett. IET*, vol. 6, no. 4, pp. 201–204, 2011.

[93]   W. Qiao, G. Cho, and Y.-H. Lo, "Wirelessly powered microfluidic dielectrophoresis devices using printable RF circuits," *Lab Chip*, vol. 11, no. 6, p. 1074, Feb. 2011.

[94]   R. D. Das, S. Dey, and C. Roychaudhuri, "Functionalised Silicon Microchannel Immunosensor With Portable Electronic Readout for Bacteria Detection in Blood," no. Ferro 53120.

[95]   N. Samanta, O. Kundu, and C. R. Chaudhuri, "A Simple Low Power Electronic Readout for Rapid Bacteria Detection With Impedance Biosensor," *IEEE Sens. J.*, vol. 13, no. 12, pp. 4716–4724, Dec. 2013.

CHAPTER 2. THE DIELECTROPHORETIC EFFECT. INTRODUCTION AND PRELIMINARY STUDIES.

Herein dielectrophoretic effect is examined in terms of trapping efficiency. For this purpose, an electronic device and a classical microfluidic configuration were designed and tested. The setup was used under different conditions generating exhaustive statistics for different DEP configurations.

The first challenge when developing a device for a particular application in any engineering work is to define its requirements and specifications. A standard electronic equipment for DEP-based manipulation of certain types of pathogens such as bacteria needs a preliminary study to define some electrical properties, such as the operating power needed or the useful frequency range. In this case a double approach has been followed. First, we have checked previous theoretical studies, based on simulations, by reviewing pre-existing literature. Then, we experimented under controlled conditions different configurations with a more open-concept equipment.

In a first attempt to define the DEP device, was proposed a multiple-purpose electronic device. It was designed bearing in mind its usage for a range of applications such as bacteria separation or trapping, for diagnostic purposes, or viable and non-viable yeasts and blood cells manipulation. A quadrature signal circuit was needed in the DEP generator in order to be able to combine counter-phased signals as explained later. This approach would provide higher manipulation abilities in case of using other cells in the future and keeping a broader scope than the proof of concept tests done in the frame of this thesis.

In order to define the needs of the system to be designed, studies were done considering the potential analysed sample conductivities and frequency ranges as described in previous works available in the scientific literature. In Table 2.1 a summary of articles where blood cells have been manipulated is shown.

The suspension medium conductivities and the frequencies used, are also included in Table 2.1. These values were used in order to establish the device working ranges of interest.

The same process was followed to characterize potential working ranges when other cells such as bacteria should be manipulated. Thus, a study of regular DEP bacteria manipulation conditions was performed. A summary

of some publications on bacterial manipulation and its relative electrical experimental conditions is depicted in Table 2.2.

Table 2.1. Summary of the characteristics, as found in literature, of previously manipulated cells by means of DEP, and of their suspension medium.

Manipulated cell	Medium Conductivity (mS/m)	DEP Frequency (kHz)	Ref
Human MDA231 cells (breast cancer)	56	80	[1]
Human T lymphocytes	56	320	[1]
Human Erythrocytes	56	450	[1]
Human MDA231 cells	10	15	[1]
Human T lymphocytes	10	58	[1]
Human Erythrocytes	10	95	[1]
Human HL60 cells	56	180	[2]
Human T lymphocytes	56	320	[2]
Human Erythrocytes	56	490	[2]
Granulocytes	10	40-45	[3]
T-lymphocytes	10	60-65	[3]
Monocytes	10	25-30	[3]

Table 2.2. Summary of publications related to DEP-based bacteria manipulations and the tested experimental electrical conditions.

Concentrated bacteria	Sample conductivity (S/m)	DEP signal applied (Hz)	Ref
Escherichia coli	1.59	100k	[4]
Escherichia coli	$10^{-4}-1$	1k	[5]
Staphylococcus aureus Pseudomonas aeruginosa	0.1	100k to 1.2M	[6]
Escherichia coli	$2 \cdot 10^{-4} - 5 \cdot 10^{-4}$	300k	[7]
Escherichia coli	$8.6 \cdot 10^{-3} - 1.2$	100k	[8]
Bacillus atrophaeus	$3 \cdot 10^{-4} - 284 \cdot 10^{-3}$	1k -60 M	[9]

Considering the previous ranges, in a first attempt to define a proof-of-concept prototype, a possible sample conductivity range from 0,02 to 2 S/m

was set. As was stated in the previous chapter, DEP is high dependent on media and particle conductivity. A successful DEP manipulation will depend in fact of the well managing of sample conductivities. From the electronic point of view, a certain solution conductivity, where a current is applied, could be translated into an electrical circuit with an equivalent impedance. This, becomes in fact one of the main components of the load of the electronic system. In a first approach, a device able to manage a wide range of conductivities, ensuring signal stability for all of them, was proposed.

In order to accomplish this objective, initial calculations were made considering a 20 μm x 20 μm electrodes with a 20 μm separation to each other, immersed in a medium where conductivity values could vary from 0,02 S/m to 1,66 S/m. These conditions were extrapolated for what we estimated to be the most restrictive case in which our system would be applied. These physical properties were then translated into an estimate of the electrical resistance:

$$R = \frac{\rho \cdot l}{A}$$
(Eq. 13)

, where ρ is the specific resistivity in $\Omega \cdot$cm, l is the distance between elèctrodes in cm, and A is the area of the elèctrodes in $cm^{2.}$. The specific resistivity was estimated from its specific conductivity (mho.cm^{-1} o S$\cdot$cm^{-1}).

The Table 2.3 below shows the relation between media conductivity and the resultant theoretical load obtained from computing Equations 1 and 2.

Table 2.3. Theoretical expected load

Conductivity [S/m]	Load [Ω]
0,02	$2,50 \cdot 10^6$
0,24	$2,08 \cdot 10^5$
0,5	$1,0 \cdot 10^5$
0,72	$6,94 \cdot 10^4$
1	$5,0 \cdot 10^4$
1,24	$4,03 \cdot 10^4$
1,5	$3,33 \cdot 10^4$
1,74	$2,87 \cdot 10^4$
2	$2,50 \cdot 10^4$

Moreover, from the analysis of literature, we explored other issues that could affect to DEP system also [10], [11]. In an electronic sinusoidal generation often the DC- offset diminution is a challenge, but for electrodes maintenance and cells this is a big issue. Two topics have been reported related electrodes and cells under a DC field. One of them is the Joule effect, which consequent temperature variation can destroy cells, such as mammalian cells that a >4ºC variation causes them death. The other one is related to the high voltage used to generate the electric field. This voltage can destroy the cells due to the number of free radicals generated by the thermal decomposition and electrolysis of the metal electrode. Also, the electrode is damaged in the process. Then we realized that a huge improvement for any electronic system based in DEP would be to provide high voltage signals without any DC residual signal. A counter-phases generator could be a feasible solution. According to these limits, the following system was proposed, designed and tested.

2.2 DEP generator design and validation

The system was mainly composed of three parts (Figure 2.1.A-C) The first one, Control Signal Generator, which generates four signals by means of an oscillator circuit so as to give a stable frequency to the DEP Generator stage.

The second part, the driver module, which adequate the power level of the control signals to be injected into the DEP Generator. And a Class E amplifier which is the responsible of the DEP signal creation according to the control signal generator.

The generator block (Figure 2.1.A) was based on the LTC6902 from Linear Technologies Company. This circuit generates synchronized quadrature square signals (0º,90º,180º,270º) that allowed to control the generation frequency of the DEP Generator. LTC6902 general features are shown in Table 2.4.

Table 2.4 LTC6902 Features

Supply Voltage (V+) to GND	-0.3V to 6V
Operating temperature range	-40ºC to 85ºC
Frequency Range	5kHz to 20MHz
Frequency Error (TA = 0°C to 70°C)	<= 2% Max
Typical Supply Current, Vs = 3V, 1MHz	400µA
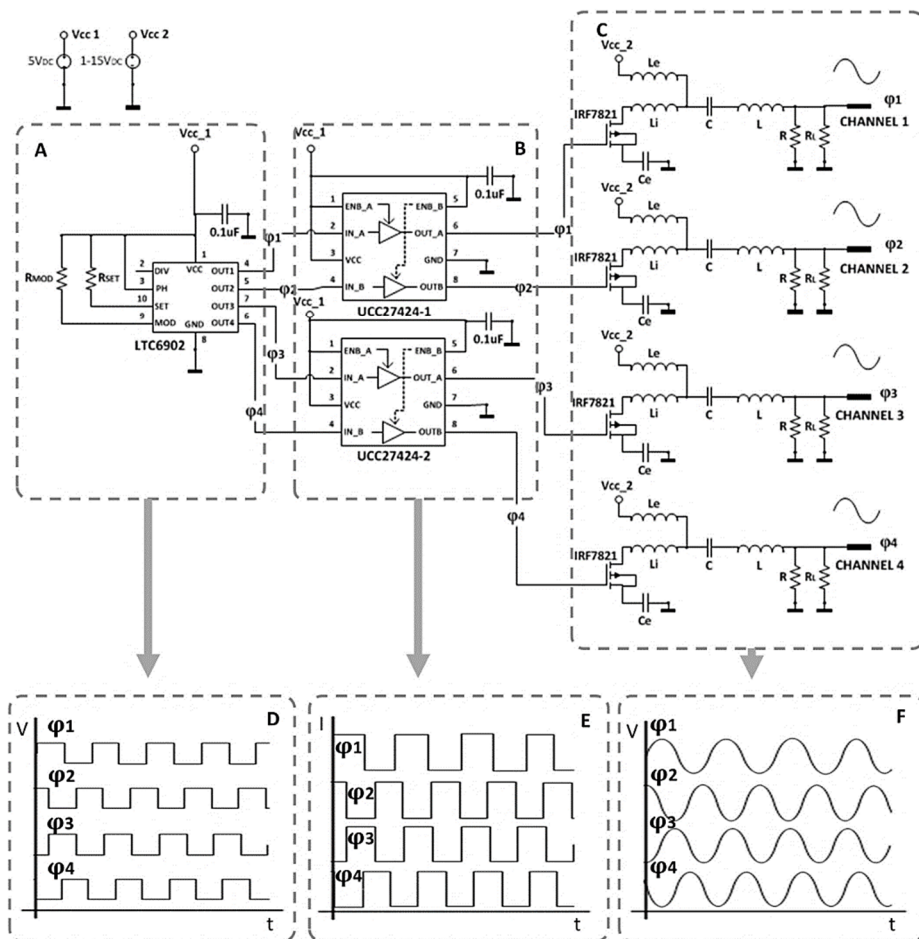
Figure 2.1.A general block diagram of DEP system

The LTC6902 frequency operation could be tuned by the following equation.

$$f_{out} = \frac{10MHz}{N \cdot M} \left(\frac{20k\Omega}{R_{set}} \right)$$
(Eq. 14)

Where M is related to the number of phases that are expected at the output (M=4), and N is selected following manufacturer directives, by knowing the frequency range used (Table 2.5).

The LTC6902 was designed for low power electronics and its outputs are limited to 400uA. As a power structure is used to create DEP signals, a power driver is needed between these modules.

Table 2.5 Relation between n value and the frequency range from LTC6902 datasheet.

N	Frequency range
N =1	2MHz to 20MHz
N= 10	200kHz to 2MHz
N= 100	< 200kHz

For this purpose the UCC27424 driver (Figure 2.1.B) is used, which boosts high frequency signals and provides enough output current level (up to 4A) to drive the DEP generator module. Its general properties are shown in the following Table 2.6.

Table 2.6 Driver features

Driver Configuration	Non-Inverting
Supply Voltage	4 -15V
Peak Output Current	4 A
Rise Time	20 ns
Fall Time	15 ns
Prop Delay	30 ns
Input Threshold	CMOS
Operating Temperature Range	-40 to 105ºC

Then, a stable sinusoidal generator module was needed. This was defined to be capable to drive a high number of electrodes or electrode arrays. Some commercial generators could be considered to feed DEP electrodes, but most of them are not prepared to work under high power and high frequency conditions or they have an elevated cost.

We found a low cost solution so as to implement the DEP generator. A Class E Amplifier [1-2] was used for this purpose, since is capable to generate stable high frequencies, with especially low offset level, to drive huge loads. Its principle is based on a resonant LC system and the basic structure is depicted in Figure 2.2. The design was defined following the expressions (15)-(18). Where ω_s is the operating frequency and Q is the expected quality factor of the amplifier.

$$L_e = \frac{0,4001R}{\omega_s} \quad \text{(Eq.15)}$$

$$C_e = \frac{2,165}{R\omega_s} \quad \text{(Eq.16)}$$

$$L = \frac{QR}{\omega_s} \quad \text{(Eq.17)}$$

$$\omega_s L = \frac{1}{C\omega_s} = 0,3533\imath \quad \text{(Eq.18)}$$
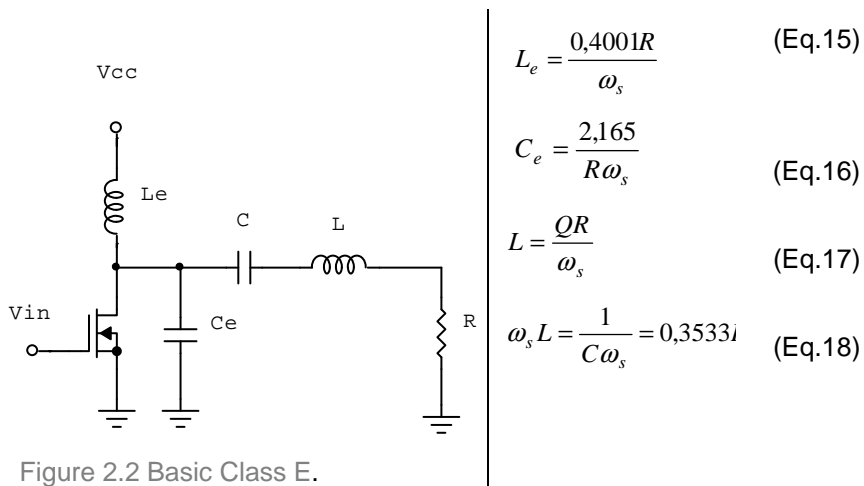
Figure 2.2 Basic Class E.

However, the original class E amplifier is time dependent on the load. As load variation is a common phenomenon inside microfluidic chip when cells are flowing inside it, a study of load variability with signal stability relation was done. As a matter of fact, a cell through a microfluidic channel could be approached to an instant power demand from the point of view of the electrodes. To ensure system viability, some simulations were carried out. A controlled switch system introduces a load variation to the basic class E in a determined period of time; this can be equivalent to a cell crossing the

50

electrodes with a certain size or to a certain flow rate of cells. Selecting a high variance (around 25%) in a short time (simulating a tiny cell or a rapid flow rate) the Figure 2.3 is obtained.

As the figure shows, instant load variations affect the system response, since the system tries to deliver the necessary instant power. In order to reduce this effect the circuit modification was applied (Figure 2.1.C).The use of R parallel manage the output voltage stability at the expense of system efficiency, but reducing the load dependence, which permits to introduce a group of cells or different flow rates without significant problems.

The Figure 2.4 shows the modified Class E simulation. In this case the system stability depends on R parallel and the load impedance can vary without be affected by the generated signal. Also, the introduction of inductive element Li helps to reduce the global consumption of the system, because the instant power demand at MOSFET conmutation is also smoothed.
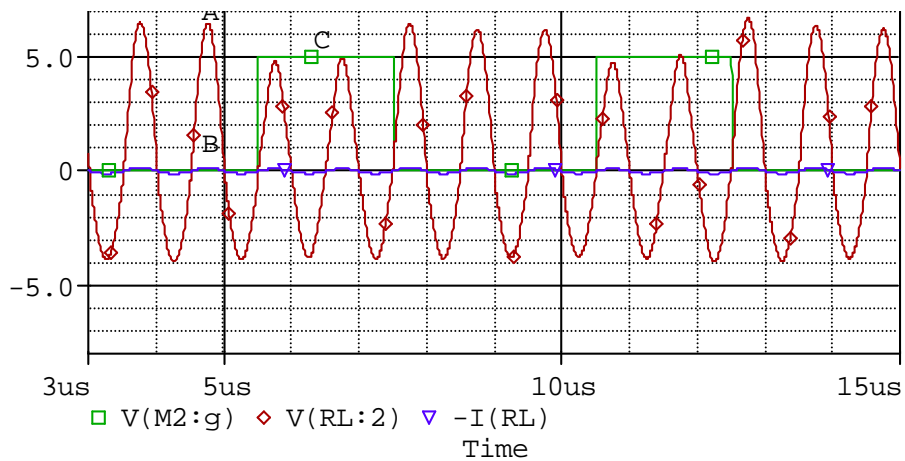
Figure 2.3 Simulation of the possible load variation; where A is the load voltage, B is the load current and C is the time of the variation load introduced.

With this configuration and for 1,66S/m of medium conductivity, an estimation of the maximum number of electrodes allowed to be connected is obtained.
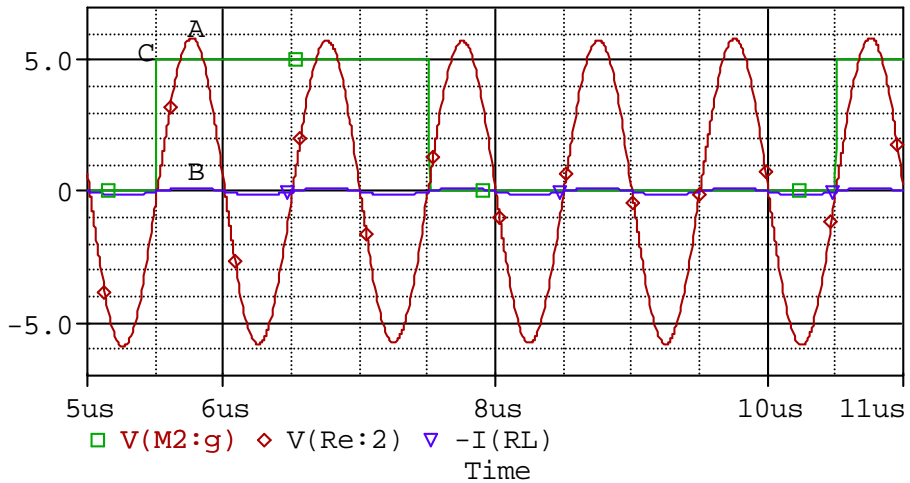
Figure 2.4 Simulation of the possible variation in the modified class E; where A is the load voltage, B is the load current and C is the time of the variation load introduced (25%).

Table 2.7 General DEP system features

Vsupply	$10V_{DC}$
Mínimun allowable load	> 1 kΩ
Maximum number of electrodes per channel (With a 1,66S/m conductivity)	25 elèctrodes
Working frequency	1MHz
Vout range (peak voltage)	1V- (V_{DC}-0.5) V
Maximum current capability	1A

Additionally, general system features are shown in Table 2.7.

Real DEP generated signals are captured and could be observed in the following Figure 2.5. As it could be guessed in the previous features table, the final circuit was finally designed for a single frequency (1 MHz). This value was selected following literature and according to the future application. Many cells could be clearly manipulated at 1MHz, but especially bacterium Escherichia Coli.

52
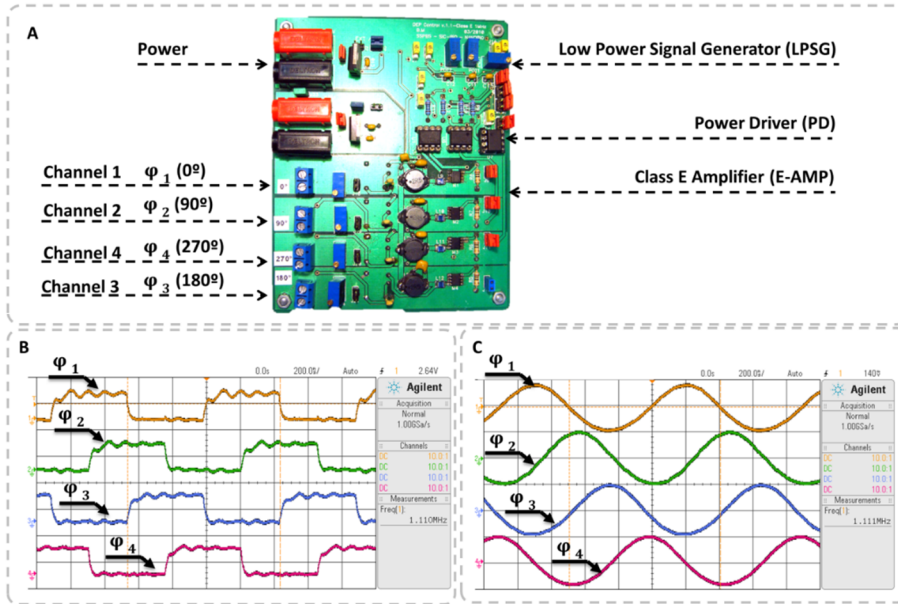
Figure 2.5 A: Custom electronic device. Final board dimensions: 100 x 120mm. B and C: Experimental signals from the designed device. B: The outputs from module a, the low power signal generator. C: the DEP signals generated by module c, the class E amplifier.

E. coli is a member of the family Enterobacteri-aceae located in the human intestine and in warm-blooded animals [14]. Many *E. coli* strains are in the humans pathogenic and produce infections or gastrointestinal diseases [15]. Usually by contact with bacteria through water or food, due to an unsanitary treatment [16]. To treat *E. coli* by means of DEP it is necessary to approach the electric model of the pathogen to the DEP formulas. Usually, *E. coli* shape is approached to an ellipsoid with two dielectric layers, then adapted Clausius – Mosotti factor from DEP equation is changed as follows [17], [18]:

$$F_{CM_i}(\omega) = 1 \Big/ \left(2 \bullet \left(\varepsilon_p^* - \varepsilon_m^* \Big/ \varepsilon_m^* + A_i \big(\varepsilon_p^* - \varepsilon_m^* \big) \right) \right) \qquad \text{(Eq. 19)}$$

where εp is the particle permittivity and Ai is the depolarization factor of an individual ellipsoid axe (i =x,y,z), which for the large axis is

$$A_x = \frac{1-e^2}{2e^3} \log\left(1 + \frac{e}{(1-e)-2e}\right) \qquad \text{(Eq. 20)}$$

where e is the eccentricity that involves the ellipsoid dimensions (b being the height and a the width),

$$e = \sqrt{1 - \left(\frac{b}{a}\right)^2} \qquad \text{(Eq. 21)}$$

Moreover, the depolarization factor for the shorter axis is

$$A_z = A_y = \frac{1-A_x}{2} \qquad \text{(Eq. 22)}$$

$\varepsilon_m/\varepsilon_0$	9.8
$\varepsilon_w/\varepsilon_0$	78
$\varepsilon_c/\varepsilon_0$	49.8
σ_m	$259 \cdot 10^{-6}$ S/m
σ_w	$58 \cdot 10^{-3}$ S/m
σ_c	0,48 S/m
d_w	8 nm
d_m	50 nm
a	3/2 μm
b	a/2 μm
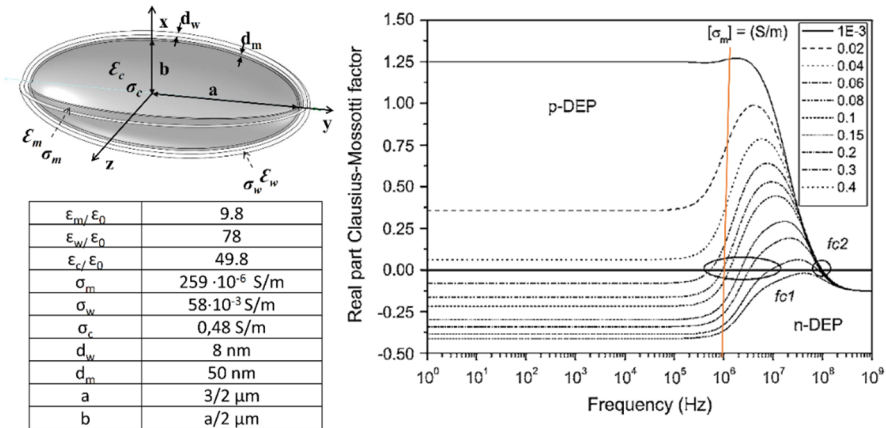
Figure 2.6. Electrical model of *E. coli* and FCM representation in a huge range of conductivities (Reproduced from M. Castellarnau et al publication)

Thus, the expression (19) could be represented according bacteria electrical properties, as it was reported in previous group publications [19] and was here reproduced in **¡Error! No se encuentra el origen de la referencia.**. Where is clearly discovered that *E. coli* could be manipulated from 500 kHz to 10 MHz, but the maximum difference between nDEP and pDEP is around 1MHz.

2.2 Microfluidic device design and fabrication

To apply DEP to manipulate *E. coli* a microfluidic device was designed. A single-PDMS channel with interdigitated electrodes was chosen for this first trial[20]. The DEP Force distribution for a small section of the chip was simulated using COMSOL Multiphysics and obtained results are depicted in Figure 2.7. The trapping of *E. coli* was expected to be close to the surface of the electrode, as higher DEP forces and electric field maxima were obtained there. This would depend also of dynamic properties, since higher flow rates would play against DEP force. Thus, some experiments had to be done to trade-off both forces.
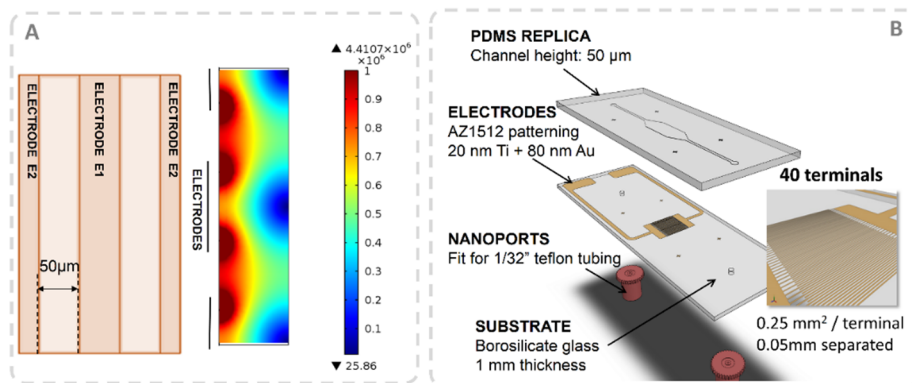
Figure 2.7 Microfluidic chip design

The microfluidic chip fabrication can be divided into three main steps: microchannel moulding (a), electrode fabrication (b) and microfluidic chip bonding (c). Each process will be detailed as follows.

a) Microchannel Molding: The SU8 50 microchannels moulds were fabricated over glass slides. First, the slides were cleaned and activated by a Piranha attack during 15 minutes. Then, a 50 µm high SU-8 50 was spun over glass slides. Once developed, the microchannel mold was obtained. Soon after, the microchannel was replicated by mixing, degaussing and

pouring a 10:1 ratio PDMS pre-polymeric solution in the mould. Finally, after a 70ºC at 1h curing process, the cast PDMS was peeled off from the master.

b) Electrode Fabrication: In order to fabricate the microelectrodes a lift-off soft lithography process was applied. First, an initial Piranha chemical attack was used. The AZ 1512 photoresist was chosen to act as a sacrificial layer. After exposure and first development of the AZ 1512, two metal layers, formed by 20 nm of Ti and 80 nm of gold, were vapor-deposited onto the surface. Then, the electrodes were obtained by removing the AZ photoresist.

c) Microfluidic chip bonding: In order to seal the microfluidic chip, the electrode surface was cleaned by using an oxygen plasma process. Then, the PDMS microchannels were aligned and attached by contact to the electrodes slide. Later, one cable was welded to each pad by conductive silver paint. Finally, an epoxy glue mix was also applied to the weld and cured at room temperature for 60 minutes. Eventually, two Nanoport Assemblies were attached to the inlet and outlet connections of the chip

2.3 Experimental and Results

A series of bacteria concentration tests were performed to analyse the DEP effects by applying a different phase signal combination. The experimental setup was carefully defined so as to supervise each flow injection to the microfluidic chip. The final setup is shown in Figure 2.8.A.

The complete fluidic module was composed of a 6 port manual valve (Valco), connected to a 5 mL syringe mounted in an infusion micropump (Cetoni NEMESYS). This syringe was connected to the microfluidic chip. Moreover, this was placed over an inverted microscope stage (Olympus IX71) with a digital camera (Hamamatsu Orca R2). The microfluidic chip electrodes were activated by the DEP multiphase generator previously described powered by an Agilent E3631A power source.

After, experimental protocol was determined. Three fractions were collected for each experiment (Figure 2.8.B): the original fraction (f1), the control fraction (f2), bacteria which escaped from the electric field – non-trapped bacteria - (f3). The fractions f2 and f3 were obtained after introducing 150 µL of *E. coli* sample (50 µL of original sample diluted in 100 µL of deionized water during the experimental process).
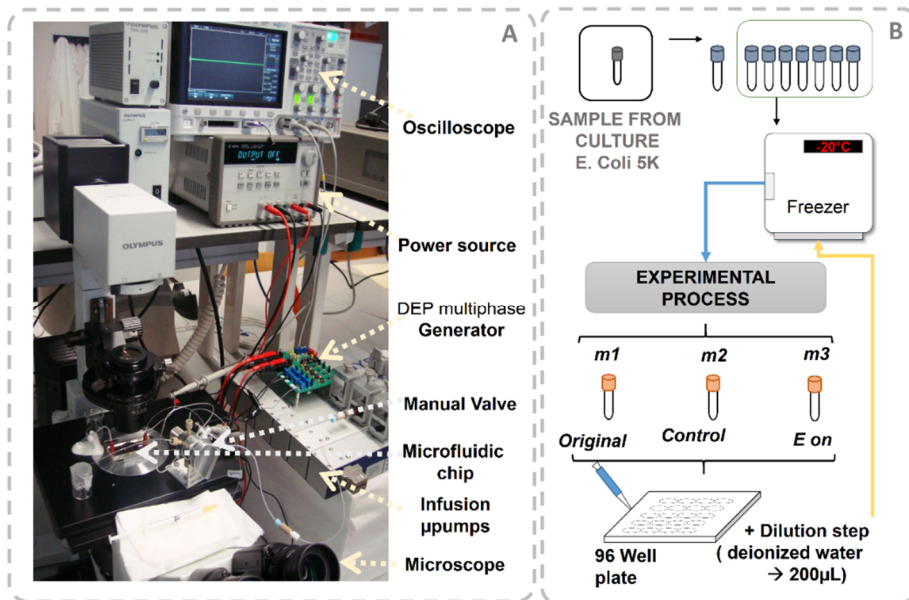
Figure 2.8 Experimental setup and graphical overview of experimental process

Then, samples were acquired following profusely the protocol from Table 2.8.

Each fraction was collected at a constant 5 µL/min flow rate by continuous deionized water pumping. Each 150 µL fraction was diluted again until reaching 200 µL, owing to the cytometer specifications, and immediately frozen to -20 °C. Once the fractions were defrosted, a flow cytometry (Beckman Coulter FC 500) bacteria counting process was applied. In order to improve the analysis accuracy, 1 µL of Green Fluorescent Nucleic Acid

Stain (Invitrogen SYTO 13) was added to each 200 µL fraction. Thus, real trapped *E. coli* could be counted as well as non-trapped.

Table 2.8 Experimental protocol

FIRST FRACTION *(Control)*			
#	µL	Step	time
1	-	The voltage applied is selected	3'
2	0	The content of the syringe is injected through the loop	3'
3	47.7	Sample arrives to the outlet. The first fraction is started to be collected	13'
4	97.7	The sample is completely out. The collection is finished	23'
5	-	Dilution, mixing and freezing of the simple in small ependorf.	-
6	100	Sample 2 is prepared	24'
SECOND FRACTION *(E on)*			
#	µL	Paso	time
7	0	Sample 2 is injected through the loop	24'
8	27.17	Sample arrives to the start point of the chamber. Selected electric field is activated.	31'
9	47.7	Sample arrives to the outlet. Second fraction is started to be collected	34'
10	97.7	The sample has completely passed through the channel. Collection is finished	44'
11	-	Dilution, mixing and freezing of the simple in small ependorf.	-
THIRD FRACTION *(Release)*			
#	µL	Step	time
12	147.7	The electric field is deactivated.	54'
13	163.43	The remaining bacteria arrive to the channel outlet. Last fraction is started to be collected	57'
14	213.43	50 µL are collected. Collection time finished.	67'
15	-	Dilution, mixing and freezing of the simple in small ependorf.	-
CLEANING PROCESS			
#	µL	Paso	time
16	0	Flow rate is incremented so as to drag the remaining bacteria inside the chip, with a cleaning solution based on Sodium dodecyl sulfate (SDS).	68'
17	300	Cleaning process finished	**69'**
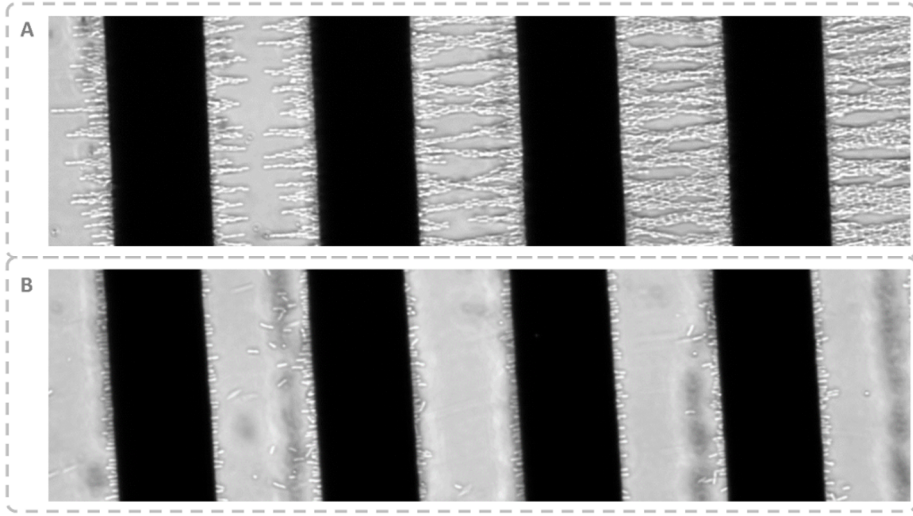
Figure 2.9. Trapped and released bacteria

However, we should point out that a small amount of bacteria was lost during the process due to the strong cell adherence to the electrodes in some cases. These could be observed in Figure 2.9, in A, electric field was activated and bacteria chains were growing further. In B, electric field was later deactivated and some bacteria were still remaining inside the chip. This effect was reduced in successive experimental tests by controlling the sample defrosting time and the cells condition at the moment of trapping, indicating that this process, and cell viability, influenced also the undesired attachment of debris and some cells to the electrodes.

As was mentioned before, there are different phase combinations to be applied so as to manipulate *E. coli*. In fact, different diphased signals could result different effective voltages inside the microfluidic chip. For instance, when two counter-phase signals (with the same ground reference) are applied to the electrodes, the effective applied voltage to the chip (VT) is defined by the following equation:

$$V_T = \left[V_m^{\varphi 1} \sin(\omega t) + V_{01} \right] - \left[-V_m^{\varphi 3} \sin(\omega t) + V_{03} \right] \qquad \text{(Eq. 23)}$$

where $V_m^{\varphi X}$ is the amplitude peak voltage of the signal, and V_{01} and V_{03} are the offset voltages. Moreover, if the two peak amplitude voltages are equal,

$$V_m{}^{\varphi 1} = V_m{}^{\varphi 3} = V_m \qquad\qquad\qquad\qquad\text{(Eq. 24)}$$

and the resultant effective applied voltage signal is

$$V_T = 2[V_m \sin(\omega t)] + (V_{01} - V_{03}) \qquad\qquad\text{(Eq. 25)}$$

According to the expression (25), the effective voltage VT is doubled and the average resultant offset ($V_0 = V_{01} - V_{03}$) can be considered almost null. Thus, different phase combinations were defined to test the effect of manipulating by different phase combinations. The expected effective voltage in each case is in Table 2.9 represented.

Two signals from the device channels were applied to the pair of interdigitated electrodes, creating different phase combinations which generate the same DEP effect. Each applied voltage was determined by equalizing the resultant potential of each pair of applied signals (V_{RMS}) to Case 1 (see Table 1). Hence, cases 1, 2, 3 and 4, it was expected to obtain similar effects since all of them had equivalent applied fields. Then, six repetitions of each Case were done to obtain statistics of concentration efficiency.

Table 2.9 Experimental Cases

Experimental Case	Applied signals	Resultant potential V_{RMS}	Applied voltage $V_{pp} = 2V_m$	Case 1 Equivalent voltage
Case 1- **Single Phase** (reference)	E1: φ_1= 0⁰ E 2: GND	$V_m/\sqrt{2}$	10Vpp	--
Case 2 **90⁰diphase**	E1: φ_1= 0⁰ E2: φ_2= 90	V_m	7Vpp	10Vpp
Case 3 **270⁰diphase**	E1: φ_1= 0⁰ E2: φ_4= 270⁰	V_m	7Vpp	10Vpp
Case 4 **180⁰diphase**	E1: φ_1= 0⁰ E2: φ_3= 180⁰	$\sqrt{2}V_m$	5Vpp	10Vpp

Vm=maximum applied voltage. E1, E2= electrode 1 and 2.

Experimental results could be observed in Figure 2.10. The median and the quartiles of each sample group (Cases) are presented in order to give a visual representation of the sample group distribution.

To report a statistical analysis, the obtained bacteria counts were introduced in SPSS Statistics Software (IBM). Since the obtained counts are independent samples, a non-parametric test was done in order to analyze the obtained results. Thus a U-Mann Whitney test was carried out, where equivalent effective-voltage Cases (Case 1, 2, 3 and 4) were analyzed in pairs. Then, no significant differences were obtained for these Cases. Moreover, these Cases were compared with the double voltage Case (Case 5). Case 5 was defined to verify if counter-phase signals could be the best option for concentration purposes, since it was expected to obtain better results with the same Vm per channel (max mum voltage) applied as in Case 1 and with the double voltage as compared with Case 4.

Table 2.10. Final experimental case

Experimental Case	Applied signals	Resultant potential V_{RMS}	Applied voltage $V_{pp} = 2V_m$	Case 1 Equivalent voltage
Case 5 180⁰diphase	E1: $\varphi_1=$ 0⁰ E2: $\varphi_3=$ 180⁰	$\sqrt{2}V_m$	10Vpp	20Vpp

In this test significant differences between samples were detected (p<0.01), since Case 5 presents a higher trapping efficiency due to its equivalent applied voltage of 20 Vpp.

Moreover, as was predicted in equation (25) DC offset must be almost null (section 1.2.1). Following this hypothesis, better results for Case 5 are also related to this fact.
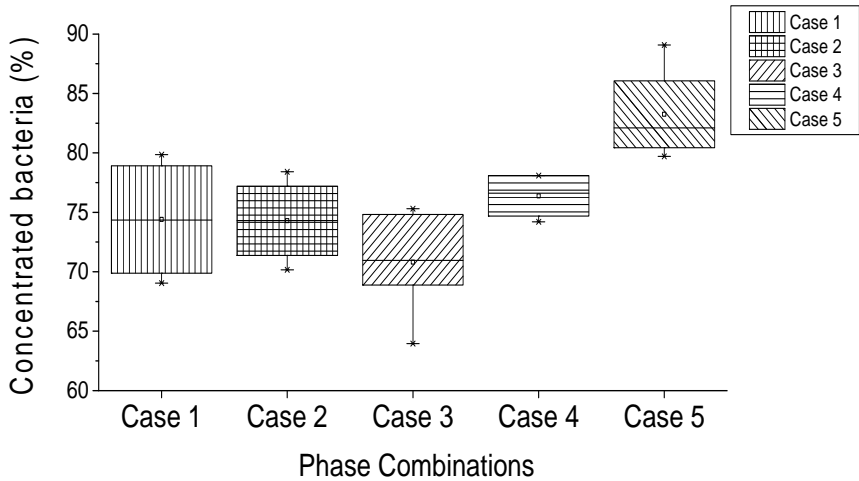
Figure 2.10 Counting of trapped bacteria ((f2-f3)/f2) relative to control sample

The experimental DC given by the designed generator, was measured and is around 30 mV in each device output. Since the culture of *E. coli* samples are variable the cancellation of this small obtained DC offset was difficult to be quantified by means of bacteria counts. Hence, an additional experiment was done to reproduce the DC effect and so, observe the effects inside the microfluidic chip. At one of the interdigitated electrodes, a 5 Vpp sinusoidal signal was applied by using our DEP generator. On the other, a DC signal coming from an external generator (2400 Keithley) was being progressively increased until some effect was detected. As observed, the microfluidic device is so sensible for offsets greater than 3V DC, where electrolysis could be physically observed (Figure 2.11. A). At this point, the electrode starts to boil and the air bubbles repel bacteria from the electrode. This effect clearly impedes a correct DEP concentration. Furthermore, when higher DC levels are applied (> 4 V) to the electrodes, the microfluidic chip fills up with air blocking the continuous flow and the electrode gets damaged (Figure 2.11. B).
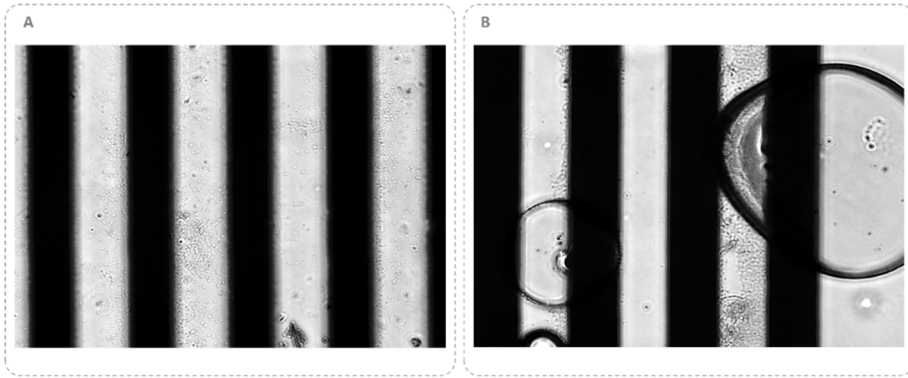
Figure 2.11. DC offset effects. A. DC effect when Voffset is 3V. B. DC effect when Voffset is 4V

2.4 Chapter conclusions

A first device for manipulating cells by DEP methods was designed. The solution is a versatile system which generates 4 sinusoidal signals, stable in frequency at 1MHz and with a maximum output voltage of 15Vpp and a maximum current of 1A. The device has been validated for concentration purposes. In this chapter, a microfluidic chip based on an interdigitated electrode and a single microfluidic cannel was used. With both equipment and microfluidic chip different experiments were carried out to concentrate *E. coli*. The experiments were done at different phase combinations, with equivalent DEP effects, so as to test the electronic device and to to prove that the phase combination could give benefits to the overall system. From the analysis of these experiments, a median 75% of concentration efficiency was obtained. Nevertheless, for counter-phased signals, the trapping efficiency increased to 83% when the applied voltage was doubled, also reducing the offset levels applied.

References

[1]   F. F. Becker, X. B. Wang, Y. Huang, R. Pethig, J. Vykoukal, and P. R. Gascoyne, "Separation of human breast cancer cells from blood by differential dielectric affinity.," *Proc. Natl. Acad. Sci.*, vol. 92, no. 3, pp. 860–864, Jan. 1995.

[2]   F. F. Becker, X.-B. Wang, Y. Huang, R. Pethig, J. Vykoukal, and P. R. C. Gascoyne, "The removal of human leukaemia cells from blood using interdigitated microelectrodes," *J. Phys. D. Appl. Phys.*, vol. 27, no. 12, pp. 2659–2662, Dec. 1994.

[3]   X.-B. Wang, J. Yang, Y. Huang, J. Vykoukal, F. F. Becker, and P. R. C. Gascoyne, "Cell Separation by Dielectrophoretic Field-flow-fractionation," *Anal. Chem.*, vol. 72, no. 4, pp. 832–839, Feb. 2000.

[4]   S. Park, Y. Zhang, T.-H. Wang, and S. Yang, "Continuous dielectrophoretic bacterial separation and concentration from physiological media of high conductivity.," *Lab Chip*, vol. 11, no. 17, pp. 2893–2900, Sep. 2011.

[5]   Y. Inoue, R. Obara, M. Nakano, and J. Suehiro, "Concentration of bacteria in high conductive medium using negative dielectrophoresis," in *2015 IEEE International Conference on Industrial Technology (ICIT)*, 2015, pp. 3336–3340.

[6]   I.-F. Cheng, T.-Y. Chen, R.-J. Lu, and H.-W. Wu, "Rapid identification of bacteria utilizing amplified dielectrophoretic force-assisted nanoparticle-induced surface-enhanced Raman spectroscopy.," *Nanoscale Res. Lett.*, vol. 9, no. 1, p. 324, Jan. 2014.

[7]   Y.-K. Cho, S. Kim, K. Lee, C. Park, J.-G. Lee, and C. Ko, "Bacteria concentration using a membrane type insulator-based dielectrophoresis in a plastic chip.," *Electrophoresis*, vol. 30, no. 18, pp. 3153–9, Sep. 2009.

[8]   M. Kim, T. Jung, Y. Kim, C. Lee, K. Woo, J. H. Seol, and S. Yang,

"A microfluidic device for label-free detection of Escherichia coli in drinking water using positive dielectrophoretic focusing, capturing, and impedance measurement.," *Biosens. Bioelectron.*, vol. 74, pp. 1011–1015, Jul. 2015.

[9]   H. O. Fatoyinbo, M. C. McDonnell, and M. P. Hughes, "Dielectrophoretic sample preparation for environmental monitoring of microorganisms: Soil particle removal.," *Biomicrofluidics*, vol. 8, no. 4, p. 044115, Jul. 2014.

[10]   D. Morganti and H. Morgan, "Characterization of non-spherical polymer particles by combined electrorotation and electroorientation," *Colloids Surfaces A Physicochem. Eng. Asp.*, vol. 376, no. 1, pp. 67–71, 2011.

[11]   Y. Kang, B. Cetin, Z. Wu, and D. Li, "Continuous particle separation with localized AC-dielectrophoresis using embedded electrodes and an insulating hurdle," *Electrochim. Acta*, vol. 54, no. 6, pp. 1715–1720, 2009.

[12]   B. Lenaerts and R. Puers, *Omnidirectional inductive powering for biomedical implants*. Springer, 2009.

[13]   M. H. Rashid, M. H. R. V González, and P. A. S. Fernández, *Electrónica de potencia: Circuitos, dispositivos y aplicaciones*. Pearson Educación, 2004.

[14]   W. H. Ewing, *Edwards and Ewing's identification of Enterobacteriaceae*. Elsevier Science Publishing Co. Inc., 1986.

[15]   G. R. Gibson, G. T. Macfarlane, and others, *Human colonic bacteria: role in nutrition, physiology, and pathology.* CRC Press Inc., 1995.

[16]   P. Feng, "Escherichia coli serotype O157: H7: novel vehicles of infection and emergence of phenotypic variants.," *Emerg. Infect. Dis.*, vol. 1, no. 2, p. 47, 1995.

[17]   H. Morgan and N. G. Green, *AC electrokinetics: colloids and*

nanoparticles, no. 2. Research Studies Press, 2003.

[18]   T. B. Jones, "Basic theory of dielectrophoresis and electrorotation," *Eng. Med. Biol. Mag. IEEE*, vol. 22, no. 6, pp. 33–42, 2003.

[19]   M. Castellarnau, A. Errachid, C. Madrid, A. Juárez, and J. Samitier, "Dielectrophoresis as a tool to characterize and differentiate isogenic mutants of Escherichia coli," *Biophys. J.*, vol. 91, no. 10, pp. 3937–3945, 2006.

[20]   K. Khoshmanesh, S. Nahavandi, S. Baratchi, A. Mitchell, and K. Kalantar-zadeh, "Dielectrophoretic platforms for bio-microfluidic systems," *Biosens. Bioelectron.*, vol. 26, no. 5, pp. 1800–1814, 2011.

CHAPTER 3. IMPROVING THE CONCENTRATING CELL METHODS. INSULATED POLES BENEFITS IN DEP DEVICES.

A novel design to achieve improved electrokinetics in the microfluidic device was developed. The microdevice was improved by integrating insulating poles to selectively disturb the electrical field. The method expanded the cell trapping areas and increased their efficiency by generating a better spatial coverage of the LOC volume. Thus, by including the poles, higher trapping efficiencies were obtained and higher flow rates were achieved leading to reduced sample preparation times.

Previous results obtained with the classical design indicated a need to improve the system to achieve lower sample processing times and higher efficiencies. Thus, the combination of the specific DEP electronic board and microfluidic device would be useful in life sciences applications in terms of speed and reliance.

A classical challenge in microbiology studies is the purification and the pre-concentration of samples prior to analytical procedures such as cell disruption or polymerase chain reaction (PCR). These methods are not always able to be performed when the sample is scarce and classical methods are often not selective enough. Moreover, most of them require long time procedures. Furthermore, the possibility to miniaturize such procedures opens a new range of potential point-of-care applications in fields as diverse as food safety control or medical diagnosis. Consequently, we centred our attention into proving the applicability of our system to this analytical field. Following previous steps, our research work focussed on the concentration ability of the microfluidic chip when counter phased signals were used, since better results were being obtained at this point, and the improvement of the microfluidic device.

As literature exhibits, many microfluidic configurations have been used for concentration purposes. Some works used a large number of interdigitated metal electrodes placed in a microfluidic channel, as we have used in the previous chapter. However, we guessed these devices only generated DEP forces near the electrode, limiting their capabilities. To solve this issue, we investigated on the use of incorporating dielectric structures to the microfluidic channel. Insulator-based structures are capable to modify the electric field in the media so as to increase the effective trapping areas. Carbon structures have been previously used for this purpose [1], [2], although this is an expensive technology with complicated fabrication methods. Hence, we believe that isolating PDMS structures could be a better technology to be used in these applications, since it is a cheap technology with rapid fabrication procedures. Thus, we believe by means of PDMS pillar we could obtain increase the trapping possibilities of our

70

microfluidic chip. To verify this hypothesis some additional simulations and tests were executed with the current microfluidic chip and with the improved version, as it will be described below.

3.1 DEP microfluidic device based on interdigitated electrodes with a regular chamber.

First, some COMSOL simulations were run out to check and refine our hypothesis. A small differential portion of the current microfluidic chip (350 µm x 200 µm x 50 µm) was designed with the Solidworks CAD program, which represented the full microfluidic chamber by applying symmetry to the borders.

To simulate the DEP force in the chamber, the electrodes from the model were activated by two counter-phased signals at 15/√2VRMS and -15/√2VRMS and the bacteria shape and properties were introduced as global parameters so as to compute DEP expression. Then, a stationary analysis was performed. The results obtained are shown in Figure 3.1.
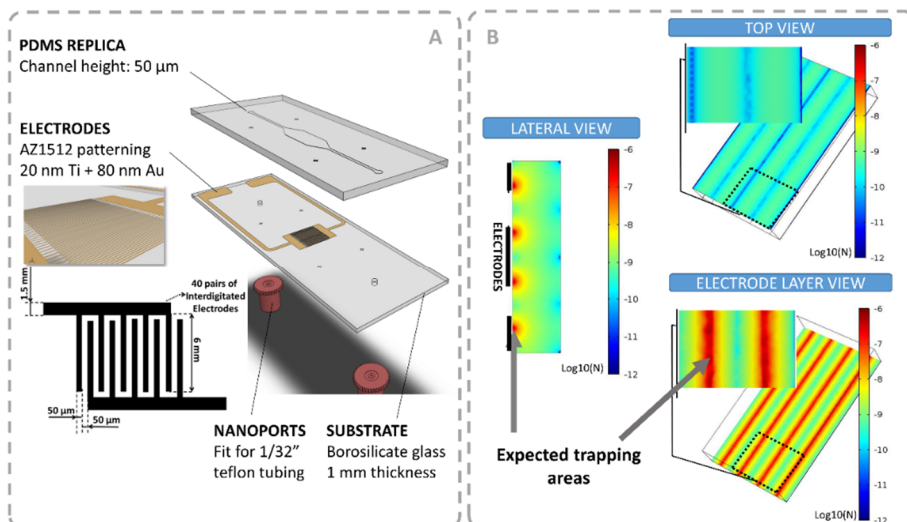
Figure 3.1.A. Interdigitated electrode with single chamber (previous design). B. COMSOL simulation of DEP force for the expected applied signal

As simulations showed, a trapping effect only in the immediate environment of the electrode was expected, since the electrical field was almost fully limited to this plane. Thus, when faster flows were used, the DEP force would be not enough to trap a valuable bacteria quantity, since no trapping effect occurred in higher sample flowing planes. Thus, the chip thickness wouldn't be exploited and a large amount of the sample analyte ignored.

3.1.1 Experimental and results

Then, even more statistical and a survival test were performed to verify the obtained simulation results. For this purpose, again *E. coli* 5K cells were used, which were treated in the same way as previous chapter experiments. In here, samples were diluted to achieve $4 \cdot 10^6$ cells/mL. The defined setup could be observed in Figure 3.2.
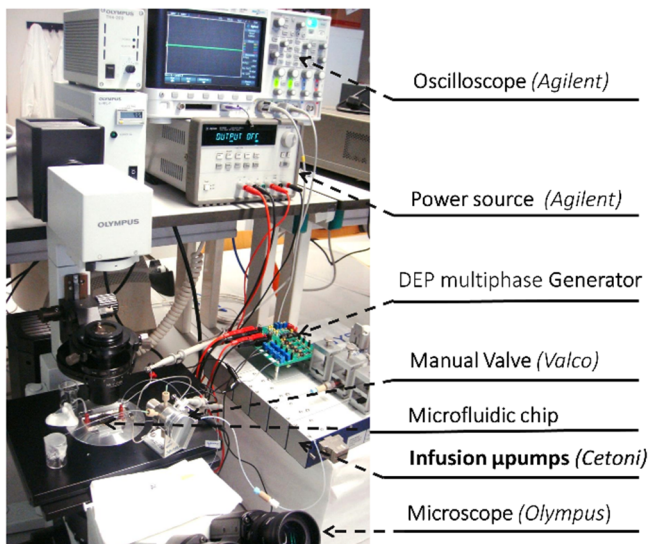
Figure 3.2. Experimental setup

Also, the experimental protocol quite differed from previous experiments: A 1 mL tube was defrosted and a first 50 µL pipetted sample (f1) was collected.

The remaining content of the 1 mL tube was introduced into the syringe, which was already connected to the valve so as to control sample injection through 50 µL loads. Next, a first load was injected into the chip at a continuous flow rate and without activating the electrical field. After this, the second fraction (f2) was collected at the outlet. Subsequently, a second load was injected at the same flow rate, merely preserving the electrical field activated. Meanwhile, the third fraction (f3) was collected. Finally, after switching off the field, the last sample was collected (f4), which was in fact the concentrated bacterial cells. Each fraction (150 µL of volume) was diluted again until reaching 200 µL, and immediately frozen at -20 °C.

 After fraction collection, the samples were defrosted, labelled with 1 µL of Green Fluorescent Nucleic Acid Stain (Invitrogen™ SYTO® 13), and counted by a cytometer (Beckman Coulter™ FC 500). During the electric field activation, electrodes were excited by two counter-phased signals of 15 Vpp each one by means of DEP board detailed in chapter 2.

A group of exhaustive cell count values was obtained from each single experiment. Then, we applied the following expression below to calculate the device trapping efficiency:

$$Trapping\ efficieny\ (\%) = \frac{f4}{f2} \bullet 100 \qquad\qquad (Eq.\ 26)$$

The obtained results are depicted in Figure 3.3, where our previous hypothesis were confirmed.

As expected, a high efficiency is obtained when the flow rate is low. However, the median efficiency is clearly dependent of the applied flow and decreases linearly at the same time that flow rate increased, which means DEP force is being overcome by the flow rate and no trapping effects is occurring further up from the electrode. Thus, this configuration will be recommended for small samples volumes, whose concentration time are not critical enough
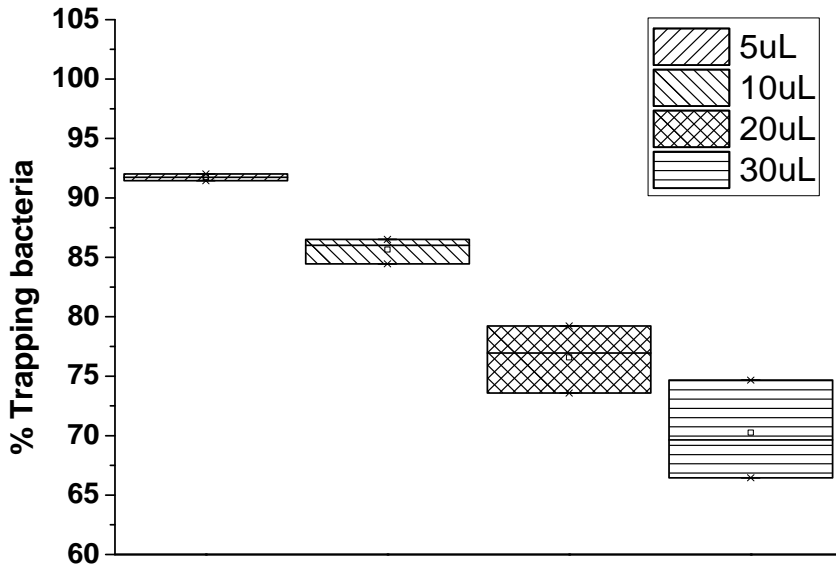
Figure 3.3. Results of trapping efficiency depending of the applied flow rate. Regular chamber case.

3.2 DEP microfluidic device trapping improvements.

In order to improve our results we look for designs which increment maximums of electric fields inside the chip. Thus, we could take profit of the current available space inside the channel filling it with trapped bacteria, since up to now only the electrode plane was storing bacteria. As stated before, in literature could be found some works based on conductive poles (3D electrodes) to improve electric field maximums distribution [1], [3], [4]. Currently, Carbon MEMS has been commonly employed for this function, which are obtained from subjecting organic structures to high temperatures (close to 900º). But due to this high temperatures, we realized carbon poles were complex to be fabricated and replicated. Also, doped silicon has been reported to be employed to make 3D electrodes. They were based on a thin doped silicon layer which included the microfluidic channel and the electrodes and which was introduced between glasses anodically bonded.

74

The creation of the doped-silicon-based microfluidic device required especially of an expensive infrastructure to make it feasible [5]. Equally well, insulating structures have been reported to be an efficient method to generate electrical field non-uniformities as an alternative, or a complement, to 3D electrodes. This techniques was named insulator-based dielectrophoresis (iDEP) [6] and it allows to generate convenient electrical field gradients without the need of integrating complex and more numerous electrodes. Also, it has been reported as an economic technique in terms of fabrication procedures [6].

Thus, we designed a microfluidic device based on dielectric poles, taking into account our infrastructure limitations. We included the dielectric poles to the chamber of the previous microfluidic chip based on interdigitated electrodes. Thus, by means of these structures, we aim to obtain higher flow rates without giving up high concentration efficiencies.

The accorded design was also COMSOL simulated, to corroborate their effects on the electric field applied and the expected DEP improvement. As stated before, an small differential of the microfluidic chip (350 µm x 200 µm x 50 µm) was represented and electrodes were activated also by two counter-phased signals at $15/\sqrt{2}$VRMS and $-15/\sqrt{2}$VRMS, parameters didn't vary from the previous simulation. The resulting simulation is shown in Figure 3.4.

Red areas show the zones with higher DEP force. From the analysis of the results, a 3D trapping effect was expected due to dielectrophoretic force, since this was incremented because of the action of the pillar. However, it was also predictable to have high trapping effects near the electrode too, which was in fact the electric field source. When comparing to the previous device, a force 10 times higher on average than the classic chamber was observed, Better results in terms of cell trapping efficiency were therefore expected
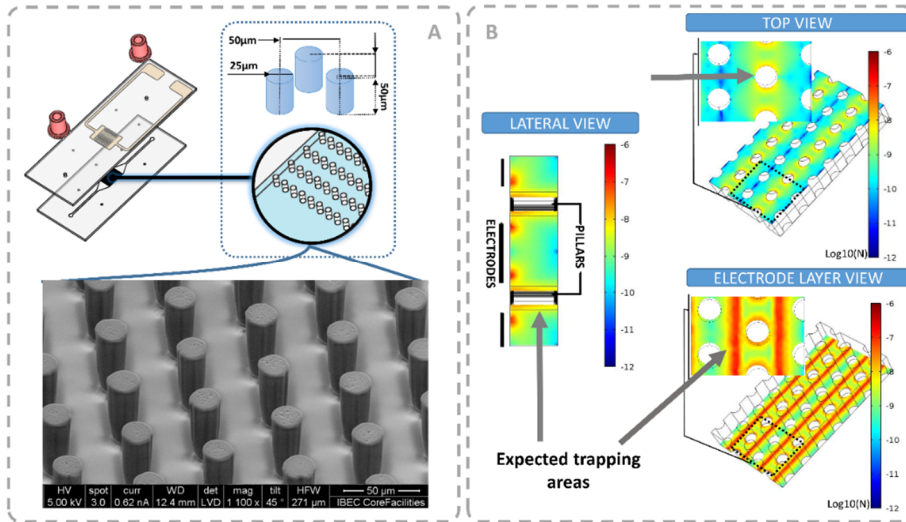
Figure 3.4. A. Poles design and real SEM image from the fabricated chamber. B. COMSOL simulations of the expected DEP Force inside the poles chamber and the expected trapping areas.

.

3.2.1 Poles chamber fabrication

The insulating posts were made by PDMS and the electrode layer design was maintained. Thus, the fabrication procedure followed the steps detailed in chapter 2, since only the PDMS chamber mould was varied. The difficulty of fabrication was in fact the exposure step, because the post shape was clearly dependent on this. In the UV exposure step, the light arrives in a different way to the pillar mould: higher light is applied to the top than to the bottom of the mask. This could cost a slight degree of the conical shape of the post. Also, the extraction of the chamber from the mould was a challenge, since the pillars were fragile at this point at could break during the process.

3.2.2 Experimental and results

A series of concentration experiments were also performed to gather consistent statistics on efficiency through exhaustive bacteria counts.
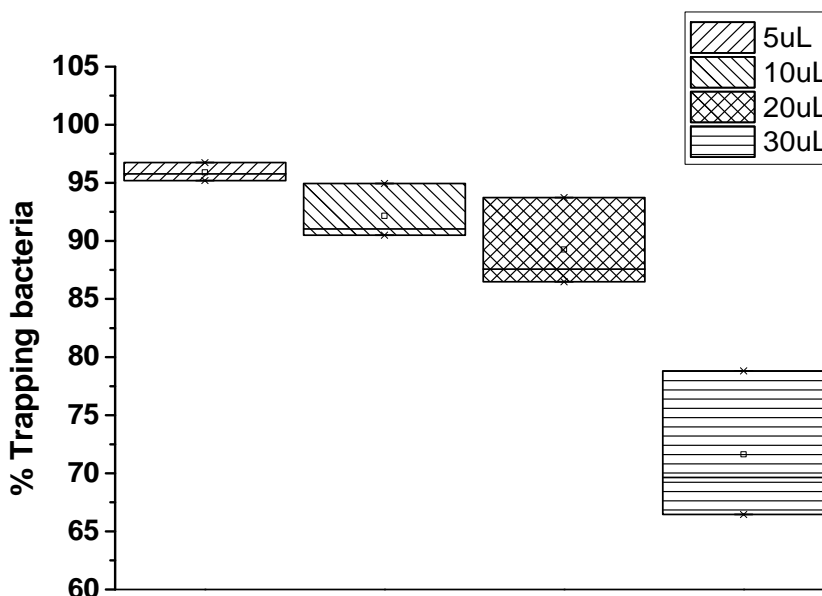
Figure 3.5. Results relative to poles chamber, depending on the applied flow rate.

Following the previous procedure, a series of concentration tests were carried out with the poles chamber, with different flow rate conditions. Results represented in the statistical box chart are shown in Figure 3.5.

The poles structure showed higher efficiency. For the lower flow rates (5 µL/min) cells were trapped with higher efficiencies in both systems. The regular chamber had a median efficiency of 91.7% and the poles chamber showed 95.9%. The difference was increased when faster flows were used. The maximum average increment of trapping efficiency (12.6%) was obtained for 20 µL/min. Moreover, poles design decreases bacteria losses at an average 44.2% for 5 µL/min, 10 µL/min and 20 µL/min. Thus, the insulating structures showed the highest efficiency, due to the maximums of electrical field that were registered around the pillars. This added structure also increased the effective trapping area in height, as simulated. Regrettably, at a current rate of 30 µL/min the flow dynamics overcame the DEP force, giving similar trapping values both devices. The results were additionally verified by a U-Mann Whitney test, comparing the obtained data

from both microfluidic devices. For the analysis, data were paired by flow rate. As a result, at 5 µL/min, 10 µL/min and 20 µL/min significant differences between devices (p< 0.05) were detected, where efficiencies were clearly improved. On the contrary, at 30 µL/min (p= 0.82) differences were not so significant.

To verify the 3D trapping effect, we decided to make some fluorescence tests. And so we were capable to verify where bacteria were attached, focusing the labelled E. coli with the microscope in the different heights. For the experiments *E. coli* SAR20 cells were used. These cells were obtained from CSH26 strains which were tagged by inserting a Ypf gene in the attB chromosome region [7]. Fluorescent *E. coli* SAR20 cells were treated with the same protocol as *E. coli* 5K cells, obtaining samples also of $4 \cdot 10^6$ cells/mL. 50 µL of fluoresced sample was introduced into each microfluidic device through the valve at a flow rate of 5 µL/min for 30 minutes, with the electrical field activated (also by two counter-phased signals of 15 Vpp). Immediately afterwards, the flow was stopped to properly observe the trapped cells (Figure 3.6)..
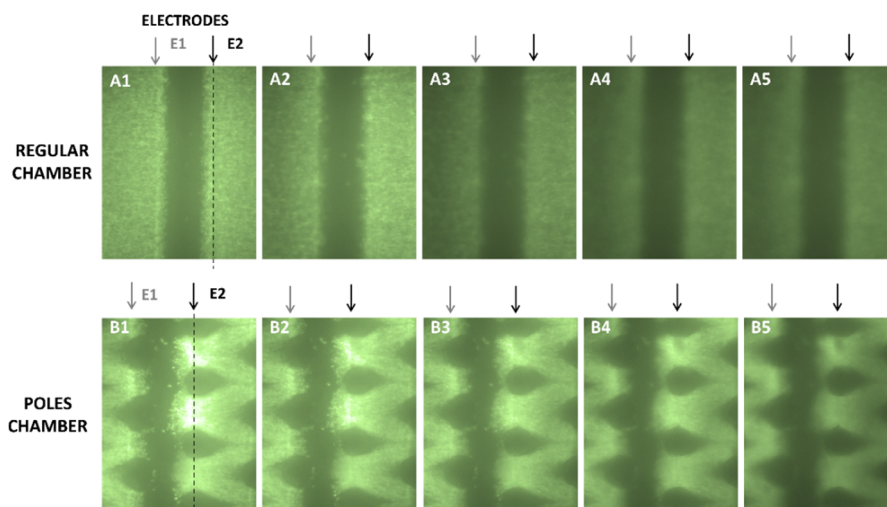
Figure 3.6. Fluorescence test results. In the top, results relative to the regular chamber. In the bottom, results relative to the poles chamber. The electrode edge is marked up with arrows at the top of each capture.

Then, by controlling the microscope focus position in the Y direction, the focused fluorescent cells at different heights of the microfluidic chip were differentiated. Consequently, it was possible to observe whether cells were trapped further up from the electrode. In the poles chamber, focussed labelled cells were distinguished in all the steps. In contrast, in the regular chamber, focussed cells were absent at a height of 8 µm. This observation corroborates the simulations and the statistical results, since a trapping effect close to the pillars was predicted

3.3. Testing E. coli survival to long-term electric field exposures

Finally, a third experiment was done to conclude that the microfluidic chip with dielectric poles was suitable to be used as a bacterial cell concentrator. Since at low flow rates cells were radiated with relatively high electrical fields for a long time, a proteomic analysis of the concentrated sample was performed so as to verify the sample viability in terms of proteins. This analysis consisted of a 15% (w/v) SDS polyacrylamide electrophoresis gel.

From each bacterial fraction obtained from a full DEP experimental process, 120 µL of sample was re-suspended in 240 µL of LB broth and incubated at 37ºC for 45 minutes. The samples were then centrifuged for 5 minutes at 300 rpm, and the resulting pellets were re-suspended in a lysis buffer composed of 100 mM Trisaminomethane/Hydrochloride –Tris/Hcl- (pH 8), 2 mM of Ethylenediaminetetraacetic acid (EDTA) and 2 % Sodium dodecyl sulfate (SDS). The samples from this process were then analysed by protein assay, which consisted of verifying the protein patterns by a 15% (w/v) sodium dodecyl sulfate polyacrylamide electrophoresis gel [19] (SDS-Page technique).

The running gel was composed of 3.75 mL of acrylamide, 25 µL of Ammonium persulfate (APS), 5 µL of Tetramethylethylenediamine (TEMED), 1.875 mL of 1.5M of Tris(ph 8.8) as a resolving buffer and 1.875 mL of deionized water. This first mixture was deposited between two glass plates in a gel caster. Soon after, some water was added to prevent air from

entering. After polymerization, the water was removed by decantation, and the stacking gel was added. This gel was composed by 650 μL of acrylamide, 25 μL of APS, 5 μL of TEMED, 1.25 mL of 0.5M of Tris/Hcl (ph 6.8) as a stacking buffer, and 3.05 mL of deionized water. Later, a 0.75 mm comb was inserted in order to create the 20-μL sample wells.
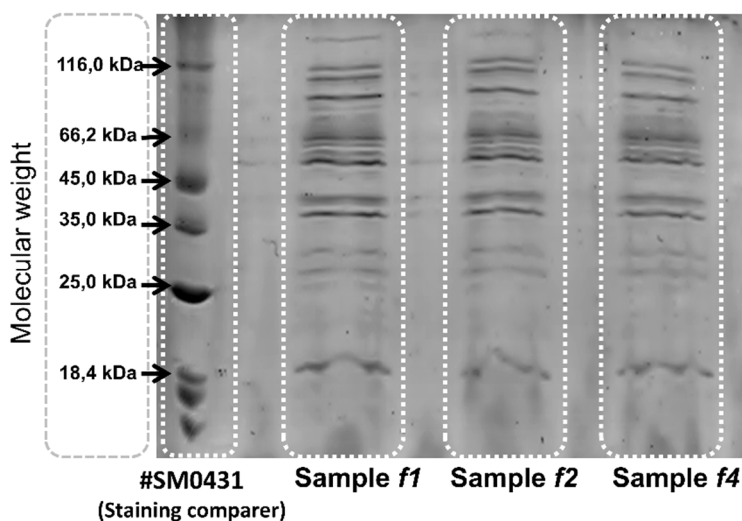
Figure 3.7. Scanned image from the resultant gel. The staining comparer was introduced in the first column. The relative molecular weight of each mark was labelled on the left.

Before loading samples into wells, they were mixed with 4 μL of 5X Loading Buffer (10% w/v SDS, 10 mM Dithiothreitol, 20 % v/v Glycerol, 0.2 M Tris-HCl (pH 6.8), and 0.05% w/v Bromophenol blue), boiled 10 minutes and spun. Moreover, the first well was filled with protein marker #SM0431 in order to locate the average molecular weight of the proteins analysed. The protein separation on the gel was performed by electrophoresis (BioRad PowerPac Basic). The electrophoresis tray was filled with 70 mL of 10X running buffer diluted in 630 mL of deionized water. The gel was then introduced, and the device was set at 20 mA per gel for about one hour. Finally, activated gels were dyed with Comassie Brilliant Blue (CBB) for 15 minutes on a rotating plate. The resultant gel was cleaned with acetic acid

and deionized water before being photographed by the ImageQuant LAS 4000 mini (GE HealthCare).

The results of the gel are shown in Figure 3.7. It could be observed that protein marks had the same intensity for all the samples, indicating that protein expression was not affected by exposure to the DEP electrical field. Thus pre-concentrated bacteria are still alive to be measured, as will be later detailed in chapter 5.

3.4. Chapter conclusions

Herein it was described a novel iDEP-based bacterial cell concentrator at continuous flow to improve the device described in the previous chapter. Both devices, one with a regular chamber and another with a poles structure, were simulated and then evaluated by means of its trapping efficiency, when different flow rates were applied. The microfluidic devices were actuated with portable electronic defined in the previous chapter. As a result, the poles structure showed greater concentration capacity, decreasing bacteria losses at an average 44.2% for flow rates less than 20 μL/min. The concentration improvement was caused by the trapping occurring around the pillars, which allowed to have a 3D trapping effect, which was also demonstrated by fluorescence experiments. Additionally, cell viability after these long exposures to the electrical field was verified by a protein analysis. From the analysis of the results it was verified that bacteria wasn't altered by the electric field, since no protein changes were detected.

References

[1]   R. Martinez-Duarte, F. Camacho-Alanis, P. Renaud, and A. Ros, "Dielectrophoresis of lambda-DNA using 3D carbon electrodes.," *Electrophoresis*, vol. 34, no. 7, pp. 1113–22, Apr. 2013.

[2]   R. Martinez-Duarte, "Microfabrication technologies in dielectrophoresis applications--a review.," *Electrophoresis*, vol. 33, no. 21, pp. 3110–32, Nov. 2012.

[3]   M. D. C. Jaramillo, R. Martínez-Duarte, M. Hüttener, P. Renaud, E. Torrents, and A. Juárez, "Increasing PCR sensitivity by removal of polymerase inhibitors in environmental samples by using dielectrophoresis.," *Biosens. Bioelectron.*, vol. 43, pp. 297–303, May 2013.

[4]   M. Elitas, R. Martinez-Duarte, N. Dhar, J. D. McKinney, and P. Renaud, "Dielectrophoresis-based purification of antibiotic-treated bacterial subpopulations.," *Lab Chip*, vol. 14, no. 11, pp. 1850–7, Jun. 2014.

[5]   C. Iliescu, G. L. Xu, V. Samper, and F. E. H. Tay, "Fabrication of a dielectrophoretic chip with 3D silicon electrodes," *J. Micromechanics Microengineering*, vol. 15, no. 3, pp. 494–500, Mar. 2005.

[6]   R. Martinez-Duarte, "Microfabrication technologies in dielectrophoresis applications.A review," *Electrophoresis*, vol. 33, no. 21, pp. 3110–3132, 2012.

[7]   A. Reisner, J. A. J. Haagensen, M. A. Schembri, E. L. Zechner, and S. Molin, "Development and maturation of Escherichia coli K-12 biofilms," *Mol. Microbiol.*, vol. 48, no. 4, pp. 933–946, 2003.

CHAPTER 4.   BIOIMPEDANCE AS A METHOD FOR BIOLOGICAL MATERIAL CHARACTERIZATION.

In this chapter impedance measurements are validated for biological material characterization. A new electronic device, capable of measuring the impedance by the 4-electrode method is designed. Different materials were measured by this method, so as to characterize a tissue sensor for in-vivo testing.

Up to this point we were able to concentrate bacterium with significant efficiency values. Thus, it was proposed to improve the system by including a bacteria level detection. Consequently, a new module was developed, able to detect biological material in lab on a chip environments by means of impedance spectroscopy (IS).

In its early stage, this module was defined to measure the bioimpedance of cells, solutions and tissues in general. With this IS device we were able to make a sweep in frequency of the biological material, so as to characterize it in terms of bioimpedance. As introduced in the first chapter, it was decided to use the 4 electrode method, since electrode impedance would be cancelled with this method. This was based on two current injection electrodes and two voltage reading electrodes. The read differential voltage was related to the cell impedance by Ohm's law.

Hereafter, by knowing the proper frequency to detect the biological material, it is possible to adequate the system to be integrated with other systems and automatize the bioimpedance value acquisition.

It must be pointed out that posterior to the design of the module, a collaboration between SIC-BIO group and the Nanobieengeenig group from the Institute of Bioengineering of Catalonia came up. In this collaboration, an IS solution based in our system, was developed for a Multisensor array previously tested at IBEC. The binomial equipment-sensor was part of the European project ARAKNES (Array of Robots Aumenting the KiNematics of Endolumial Surgery), which involved the design of a complete robotic platform for endolumial surgery. In fact, the objective of the Nanobioenginering group was to develop a real-time monitoring system based on an array of sensors capable of detecting, by different techniques, the ischemia on the stomach tissue during a surgery.

Ischemia is a damage caused by an insufficient supply of blood to an organ [1], [2]. Normally is generated by an obstruction or a narrowing of the arteries. When this occurs, the oxygen of the affected area is reduced and

84

tissue could be damaged or even die. In case of tissue from the gastrointestinal truck, this damage cause mortality in the 60% of cases [3]. Moreover, ischemia is often difficult to be diagnosed, since it no express clear symptoms in the first phase [4]. Thus, to real-time monitor the possible tissue variance could help to a necessary prompt diagnostic.

Thus, the Nanobioenginering group defined a multisensory array with different sensors, two for measuring potassium, three for pH and one for impedance, based on four non-treated pins.
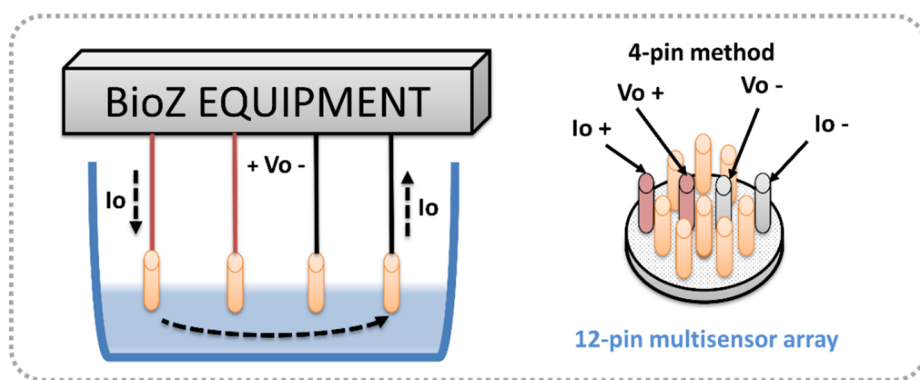
Figure 4.1. Different electrode configuration for bioimpedance measurement.

4.1. IS Equipment

According to the chosen IS method, a first device was designed (Figure 4.2). This was grounded in two mainly modules: a) The current injection module and b) The impedance reading module. The current injection module (a) was based on a Low-power signal generator, a DC filter and a V-I converter.

A DC filter was applied to an externally injected sinusoidal signal, based on a second-order Sallen-Key topology in its high-pass filter configuration. This allowed avoiding noise and DC levels of the generated signal, since this could create electrolysis and damage the injection electrode, as was

verified in chapter 2. Finally, the V-I converter was based on the Howland Current converter configuration that with the injection of a variable AC signal generated a stable current to be injected in the electrodes.

The applied current was selected by means of Ri (Vin was calculated to have a gain of 1.62:

$$I_0 = \frac{V_{in}}{R_i}$$
(Eq. 27)
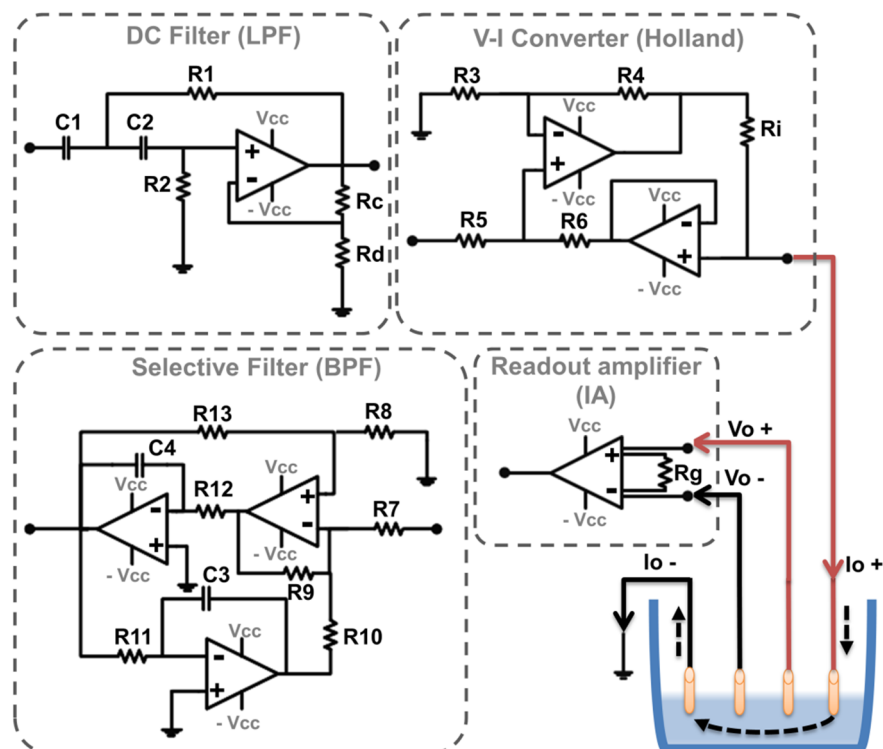
Figure 4.2. Block Diagram of the Bioimpedance system.

The second part was formed by a readout circuit based on an Instrumentation Amplifier (IA) and a selective band pass filter (BPA). The IA allowed to obtain the related voltage to the bioimpedance material value.

Then, the selective BPF helped to tune the reading circuit to the applied frequency. Thus, was possible to manually tune the whole system to the

desired frequency so as to look for the best conditions to detect the material. The specifications of the designed device are shown in Table 4.1.

Table 4.1.Datasheet of the designed IS device

Power Supply Voltage *(Provided by PSU25A-14E converter)*		± 15 Vdc and +5V	
Minimum input voltage		60mVpp	
Maximum Input Voltage		8 Vpp	
Maximum Output Delay Error (0) *Maximum Delay Error between V Read and Vload signals*		0,95%	
Optimal Operating Frequency		70kHz	
Output Frequency Range		68kHz-75kHz	
Maximum Allowed load		2.5kΩ	
Minimum Allowed load		1Ω	
Maximum Current Output		3,56mAp-p	
Current Output –Programmed- *(According to Selector Resistor)*		***Current Range Selector***	***Maximum current available***
		1M	53uApp
		200k	96uAp-p
		100k	150uAp-p
		50k	0.9mAp-p
		10k	1.4mApp
		5k	2,3mAp-p
		2k	3,56mAp-p
		1k	3,56mAp-p
Reading module Gain options		2.10/3.39/10	
Injection module Gain		1,62	
Related expressions			
| Bio-Impedance|		$$\|Z\| = \frac{Vread\ [Vpeak]}{G \cdot Idesired\ [Ipeak]}$$	
Phase		$$phase[º] = \frac{(read_{delay} + Device_{delay}) \cdot 180}{T/2}$$	

Prototype. Top view

+ Vo / - Vo / - Iin / + Iin Front panel connections

Vin / Vread /Power Rear panel connections

4.2. pH and K+ potential adapters and BioZ device improvements.

Regarding to the collaboration with the ARAKNESS project, in a first stage the given prototype defined in 4.1 was used to perform an IS analysis from 2 different tissues (chicken lean and adipose tissue). This study was reported in a UB thesis [5]. In fact, this helped to verify the reported values from *Oathman et al* [6], where 68 kHz was defined as the best frequency to clearly distinguish ischemic from non-ischemic tissue by means of impedance. Hence, 70 kHz was chosen as the best frequency to be applied in the following in-vivo experiments.

In a second stage of the collaboration, a second board was designed including adapted reading modules to facilitate the acquisition of the measures by the ARAKNES final equipment.

So as to adapt the read potential from pH and K+ sensors, which experimentally could vary between -200mV and 400mV, to the acquisition module, a signal adapter stage was needed. In this case, the acquisition module also needed 0-1V input signals with an output impedance matched at 600Ω. Thus, the adapter was designed (Figure 4.3). This was based on a readout amplifier, a level corrector, a noise filter and an impedance output adapter. First, the readout circuit was based on the instrumentation amplifier INA121 from Texas Instruments, which can be gain adapted by the external resistor Rg following expression:

$$G = 1 + \frac{50k\Omega}{Rg}$$
(Eq. 28)

After, as the original signal could acquire negative values, a level corrector was applied. This was obtained by means of an adding configuration, which was connected to a stable voltage reference of 200mV coming from the National. Semiconductor LM10CN circuit. This allows us not having signals under 0V, as was established by the requirements of the ARAKNES acquisition module.

Then, after buffering the signal, a noise filter was applied based on the LPF Sallen-Key topology, which had a cut-off frequency of 10Hz. Finally, read signal was impedance and current matched by the power amplifier LME49710 from Texas Instruments.
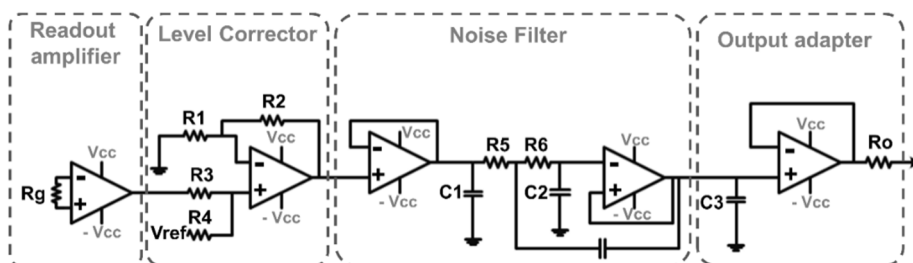
Figure 4.3. K+ potentiometric adapter

Also, the IS module was also modified. A sinusoidal generation stage (Figure 4.4) was added to the injecting module.
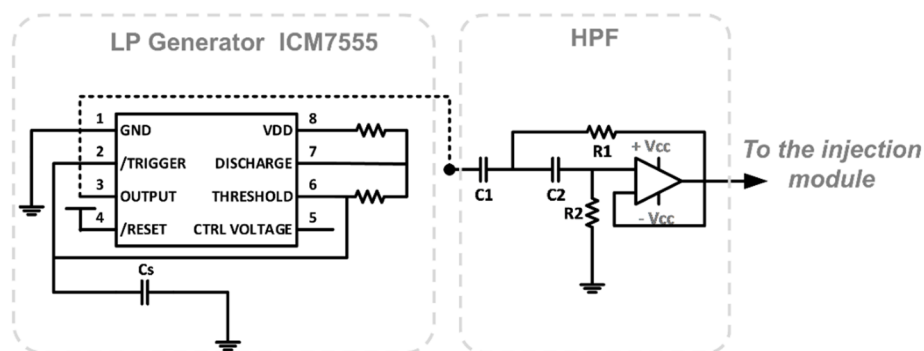
Figure 4.4. Modification of the injection module.

The Low power signal generator was based on an ICM7555 which generates stable high frequency squared signals, and a high pass filter. This, combined with the following LPF permitted to obtain a sinusoidal signal of 70 kHz. The reading stage was improved (Figure 4.5) so as to convert the AC read voltage in a DC signal, between 0 a 1 V, to make it readable for the ARAKNES equipment.

Table 4.2 The datasheet of the device adapted to ARAKNES specificactions.

General Features	
Power Supply Voltage *(Provided by PSU25A-14E converter)*	± 15 Vdc
Maximum Output voltage per channel	1 Vdc
Output impedance For each output channel	600Ω
Impedance Meter General Features	
Operating Frequency	70kHz
Maximum Allowed load (1)	**500Ω**
Minimum Allowed load	1Ω
Output current	3 mAp-p
Gain	0.75
Related expressions	
| Bio-Impedance | value	$$\|Z\| = \frac{Vread\ [Vdc] * Gain}{Idesired\ [Ipeak]}$$
PH Meter General Features	
Maximum input range	-200mV to 350mV
Maximun output range	0 to 1.2Vdc
Potassium Meter General Features	
Maximum input range	-200mV to 400mV
Maximun output range	0 to 1.2Vdc
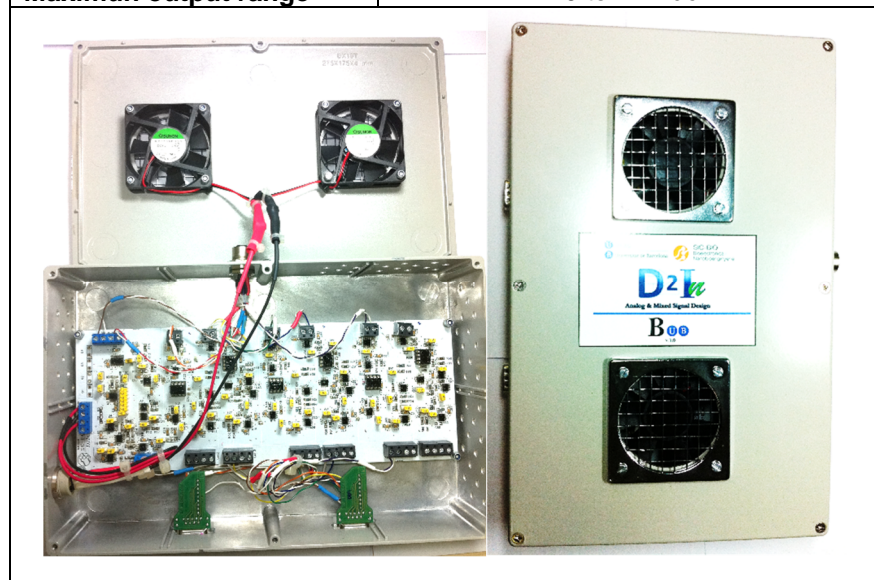
Equally as K+ and pH sensors, the output had also an output impedance of 600 Ω. The adapting circuit substituted the HPF for a 2on order LPF, with a cutoff frequency of 58 kHz, since 70 kHz was chosen as the best frequency to detect ischemia by means of impedance as previously mention. Also, a rectifier bridge so as to convert to a DC level the applied signal was applied
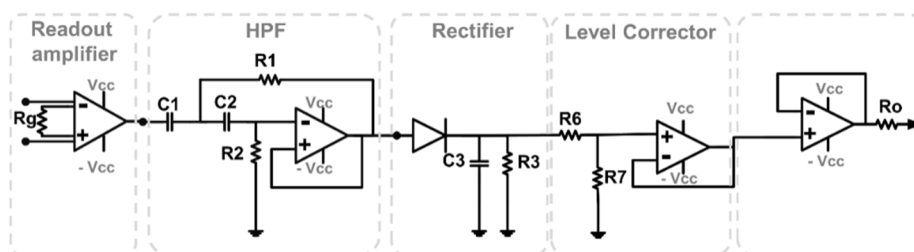
Figure 4.5. Modified read stage IS module

Finally, the signal was level corrected and impedance matched to accomplish the given specifications. The final device had the specifications given in Table 4.2.

4.3. Experimental definition, protocol and setup

The following tests were defined to validate the sensor and characterize the global system; the final application was taken into account for the test definition:

a. A measure with a commercial reference and the custom references from the sensor array to corroborate the stability of the custom reference in time.

b. A measure with a commercial pH sensor and the custom pH sensor of a known pH solution with a steering magnet inside (to ensure solution stability) in time. Hence, we verified the pH sensor accuracy and stability in time.

c. Measures with the complete array of different solutions of pH and potassium to characterize the sensor.

d. Measures of different tissues immersed in pH solution which value will be close to the expected in the pork stomach (1.9pH).

The system was connected to an acquisition card from National Instruments so as to simulate the ARAKNESS host. Moreover, the sensor array was connected to the electronic system by means of 12 pin shielded connector from Binder-connector. Furthermore, the array was placed into a floating support, which ensure electrode submersion and allows setting the distance with external electrodes if necessary.
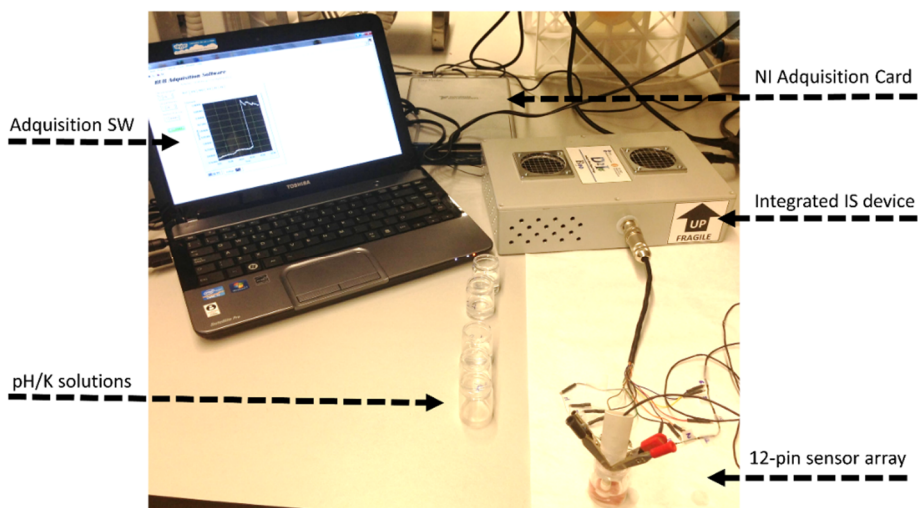
Figure 4.6. Experimental setup

Before the experiment, electrodes were cleaned with deionized water. Then, in case of solution measures, electrodes were first submerged in the swelling solution and leaved since signal were stabilized. Hereinafter, electrodes were introduced in successive solutions while the apparatus obtain the real time measure regarding to the introduced pH or K+ value. Additionally, related impedance was also measured during the experimental process.

4.4. Sample preparation

pH Samples were based on a solution of 0.1M tris(hydroxymethyl)aminomethane pH desired pH adjusted by HCl addition

and by measuring with a pH meter. We obtained samples from 0.7 to 2.5 pH and from 6 to 8pH.

K+ samples were composed of 0.1M KCl adjusted to 1.9pH and diluted with tris(hydroxymethyl)aminomethane at a pH of 1.9 (1.9 pH is the expected pH inside the stomach) so as to obtain different K+ sample concentrations maintaining the sample pH. As a consequence, we obtained from 10^{-5} M to 10^{-1}M KCl solutions.

4.5. Electrodes functionalization
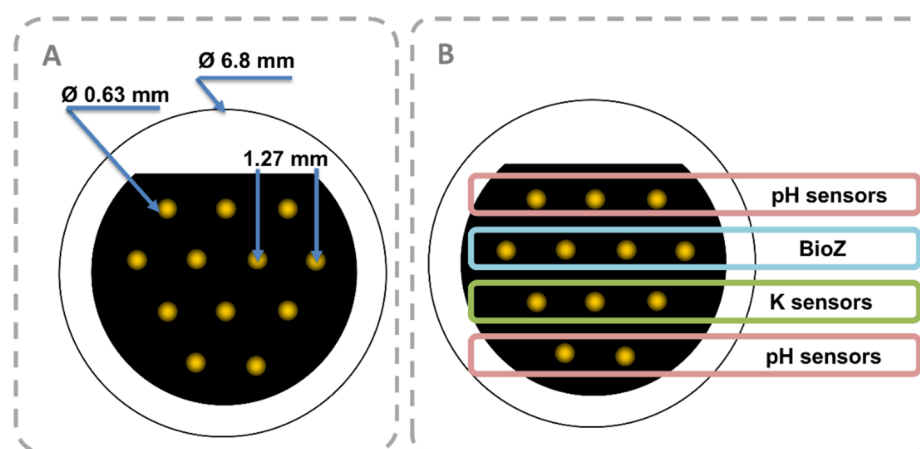
Figure 4.7. A. 12-pin array dimensions. B. Sensors distribution along the array.

The electrodes were functionalized by Nanobiengineering group. As they reported [2], the electrochemical sensor array (MCS 12 series from Omnetics Connector Corporation) of 12 electrode pins of beryllium copper alloys was washed with double deionized (MilliQ) water and dried under nitrogen atmosphere. Hereinafter, the electrode pins were covered with a biocompatible resin (EPOTEK 301-2 by Epoxy Technology) and cured at 80 °C for 3 h. Then, they were cleaned with pure ethanol by sonication for 2 min. Soon after, a second cleaning process was done by the application of nitrogen gas. Afterwards, the contact pin surfaces were covered with carbon ink (Dupont) and dried at 130 °C for 6 min. Once dried, a layer of

Ag/AgCl ink (Dupont) was deposited. Then, reference electrodes (RE) were covered with Nafion (Perfluorinated ion-exchange resin from Sigma). Then, they were kept under vacuum for 48 h under vacuum and after dried at 100 °C for 1 h. Moreover, working electrodes (WE) were covered with an ISE membrane. This membrane was made by 1.0 wt% hydrogen ionophore IV, 1.33 wt% KTClPB (potassium tetrakis (4-chlorophenyl) borate from Fluka),68.0 wt% 2-nitrophenyl octyl ether, and 29.67 wt% PVC (poly(vinyl chloride) from Fluka) of high molecular weight. This mixture (300g) was dissolved in 3 mL of THF (Tetrahydrofurane from Panreac). Finally, WE pins were dried an overnight.

4.6. Results
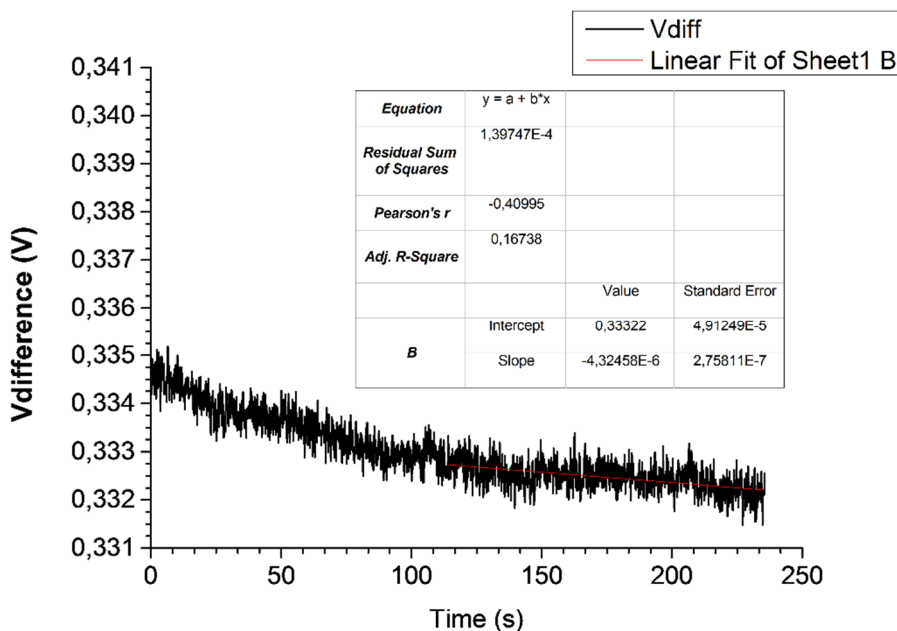
Figure 4.8. Reference electrode stability. The measure is referred to a commercial AgAcl reference. A linear fit was added to the measure for the range when reference is apparently stable.
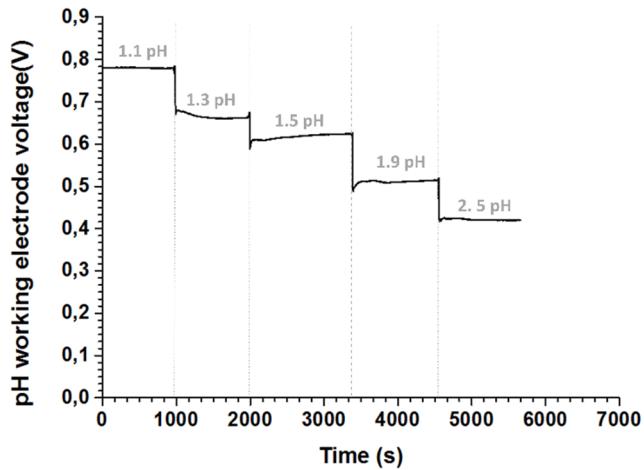
Figure 4.9. Results for a measure with a pH custom working electrode referred to a commercial reference electrode.

First, electrode reference was verified. An array provided of reference pins was introduced in a stable solution within a commercial Ag/Agcl glass reference of 3cm. The commercial reference was placed at 0.5mm from the custom array. Both were immersed in a solution of 6.5 pH and left for a long time. The voltage difference between them was measured with the National Instruments acquisition card. Thus, if custom reference has drifts, they were detected. The obtained results are depicted in Figure 4.8 were custom reference shown a god linearity and stability in time.

As measured, a 0,002 V of drift was obtained in the first period. After, signal has a variation of +/- 0,001V. Then, working electrodes of pH were tested individually. In here, also a commercial reference was used, to observe the possible drifts caused by the custom working electrode. Working pH electrodes were stable to the ph change (Figure 4.9) and the difference between levels could be quickly distinguished. However, little drifts were observed during the signal value stabilization. Finally the complete 12-pin array was tested.
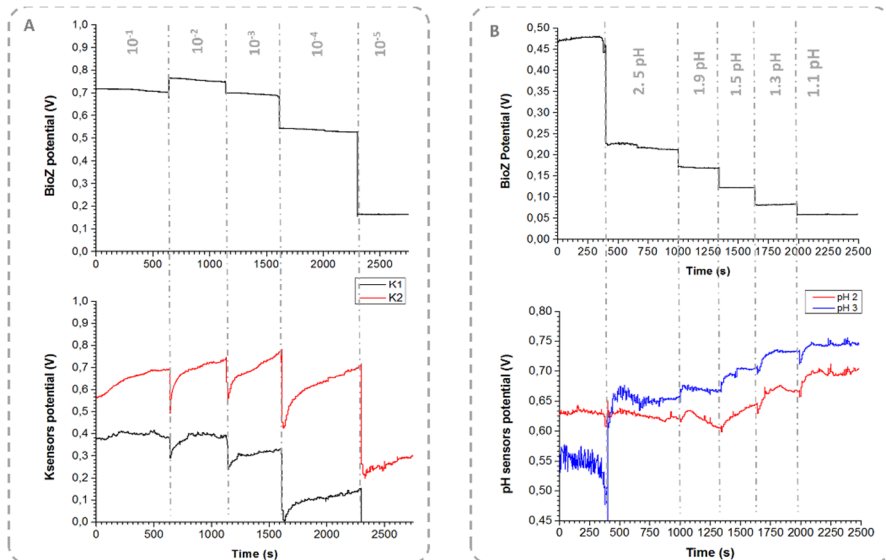
Figure 4.10. A. Results for the array immersed in potassium solution. B. Results for the array immersed in pH solutions. In both images, every signal step is related to a change of solution.

The array was immersed in different solutions of pH, from 1.1 to 2.5pH, and potassium, from 10^{-1} M to 10^{-5} M. The associated voltage of each level is captured as a function of the time.

The results for every sensor could be observed in Figure 4.10. Where could be seen pH and potassium levels could be distinguished, despite working membranes are quite sensible (they were handmade produced) and some lack of stability is observed during the experimental process. Also, the lack of stability was due to using both working and reference electrodes, whose drifts were added. Membranes increased lacks during the experiments and after they were stored for a long time. Thus, special atmosphere was needed for storing them. However, these high drifts didn't appeared with tissue test. A fourth experiment was done with different pork tissue, adipose and lean tissue, immersed in pH solution of 1.9 (pH pork stomach), trying to emulate the expected conditions of an in-vivo experiment.
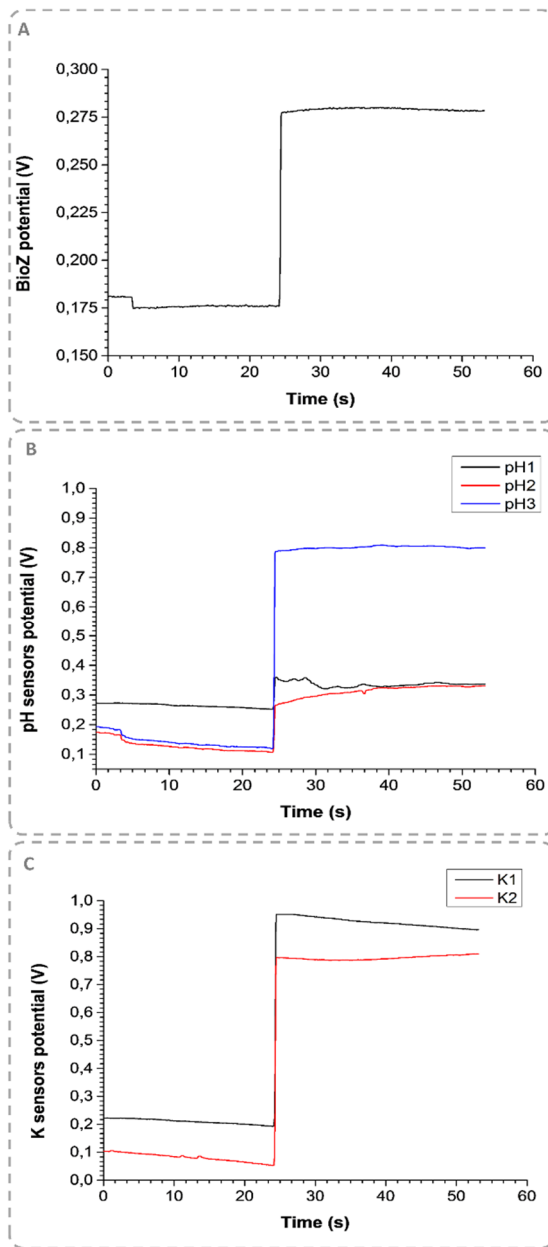
Figure 4.11. Results for the array in contact with tissue (immersed in a simulated stomach fluid of 1.9pH). A. BioZ difference between adipose and pork lean. B. pH difference between adipose and pork lean. C. Potassium difference between adipose and pork lean.

As results shown (Figure 4.11), tissue helps to membrane adhesion and the obtained results were clearly more stable in this case. In all sensors could be distinguished the differences between both tissues and its properties. Meanwhile, the buffer solution didn't affect the detection.

4.7. Chapter conclusions

In this chapter, a IS electronic solution for tissue impedance monitoring was presented. Initially the device was intended to be used as an integrative part of a complete bioimpedance and DEP Lab-on-a-Chip system. A version of the module was designed and tested to be enclosed in the ARAKNES European project, so as to give an electronic solution monitoring the signals from a sensor capable to detect ischemia inside the stomach.

The first electronic design comprises a scalable IS sensor, based on a Howland cell and a readout electronic so as to measure impedance tissue by means of 4-electrode method. The second device, was more focused on the in-vivo experiment to measure ischemia inside a pork stomach. Thus, the electronic was adapted to be autonomous, working at the ischemia working frequency. Additionally, some potential adaptors were designed to read all the signals available in the array of sensors. The whole system was tested for different solutions as well as different pork tissues. Sensors had shown better response in case of tissue measures, where membranes remain more stable at the tip of the array.

References

[1]   C. K. Chou, "CT manifestations of bowel ischemia.," *AJR. Am. J. Roentgenol.*, vol. 178, no. 1, pp. 87–91, Jan. 2002.

[2]   I. B. Tahirbegi, M. Mir, and J. Samitier, "Real-time monitoring of ischemia inside stomach.," *Biosens. Bioelectron.*, vol. 40, no. 1, pp. 323–8, Feb. 2013.

[3]   M.-C. P. Shih and K. D. Hagspiel, "CTA and MRA in mesenteric ischemia: part 1, Role in diagnosis and differential diagnosis.," *AJR. Am. J. Roentgenol.*, vol. 188, no. 2, pp. 452–61, Feb. 2007.

[4]   G. Thuijls, K. van Wijck, J. Grootjans, J. P. M. Derikx, A. A. van Bijnen, E. Heineman, C. H. C. Dejong, W. A. Buurman, and M. Poeze, "Early diagnosis of intestinal ischemia using urinary and plasma fatty acid binding proteins.," *Ann. Surg.*, vol. 253, no. 2, pp. 303–8, Feb. 2011.

CHAPTER 5. COMBINING MANIPULATING METHODS WITH ELECTRIC MEASURES. USING DEP AND BIOIMPEDANCE TOGETHER FOR A RAPID DETECTION OF *E. COLI* IN WATER.

In this chapter the whole system is characterized for water E. coli contamination detection. The strengths of both modules are combined to detect minute amounts of E. coli in large sample volumes. A unique lab-on-a-chip device is designed, fabricated and tested also for this purpose.

In the previous stages of this thesis, the different modules, which constitute the basis of the system which we aimed to develop were designed and tested. As a concluding step towards our main integration objective, these modules were adapted to reach a final proof of concept solving a current bioanalytical issue: to hold a combined DEP and Bioimpedance device for a rapid detection of *E. coli* in the water. We aimed to improve current detection methods by combining a microfluidic protocol, bioimpedance and electrokinetics . We also presumed that combining these techniques we would be able to reduce laboratory procedures, since they normally are time consuming [1], [2]. Pathogenic bacteria detection protocols are expensive in terms of equipment and time, typically requiring different equipment and several days to obtain results [3], [4]. Techniques like pathogenic-specific antibody coated magnetic beads [5], [6] or hybridization of DNA fragments of bacteria [7] improves the analysis time, but still need complex equipment and take several hours to carry out.

Our work resulted in a completely adapted equipment to quickly concentrate bacteria with DEP technique at relatively high flow rates, while monitoring in real-time its concentration by means of bioimpedance measurements. Furthermore, the changes in the bacteria medium during the measurements have been studied in detail to track conductivity variations which is key to correctly track concentration variations by the measured impedance. These biologically induced changes, and their effect on bioimpedance measurements, are generally not treated in scientific literature and are a limitation which we have solved by stablishing a specific microfluidic protocol.

5.1 Microfluidic chip design.

The used microfluidic device was an adapted version from the interdigitated device presented in chapter 2. Its design is depicted in Figure 5.1. As stated before, this was based on two interdigitated electrodes, which were shared between the DEP generator and the IS module, and 2 lateral electrodes,

which were used to inject the necessary current to achieve the impedance measure.

The interdigitated electrodes were also formed by 40 pairs of 6 mm x 50 µm electrodes separated by 50 µm. The lateral electrodes (6 mm x 300 µm) were separated by 200 µm from the interdigitated ones.
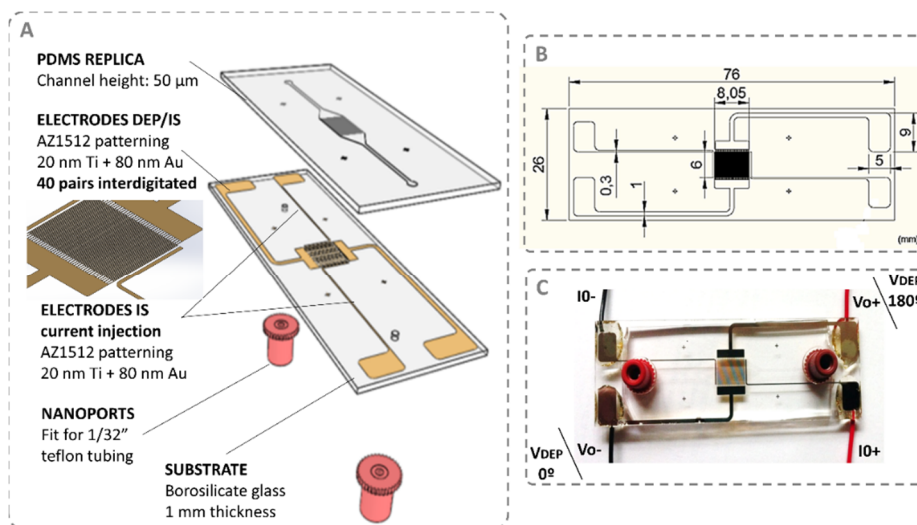
Figure 5.1. Microfluidic chip design. A. Parts of the device. B. Electrode measures. C. Real device.

These electrodes were attached to a PDMS micro-fluidic chamber with a volume of 4.8 µl. The fabrication of the microfluidic chips followed the protocol defined in chapter 2.

Later, some first validation experiments were carried out. So as to guess the theoretical limits of the *E. coli* impedance, manual measurements were done with a commercial impedance analyzer. The designed microfluidic chip was connected to a commercial analyser Agilent and filled with milk, water (1.41 uS/cm of conductivity) and non-diluted sample of *E. coli* 5K. The obtained results are shown in Figure 5.2 below.

As first measures indicate, the conductivity of an undiluted *E. coli* sample has an elevated conductivity and so low impedances are expected as much bacteria will be concentrated inside the chip.

However, the dilution of the *E. coli* sample in MilliQ water will increase our measure baseline, since this is a low conductive medium. Besides, it was observed that measures will be more stable in a mid-frequency range, where the frequency response of both states could be better distinguished.
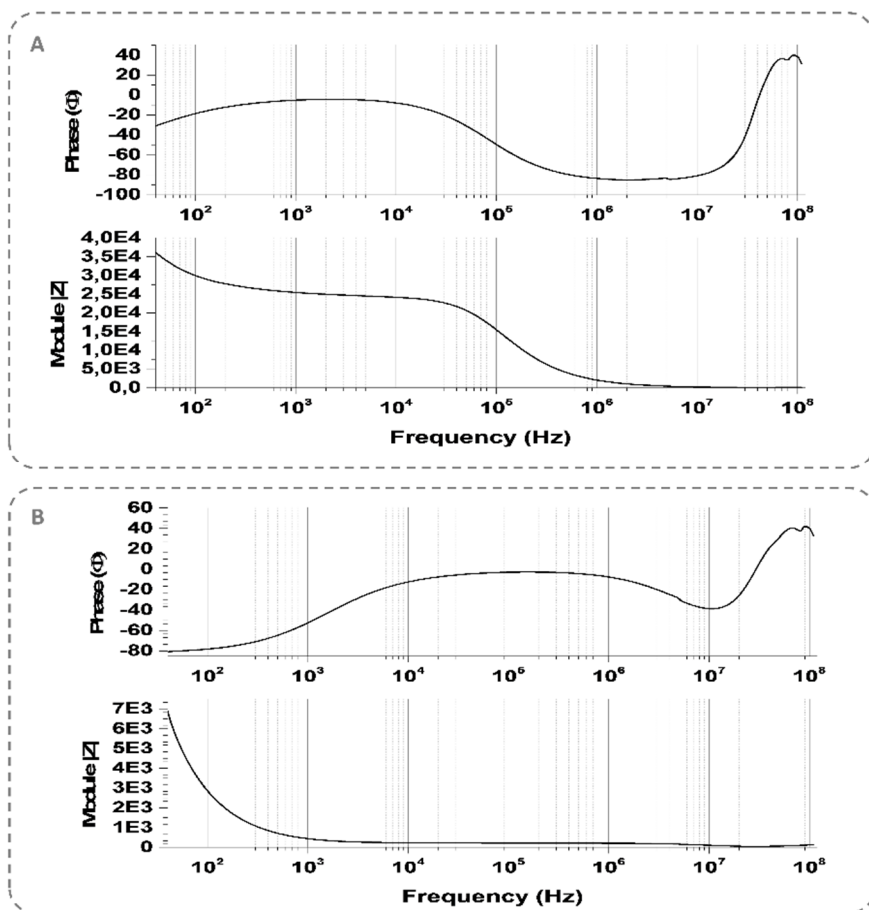
Figure 5.2. A. Chip impedance when it is filled with MilliQ water. B. Chip impedance when it is filled with *E. coli* 5K original sample

5.2 Combined DEP and IA device

The combined device is based on the designed DEP and IS module (Figure 5.3). Only two channels from original device were used, as they have shown better results in previous experiments. Both channels were connected to electrodes labelled as VDEP 0⁰ and 180⁰ respectively by means of a multiplexer, since this electrode were shared with the impedance readout electronics. As previously stated, each channel was tuned to inject 1MHz signals of 15Vpp each one. This level was also grounded on: a) A square LV signal generator that provides four shifted and frequency stable signals. b) A power driver which boost the signal from the previous module so as to activate the following stage. c) A Class E Amplifier, which generated the DEP sinusoidal signal, stable in frequency and with enough power to drive the microfluidic chip within high conductivity media.
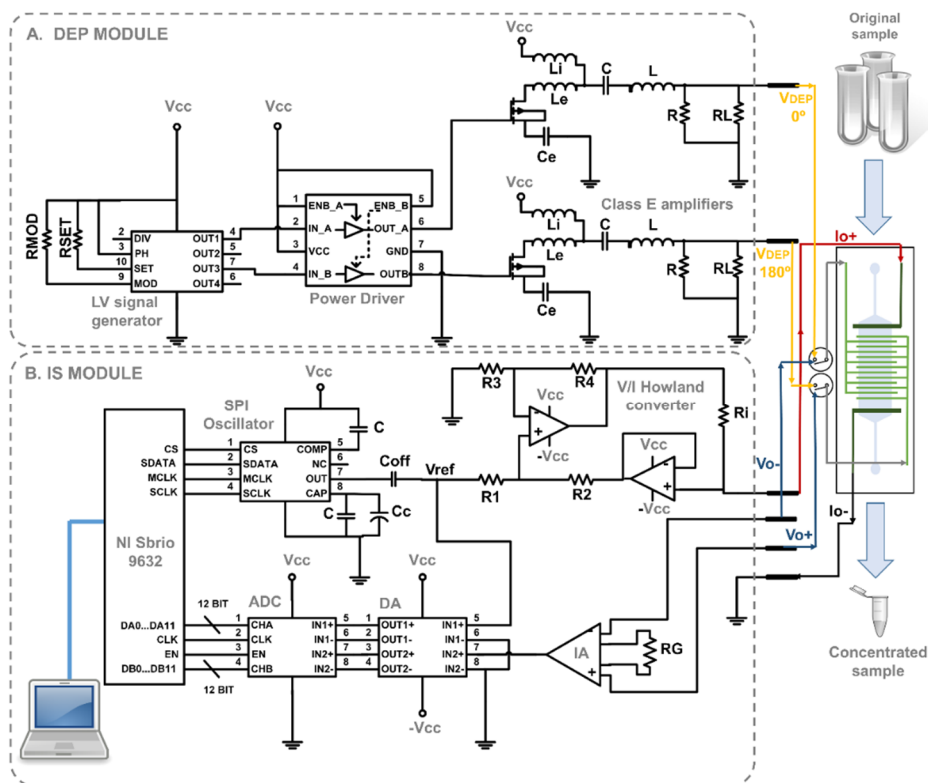
Figure 5.3. Combined DEP and IS device, schematic.

The IS module was adapted for this application. This was done in collaboration with J. Punter, who adapted his reading stage [8]–[10] for being implemented with the current IS electronic This National Instruments (NI) sbRio based module was also used in his thesis for measuring impedance haematocrit by the 3-electrode method.

In this case, the micro-fluidic device impedance measurement was based on the 4 electrode method. This is composed of two Current Injection (labelled as Io+ and Io-) electrodes and two voltage Reading (labelled as Vo+ and Vo-) electrodes. The main advantage of this system is that electrode impedances are cancelled, obtaining a more reliable measure.

The circuit specifications were defined taking into account the sample medium impedance, and considering the micro-fluidic device characteristics and the frequency range where bacterium could be discriminated [11], [12]

The IS module can be divided into two main stages: a) The current injection module. b) The reading stage

The current injection module (a), generates a frequency configurable voltage sinus signal (Vref), by way of a signal generator AD9833 (Analog Devices) and a voltage to current convertor. The signal generator AD9833 provides a stable voltage signal with a wide variable frequency range, 0 MHz to 12.5 MHz, which is driven by an SPI bus connected to the NI SbRio Later, V_{ref} is transformed into a controlled current by means of a voltage-to-current converter based on a Howland-source configuration. The Howland cell is formed by two AD8066 (Analog Devices) operational amplifiers, which assure a wide bandwidth and a high slew-rate, while maintaining a low offset performance. As previously defined in the chapter 4, the Howland output current will depend on the applied resistance R_i and input reference signal (V_{ref}). It must pointed out that the applied current will be independent of the connected load. In fact, this is the most valuable feature of the

Howland cell. The obtained controlled current will be injected into the lateral electrodes (labelled as Io+, Io-).

The reading module (b) consists on an Instrumentation Amplifier (IA), which measures the differential voltage between the interdigitated electrodes. This is based on an INA163 (Texas Instruments) which allows a wide bandwidth with a low spectral noise and low Total Harmonic Distortion. The measured voltage (V_o) is related to the differential voltage between the interdigitated electrodes, G being the instrumentation amplifier gain (relative to RG).

$$V_o = G \cdot (V_{Electrode1} - V_{Electrode2}) \hspace{2cm} \text{(Eq. 29)}$$

After, the obtained measure is digitalized and post processed to calculate the equivalent impedance value through the voltage signals provided by the previous stage.

This step consists in a 12 bit, dual, low power analog-to-digital converter ADC12D040 (ADC) (Texas Instruments). This is capable of converting signals at 40 MSPS simultaneously. 12 bit resolution does not represent an inconvenience for the final system resolution, since Vo is scaled to the full range of the ADC analog input. The analog inputs are converted from single ended to differential with a differential amplifier (DA) AD8138 (Analog Devices), with a high slew rate, with low distortion and input noise. The impedance measurement is carried out with a programmed digital lock-in (DLIA) based on the Frequency Response Analyzer (FRA) approach. This final stage is included on the real-time platform sbRIO9632 (National Instruments), which facilitates the creation of the software for data processing and hardware control by means of its 400 MHz processor and an FPGA Spartan-3 (Xilinx). The FRA is a mathematical process, which adopts sine and cosine signals related to V_{ref}. Then, by using two multipliers and a filter stage, the real (V_{real}) and imaginary (V_{im}) component values of the measured signal V_o are obtained, which are in fact related to the impedance of the *E. coli* ($|Z_{E. coli}|$).

$$V_{real} = \frac{1}{2V_{RS}} \cdot V_o \cdot \cos(\varphi_{IS}) \; ; \; V_{im} = \frac{1}{2V_{RS}} \cdot V_o \cdot \sin(\varphi_{IS}) \tag{Eq. 30}$$

$$|Z_{E.coli}| = \left(\frac{2\sqrt{V_{real}^2 + V_{im}^2}}{|V_{ref}|^2} \right) \cdot R_i \tag{Eq. 31}$$

Also, the sbRIO9632 allows to configure its clock signals, which allows us to adjust the system to have real-time control of the chip electrodes multiplexing. As stated in section 5.1, the micro-fluidic chip had two interdigitated electrodes, which were shared between the DEP generator and the IA readout electronics. When an IA measurement was done the DEP generator was disconnected, suspending the trapping process. Having the possibility of controlling accurately the timing of this process, allows not to lose bacteria during the transition of both states.

Furthermore, when DEP voltage signals are disconnected, the bacterial concentration is better distributed along the electrodes and also better monitored. The impedance analysis process last for a period of the applied current signal, plus 1 ms for multiplexor switching times and stabilization. Moreover, sbRio platform allowed us also to develop an embedded hardware control with a multiplexed R_i to obtain an auto-scale current injector or an auto-scale of RG to adjust the applied G to the IA, as well as controlling automatically the applied frequency to the SPI oscillator. These also improved the signal acquisition. Moreover, the real-time platform allows the system configuration and data display, with a user-friendly front-end user panel, by means of an external computer connected to the platform with a standard Ethernet connection. In this application the system user can configure the experimental variables, such as measurement time for signal multiplexing, signal operation frequency and output gain, while displaying the impedance measurements related to the actual bacteria concentration level.

108

5.3 Bacteria culture and sample control

A laboratory sample formed by *E. coli* 5K strains (Genotypes: F⁻, hdsR, hdsM,thr, thi, leu, lacZ) was grown overnight in 10 mL of Luria–Bertani (LB) broth at 37 °C. The achieved cell concentration (estimated by performing viable cell counts in LB agar) was 10^9 cells/mL. Then, the *E. coli* culture was pelleted by centrifugation at 5000 rpm for 5 minutes. Bacteria were then re-suspended in 10 mL of deionized water. Finally, the samples were finally diluted at a final concentration of $2 \cdot 10^7$ cells/mL and frozen in 1 mL collecting tubes for being used later in the experiment.

As *E. coli* concentration was measured by means of impedance analysis, bacteria sample conductivity was monitored by using a commercial bench top conductivity meter Corning 441. Prior to the experiments, bacteria samples were diluted in deionized water with a conductivity of $8.2 \cdot 10^{-5}$ S/m, but the conductivity of the samples at the time of the experiment was subject to variations. This was due in part to the process of storage and thawing. Thus, a sample conductivity analysis was performed to control the sample before starting the experiment. The conductivity meter probe was calibrated by the given calibration solutions from Corning brand (2 point calibration). After, the probe was introduced into the 1 mL collecting tubes until the electrode was totally covered by the bacteria sample

5.4 Experimental setup

The experimental setup is depicted in Figure 5.4. The micro-fluidic chip was placed over an inverted microscope stage (Olympus™ IX71) connected to a digital camera (Hamamatsu™ Orca R2). Moreover, the micro-fluidic chip was connected to a 6-port manual valve (Valco™).

This valve was connected to a 5 mL syringe filled with de-ionized water ($8.2 \cdot 10^{-5}$ S/m) and placed on an infusion micro-pump (Cetoni™ NEMESYS).This syringe, push on water into the valve at the flow rate indicated in the NEMESYS software.
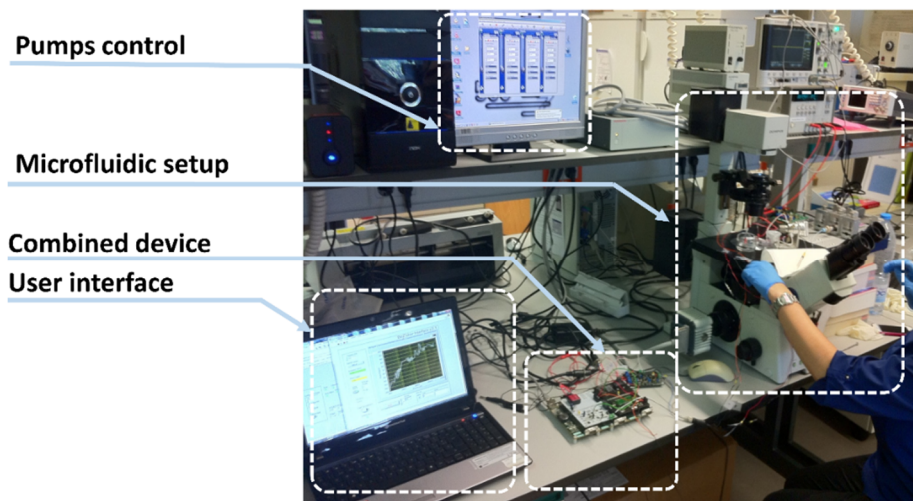
Figure 5.4. Experimental setup

Thus, a controlled continuous flow rate is obtained. In the loop of the valve, another syringe with the *E. coli* sample was connected. Thus, this 6-port valve allowed us to control the injection of the sample previously introduced in the loop. In addition, this permits to control accurately the volume of the injected sample.

Finally, the four micro-fluidic chip's gold electrodes were connected to the combined DEP and IA device. The flowing bacteria sample was pre-concentrated through the generated DEP generation and concentration was measured through IA monitoring. The electronic module was controlled by the sbRio real-time platform for continuous concentration monitoring, connected to a remote computer through a standard Ethernet connection, which enables the system configuration and data display.

5.5 Experimental results

The combined device was validated by some repetitions of *E. coli* concentration and impedance measurement tests. First of all, the system was validated as an autonomous bacteria concentrators and impedance sensor of the bacteria presence. For this, a first test was defined, which consisted of injecting continuously the prepared *E. coli* sample. This was done by using the valve connected to the micro-fluidic chip and configuring the injection NEMESIS pump at a 5 μL/min flow rate. During the experimental process, bacteria were concentrated by DEP created by the application of two counter-phased signals of 15Vpp. The automation software was setup to make a 3 ms impedance measure every 30 seconds. As detailed before, DEP is continuously active except during the 3 ms when impedance is measured. At this point of the study, the conductivity of the solution was not taken into account during the experiments, although this affected the measure, as it will be explained later on. For this first test, different frequencies for the IS applied current were considered. Considering the device features, the microfluidic chip design and the previous studies of the impedance of the chip in "vacuum", the test was defined at a current of10 μA with a variable frequency range from 500 Hz to 5 kHz, at 100Hz sample intervals. We expected to discriminate bacterium with this setup definition.

Regrettably, the obtained bioimpedance (|Z|) showed an unexpected behaviour (Figure 5.5) despite the adequate protocol. In this case, impedance value is decreased at the same time as trapped bacteria concentration increases inside the chip. Furthermore, this fact occurs regardless of the applied frequency.

This response caused the re-study of the protocol and a deep investigation the phenomena, which was occurring inside the microfluidic chip. As impedance was directly related to the media conductivity we observed, by means of the commercial Corning conductimeter, what takes place inside the sample when time pass by We left an original sample being measured

by the conductimeter for hours. The recorded values shown that the sample could change its conductivity value from $0.5 \cdot 10^{-3}$ S/m to $2.5 \cdot 10^{-3}$ S/m until it stabilized.
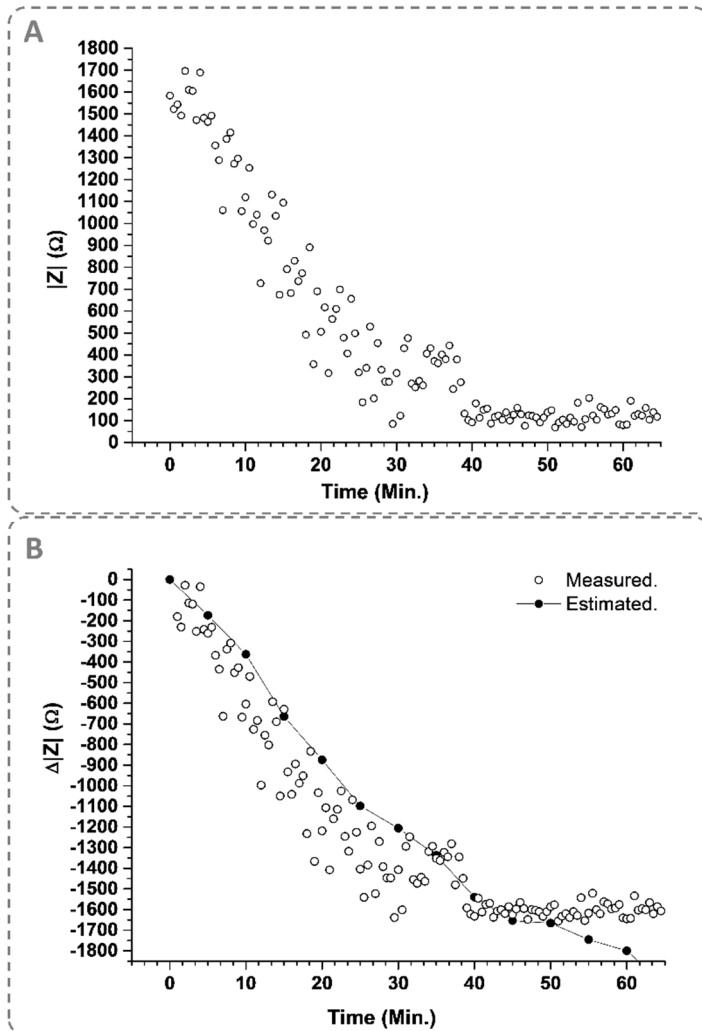

Figure 5.5. A: *E. coli* impedance measured during DEP concentration. B: Experimental versus estimated impedance value relative to incremental changes.

As was reported, bacteria have a natural process of losing conductivity during its life, which causes changes in its media. Also the natural mortality cycle of this bacterium, varies the media properties.

Hence, to verify the hypothesis, we inverted the process by calculating the expected theoretical bioimpedance using the given conductivity values from the Corning meter. This conductivity change, related to the original sample prior to the trapping process, was then translated into a theoretical variation in impedance, which is represented in Figure 5.5.B This theoretical impedance, related to measured bacteria sample in-tube conductivity, was calculated considering the geometric characteristics of the microfluidic chip. In Figure 5.5.B. impedance variation ($\Delta|Z|$) through time for the measured on-chip impedance, during the trapping process, and for the estimated on-tube impedance are shown. Results show a very similar behaviour through time of both measurements. The obtained data variations in the first 40 minutes, before conductivity stabilization, were -52.41 Ω/min for measuring impedance and -54.79 Ω/min for conductivity related impedance. These results verified that media sample conductivity was being measured instead of the trapped bacteria concentration, which remarks the need of correcting the experimental protocol.

Thus, a 2-D finite element method (FEM)-based study with Multiphysics software (Comsol) was carried out so as to verify the effect of media conductivity changes and its dominating effect on the bioimpedance measurements when left uncontrolled, looking for finding more details about this behaviour. The modelled *E. coli* was defined with the real *E. coli* 5K physical and electrical properties, considering all its layers: σ_{wall}= 0.68 S/m, ε_{r_wall}=74, $\sigma_{membrane}$= 5 x 10^{-8} S/m, $\varepsilon_{r\_membrane}$=9.5, $\sigma_{cytoplasm}$= 0.19 S/m, $\varepsilon_{r\_cytoplam}$=49.8. Then different medium conductivities were defined, as well as the potential to be applied to the external lateral electrodes. Current conservation and an initial state of potential 0 were applied in all the layers.

For this simulation, an adaptive physical controlled and extra fine mesh was applied. A frequency domain analysis at 1.7 kHz was performed. In fact, this was the chosen frequency where bacteria changes could be clearly discriminated, as it will be detailed later on. Thus, surface current density (ec.normJ) analysis of bacteria under these conditions was obtained (Figure 5.6.).
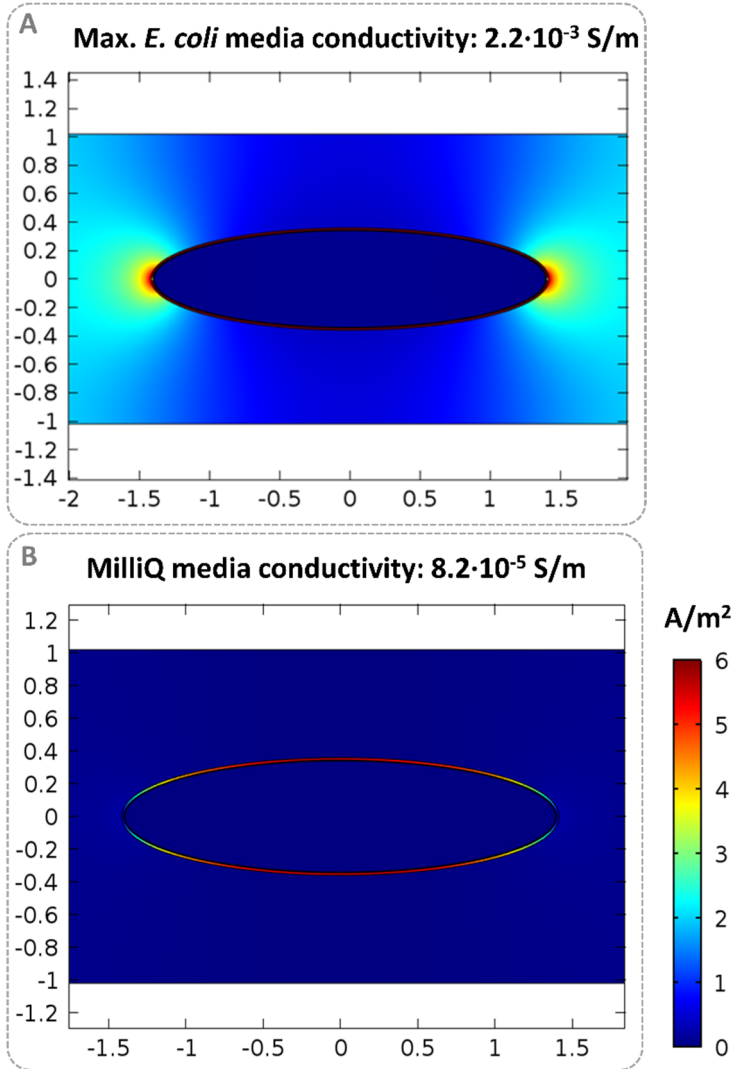
Figure 5.6. COMSOL simulation related to the effects of having different media conductivities when a current is applied. A. Current normalized density (A/m²) when the media solution is altered by *E. coli*. B. Current normalized density (A/m²) when the media solution is MilliQ water.

From the analysis of the obtained simulations it was possible to deduce that in case of a single bacteria diluted on a buffer with a conductivity which varies from $0.5 \cdot 10^{-3}$ S/m to $2.5 \cdot 10^{-3}$ S/m, current density is 99.9% located outside the bacteria. Hence, this confirms that the obtained curve of our

previous experiment was totally related to sample buffer conductivity rather than the bacteria concentration.

However, when buffer conductivity is stable and at the conductivity levels of Milli-Q water, ($8.2 \cdot 10^{-5}$ S/m) current density is mainly located in the cell membrane (Fig. 5. D), crossing the cells making a path and so, obtaining an impedance variation which is clearly related to the amount of trapped bacteria. Hence, when the cells' media is not controlled by cleaning processes, impedance variations are strongly related to changes in the conductivity of the media due to bacteria changes [13], [14]. To solve this issue a new experimental protocol was defined. This was based on an intervening cleaning process, which assure the media properties to obtain a reliable impedance measurement.

In the resulting protocol the micro-fluidic chip was first filled with Milli-Q water media to obtain the threshold impedance measurement. Afterwards, a 50 μL samples of *E. coli* were injected through a controlled valve to the micro-fluidic chip and trapped by DEP forces while flowing continuously at 10 μL/min.

It is important to point out that higher flow rates were used compared with other solutions for DEP and IA combination, where 2-4 μL/min were used [15]. After each 50 μL sample of bacteria was injected into the channel, 50 μL of Milli-Q water, with a specified conductivity of $8.2 \cdot 10^{-5}$ S/m, was automatically injected at 10 μL/min to ensure filling the complete microfluidic chamber with a steady medium conductivity for the impedance measurement. Once the Milli-Q water was injected, the impedance electronic module was activated and the DEP generator was automatically deactivated by means of multiplexor. Afterwards, another 50 μL sample of *E. coli* was injected and the process repeated until all the samples were injected. So, the impedance measurement was always activated after each 50 μL bacteria sample was injected, trapped and with Milli-Q water cleaned.
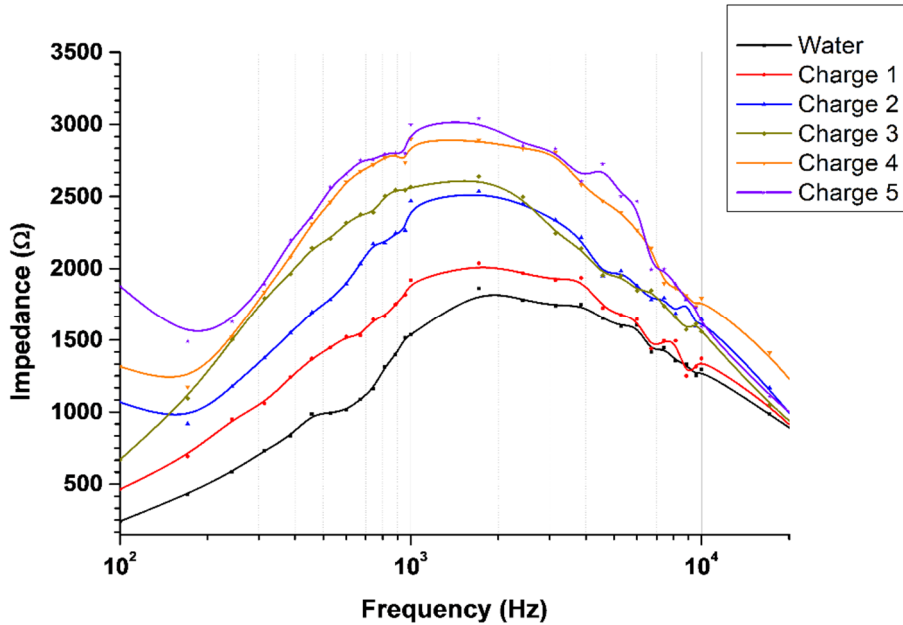
Figure 5.7. IS of a first single experiment for the whole available frequency range

A first measure (Figure 5.7) of the available IS device frequency range, defining a frequency sweep of 100 Hz, was performed as a proof-of-concept, so as to verify the system viability and the new defined protocol.

Later, the whole process was performed to scan the *E. coli* bioimpedance in some chosen frequencies. Scanning a simple frequency instead the whole range and so improving acquisition times and precision. The DEP was again generated by applying two 15 Vpp counter phased signals through the interdigitated electrodes. Then, 4 contiguous impedance measurements were performed each time in order to evaluate the precision of the measure. Three frequencies were chosen for these experiments: 500, 1700 and 5000 Hz. The results of the experimental impedance measurements are depicted in Figure 5.8.

Figure 5.8 is representing the obtained increment of impedance ($\Delta|Z|=|Z|-|Z_0|$) between the different impedance measurements for every bacteria

sample injected (|Z|) and regarding to the initial media impedance magnitude measurement ($|Z_0|$).
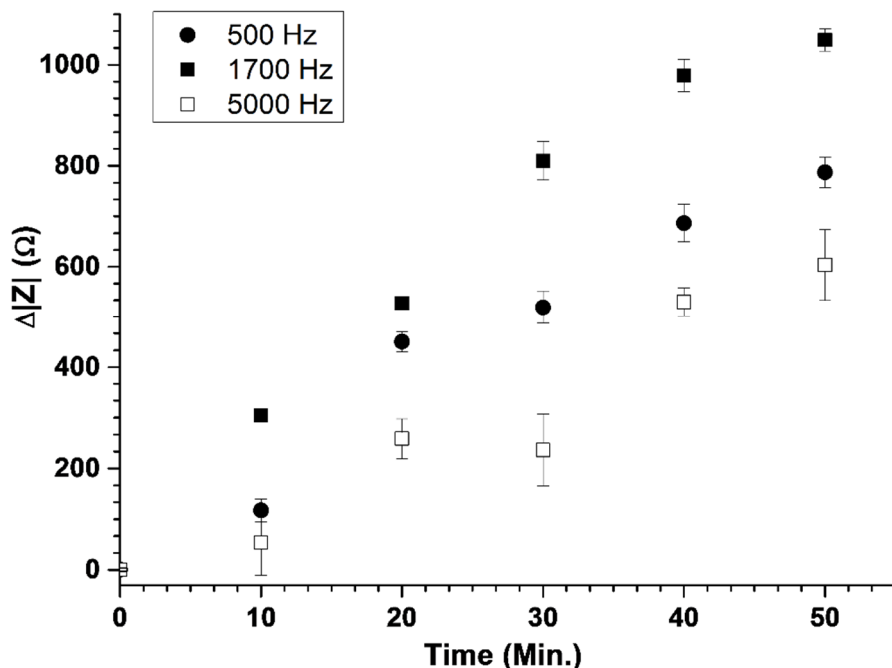
Figure 5.8. Experimental results from *E. coli* measured in several repetitions at different frequencies, with the corrected protocol.

Figure 5.8 depicts Δ|Z| measurements through time for the initial and final frequency value, 500 Hz and 5 kHz respectively, as well as the 1.7 kHz frequency Δ|Z| measurements, which resulted being more sensitive to bacteria changes. At this frequency an accuracy error of less than 2% of bacteria concentration with a correlation of 0.988 was obtained. Moreover, precision was evaluated by means of the coefficient of variation, which was the standard deviation of the 4 experiments divided by the mean value of the 4 measures. The mean value of the coefficient of variation was 3.1% for the whole range. Notwithstanding, the device shows more precision in case of lower bacteria concentration levels, where a coefficient of variation below 3% was obtained. Hence, Δ|Z| related to *E. coli* concentration could be observed with a certain precision, by utilizing the new cleaning protocol.

Having a steady and low conductivity media, the system viability issue is solved.

Furthermore, this conjunction of the DEP module and this microfluidic chip, has shown in previous chapters an effective trapping efficiency of 85.65 ± 1.07 %, in a single 50 µl bacteria sample injected at continuous flow of 10 µL/min. It must be remarked1, this was calculated by exhaustive cytometry analysis of the escaped and the collected bacteria [16].
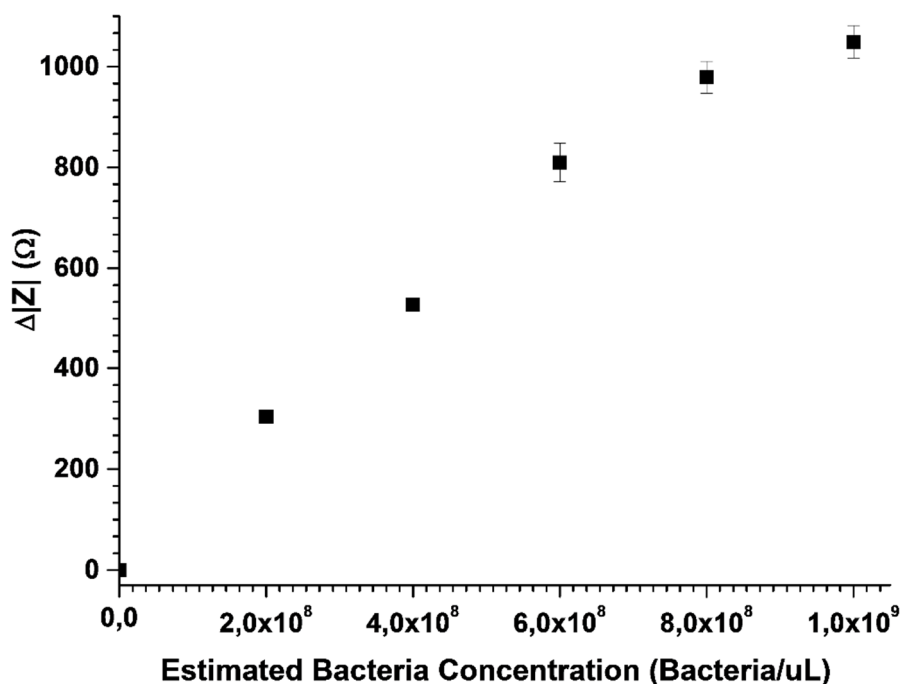
Figure 5.9. Impedance *E. coli* measurements at 1700 Hz related to estimated bacteria concentrations.

Although the whole process trapping efficiency had not been again measured by a cytometer and the viability of the system has been proved, each sample load could be estimated as an increment of bacteria concentration of about $2 \cdot 10^8$ bacteria/mL inside the micro-fluidic chip. In Figure 5.9 an estimation of the internal concentration related to the Δ|Z| measurements for each bacteria load (bacteria/µL) is depicted. The

measured impedance values were related to the quantity of bacteria concentrated with a correlation of 0.988 and a coefficient of variation of 3.1%.

5.6 Exploring further applications: additional studies.
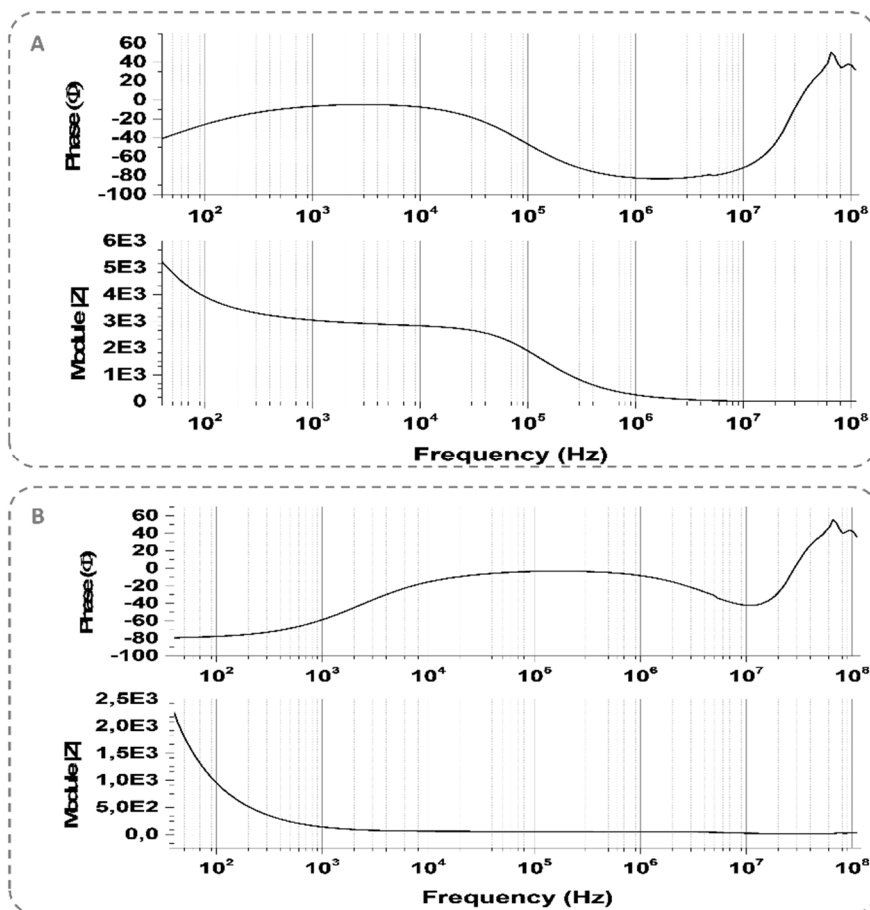
Figure 5.10. Impedance of 4chips connected in parallel and filled with MilliQ water. B. Impedance of 4chips connected in parallel and filled with *E. coli* 5K original sample

Also, the possibility of using some chips in parallel was also explored. Thus, in future it will be possible to make some parallel experiments by multiplexing signals.

The expected load was simulated by connecting four chips in parallel to a commercial impedance analyser. Then, it was filled with original undiluted *E. coli* sample and measured. Results are depicted in Figure 5.10.

Additionally, it was calculated if the expected load from connecting multiple devices could affect the designed DEP system module. From the analysis of the results (Table 5.1) it was deduced that a multiple chip system would be possible, since the variation of load from connecting multiple devices affects slightly to the global consumption of the DEP system.

Table 5.1. Equivalent load when various chips are connected to the DEP device.

Chips filled with MilliQ water				
Setup	**Vcc**	**Icc**	**P (W)**	**RL total**
C1	9	0,235	2,115	38,30
C1 + C2	9	0,241	2,169	37,34
C1+ C2 + C3	9	0,245	2,205	36,73
C1+ C2 + C3 + C4	9	0,25	2,25	36,00
Chips filled with E. coli 5K original sample				
Setup	**Vcc**	**Icc**	**P (W)**	**RL total**
C1	9	0,227	2,043	39,65
C1 + C2	9	0,234	2,106	38,46
C1+ C2 + C3	9	0,245	2,205	36,73
C1+ C2 + C3 + C4	9	0,247	2,223	36,44

5.7 Chapter conclusions

A combined device based on DEP and bioimpedance has been designed, developed by adapting the modules defined in previous chapters. This becomes a specific solution to concentrate bacteria in bench-top setups. Moreover, a new dedicated microfluidic device was designed, which permits to combine DEP and bioimpedance in a unique chip. Thus, bacteria injection, trapping and continuous rapid impedance is performed to detect bacteria concentration in water. In here, *E. coli* 5K was used to validate the system. Concentration and real-time detection of the trapped bacteria inside the micro-fluidic chip was proven. Additionally, the protocol was improved to work at relative high flow rates, up to 10 µL/min, comparing to other publications [17], [18]. Also, it was discovered the affection of bacteria media conductivity and its variability, which fact wasn't already taken into account in other publications that measured *E. coli* by bioimpedance. This supposed a challenging issue, which was solved by a new automated protocol, strengthening the system versatility and robustness. Hence, bacteria can be concentrated to given specifications while performing analytical procedures.

References

[1]   P. T. Feldsine, M. T. Falbo-Nelson, and D. L. Hustead, "ColiComplete® substrate-supporting disc method for confirmed detection of total coliforms and Escherichia coli in all foods: comparative study," *J. AOAC Int.*, vol. 77, no. 1, pp. 58–63, 1994.

[2]   F. Pouch Downes and K. Ito, *Compendium of Methods for the Microbiological Examination of Foods*, 4th ed. American Public Health Association, 2001.

[3]   M. D. Zordan, M. M. G. Grafton, G. Acharya, L. M. Reece, C. L. Cooper, A. I. Aronson, K. Park, and J. F. Leary, "Detection of pathogenic E. coli O157:H7 by a hybrid microfluidic SPR and molecular imaging cytometry device.," *Cytom. A*, vol. 75, no. 2, pp. 155–162, Feb. 2009.

[4]   A. K. Deisingh and M. Thompson, "Detection of infectious and toxigenic bacteria.," *Analyst*, vol. 127, no. 5, pp. 567–581, May 2002.

[5]   B.-K. Hahm and A. K. Bhunia, "Effect of environmental stresses on antibody-based detection of Escherichia coli O157:H7, Salmonella enterica serotype Enteritidis and Listeria monocytogenes.," *J Appl Microbiol*, vol. 100, no. 5, pp. 1017–1027, May 2006.

[6]   V. M. Bohaychuk, G. E. Gensler, R. K. King, J. T. Wu, and L. M. McMullen, "Evaluation of detection methods for screening meat and poultry products for the presence of foodborne pathogens.," *J Food Prot*, vol. 68, no. 12, pp. 2637–2647, Dec. 2005.

[7]   B.-X. Hong, L.-F. Jiang, Y.-S. Hu, D.-Y. Fang, and H.-Y. Guo, "Application of oligonucleotide array technology for the rapid detection of pathogenic bacteria of foodborne infections.," *J Microbiol Methods*, vol. 58, no. 3, pp. 403–411, Sep. 2004.

[8]   J. P. Villagrasa, J. Colomer-Farrarons, and P. L. Miribel, "Bioelectronics for Amperometric Biosensors," 2013.

[9]   J. Punter-Villagrasa, J. Cid, J. Colomer-Farrarons, I. Rodríguez-Villarreal, and P. L. Miribel-Catala, "Toward an anemia early detection device based on 50-µL whole blood sample.," *IEEE Trans. Biomed. Eng.*, vol. 62, no. 2, pp. 708–16, Feb. 2015.

[10]   J. Punter-Villagrasa, B. del Moral-Zamora, J. Colomer-Farrarons, P. Miribel-Catala, I. Rodriguez-Villarreal, J. Cid, and B. Prieto-Simon, "Towards a portable point-of-use blood analysis with EIS technique device," in *2014 IEEE 11th International Multi-Conference on Systems, Signals & Devices (SSD14)*, 2014, pp. 1–6.

[11]   M. S. Cheng, J. S. Ho, S. H. Lau, V. T. K. Chow, and C.-S. Toh, "Impedimetric microbial sensor for real-time monitoring of phage infection of Escherichia coli.," *Biosens Bioelectron*, vol. 47, pp. 340–344, Sep. 2013.

[12]   L. Yang, "Electrical impedance spectroscopy for detection of bacterial cells in suspensions using interdigitated microelectrodes," *Talanta*, vol. 74, no. 5, pp. 1621–1629, 2008.

[13]   M. Varshney and Y. Li, "Interdigitated array microelectrodes based impedance biosensors for detection of bacterial cells.," *Biosens Bioelectron*, vol. 24, no. 10, pp. 2951–2960, Jun. 2009.

[14]   M. Li, S. Li, W. Cao, W. Li, W. Wen, and G. Alici, "Improved concentration and separation of particles in a 3D dielectrophoretic chip integrating focusing, aligning and trapping," *Microfluid. Nanofluidics*, vol. 14, no. 3–4, pp. 527–539, 2013.

[15]   S. G. Dastider, S. Barizuddin, Y. Wu, M. Dweik, and M. Almasri, "Impedance biosensor based on interdigitated electrode arrays for detection of low levels of E.coli O157:H7," *2013 IEEE 26th Int. Conf. Micro Electro Mech. Syst.*, pp. 955–958, Jan. 2013.

[16]   B. del Moral Zamora, "Towards Point-of-Use Dielectrophoretic Methods: A New Portable Multiphase Generator for Bacteria Concentration," *Micro Nanosyst.*, vol. 6, no. 2, Apr. 2014.

[17]   S. Park, Y. Zhang, T.-H. Wang, and S. Yang, "Continuous dielectrophoretic bacterial separation and concentration from physiological media of high conductivity.," *Lab Chip*, vol. 11, no. 17, pp. 2893–2900, Sep. 2011.

[18]   L. Rozitsky, A. Fine, D. Dado, S. Nussbaum-Ben-Shaul, S. Levenberg, and G. Yossifon, "Quantifying continuous-flow dielectrophoretic trapping of cells and micro-particles on micro-electrode array.," *Biomed. Microdevices*, vol. 15, no. 5, pp. 859–65, Oct. 2013.

CHAPTER 6. CONCLUDING REMARKS AND FUTURE PROSPECTS

Herein the objectives of the presented thesis are revised to retake and frame the different issues that have been solved and the achievements accomplished through the thesis. Additionally, some future directions are exposed which are related to this work.

We defined the following thesis objectives:

I)   To prove the feasibility of custom DEP generator for controlling bacteria and other bio-entities and to find the best electric field generating strategy to accomplish this.

II)   To look for the best microfluidic chip option for bacteria pre-concentration purposes on Bioanalytical applications.

III)   To develop and test the feasibility of custom bioimpedance devices to be integrated with point-of-use dielectrophoretic equipment.

IV)   To use the previous studies to design a complete electronic equipment, taking advantage of a combination of both techniques to have an autonomous system

V)   To demonstrate the proof of concept of the full device with the real case of *E. Coli* concentration and to integrate microfluidic protocols to solve specific issues resulting from the manipulation of real biological samples, and their associated bioactivity, such as the medium conductivity drift over time

Relative to I), in chapter 2 it was explored the dielectrophoresis (DEP) applications possibilities, by investigating the possible limits of the electronic device, in terms of sample conductivity and frequency. A microfluidic device was defined which was based on an interdigitated electrode, since in literature was reported to be effective for concentration purposes. The fabricated microfluidic device was prepared for E. coli concentration. The custom electronic device designed for this purpose, was able to generate sinusoidal signals so as to manipulate E. coli by means of DEP inside the microfluidic chip. The general features of the designed device were defined in Table 2.7. The device was tested by 5 different test variants, with the aim of validating the device and looking for the best option to concentrate bacteria. Playing with electric field gradient, combination signals were applied with the same equivalent applied signals inside the microfluidic chip. As a result, it was demonstrated that the electronic device was able to concentrate E. coli by using DEP. Moreover, it was detected

126

that the best combination of diphased signals for concentrating purposes was using counter-phased signals. Using this option, applying 10Vpp per channel, and with a flow rate of 5 µL/min a median 83% of concentration efficiency was obtained. The related publication [1] from this work is attached in Annex 1.

Afterwards, and relative to (II), a second study was performed little increasing the amplitude of the applied signals, to increase trapping effects, and varying the flow rate. This was described in chapter 3. Here was verified that the designed microfluidic chip was able to trap bacteria only in the electrode plane, reducing its features when flow rate was increased. This was also checked by COMSOL simulations. A second microfluidic device was then designed, with the aim of improving the obtained results from previous experiments. The device was based on insulator-DEP (iDEP). By means of dielectric pillars, we were able to increase considerably the trapping efficiency at higher flow rates. A maximum average increment of trapping efficiency of 12.6% was obtained for relative high flow rates (20 µL/min). But bacteria losses also were reduced at an average 44.2% for 5 µL/min, 10 µL/min and 20 µL/min. These results were published in the special issue of Electrophoresis [2] (Anex 2)

Later, it was addressed the possibilities of including an bioimpedance module to the general equipment, which fact was relative to objective (III). A first impedance device was defined, related in chapter 4, which was in a first step tested with a multi-sensor array with 4 untreated IS pins. The device was proven to be able to measure differences of bioimpedance of different pH and potassium solutions, using a 4-electrode measurement system. The system characteristics were represented in Table 4.1. Also, the device was used in a European project in collaboration with the Nanobioenginyering from IBEC. In here, the device was adapted to read signals from an array with potassium and pH sensors, as well as Bioimpedance at the given frequency. This device within this sensor, dedicated to measure ischemia inside the pork of a stomach, was verified

to be able to discriminate different tissues. The device features were defined in Table 4.2.

Finally, it was explored the use of impedance module with electrodes inside a microfluidic chip and its integration with the DEP module, which fact is relative to objective (IV). This was described in chapter 5. A new autonomous device based on the previous modules was designed, so as to facilitate the combination of both techniques in a single microfluidic chip. The electronic was adapted and embedded into a sBrio system from National Instruments system, which permits to automatize the application of the DEP, to concentrate bacteria, and control the impedance device to obtain a real-time measurement relative to the amount of bacteria inside the microfluidic chip. Concentration and real-time detection of the trapped bacteria inside the micro-fluidic chip was proven. Tests were done at relatively high flow rates, up to 10 μL/min. Additionally, the effects of bacteria media conductivity and its variability were studied and taken into account for the final protocol, which wasn't already taken into account in other publications, to the best of our knowledge. Then, bacteria concentration levels were detected at 1.7 kHz with an accuracy error of less than 2% and with a correlation of 0.988. Thus, a combination of both techniques is possible and useful to reduce long-term laboratory procedures. Also these results were published [3] and are enclosed in Anex 3.

Although the defined work objectives are already accomplished, some other works relative to this thesis were left out of the scope of this thesis that could be developed in a future. A device which integrated not only the electronics, but also all the microfluidic units would be a good option to explore in a while. Some viability studies were done before finishing this thesis. These included the integration of a dielectrophoretic generator and an IS measurement, controlled by a laptop, a microfluidic chip based on iDEP structures and an integrated electronically controlled pumping unit based on a piezoelectric system (Figure 6.1).
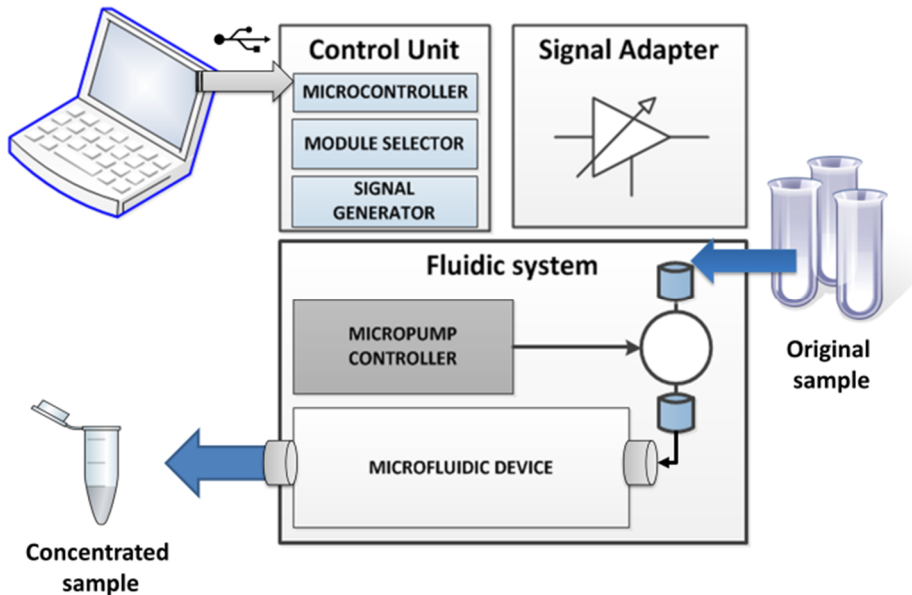
Figure 6.1. Overview of the proposed system

Thus the whole system would be completely autonomous, a clear Point-of-Care device, which will open new fields of applications, such as detection of pathogens or illnesses in non-developed countries. Moreover, DEP selectivity could be also exploitable to make a cell discriminator, not only able to separate, but also to measure the different collected cells.

References

[1] B. del Moral Zamora, "Towards Point-of-Use Dielectrophoretic Methods: A New Portable Multiphase Generator for Bacteria Concentration," *Micro Nanosyst.*, vol. 6, no. 2, Apr. 2014.

[2] B. del Moral Zamora, J. M. Álvarez Azpeitia, A. M. Oliva Brañas, J. Colomer-Farrarons, M. Castellarnau, P. L. Miribel-Català, A. Homs-Corbera, A. Juárez, and J. Samitier, "Dielectrophoretic concentrator enhancement based on dielectric poles for continuously flowing samples.," *Electrophoresis*, vol. 36, no. 13, pp. 1405–13, Jul. 2015.

[3]   B. del Moral-Zamora, J. Punter-Villagrassa, A. M. Oliva-Brañas, J. M. Álvarez-Azpeitia, J. Colomer-Farrarons, J. Samitier, A. Homs-Corbera, and P. L. Miribel-Català, "Combined dielectrophoretic and impedance system for on-chip controlled bacteria concentration: Application to *Escherichia coli*," *Electrophoresis*, vol. 36, no. 9–10, pp. 1130–1141, 2015.

Authors (signature): Punter-Villagrasa, J.;del Moral-Zamora, B.; Colomer-Farrarons, J.; Miribel-Català, P.; Cid.J.; Rodríguez-Villareal, I.; Prieto-Simón, B.

Title: Towards a portable point-of-use blood analysis with EIS technique device.

Book: Proc. Multi-Conference on Systems, Signals & Devices (SSD), 2014 11th International

Publisher: IEEE

Number or authors: 7

Volume: --- **Number:** --- **Pages, Initial:** 1 **final:** 6 **Year:** 2014 **Place of publication:** Barcelona (SPAIN) **ISBN:** 978-1-4799-3865-0 **Legal Deposit:** ---

Key: Paper **Publication code:** 289711 **Order:** 004

Authors (signature): Punter-Villagrasa, J. ; del Moral-Zamora, B. ; Colomer-Farrarons, J. ; Miribel-Catala, P. ; Cid, J. ; Rodriguez-Villarreal, I. ; Prieto-Simon, B.

Title: A portable point-of-use EIS device for in-vivo biomedical applications.

Book: Design of Circuits and Integrated Circuits (DCIS), 2014 Conference on

Publisher: IEEE

Number or authors: 7

Volume: --- **Number:** --- **Pages, Initial:** 1 **final:** 6 **Year:** 2014 **Place of publication:** Madrid (SPAIN) **ISBN:** --- **Legal Deposit:** ---

Key: Paper **Publication code:** 289712 **Order:** 005

Authors (signature): del Moral-Zamora, B.; Punter-Villagrassa, J.; Oliva-Brañas, A.M.; Álvarez-Azpeitia, J.M.; Colomer-Farrarons, J.; Samitier, J.; Homs-Corbera, A.; Miribel-Català, P.Ll.

Title: Combined dielectrophoretic and impedance system for on-chip controlled bacteria concentration: Application to Escherichia coli

Book: ELECTROPHORESIS. Special Issue: Focus on the London Dielectrophoresis 2014 Meeting

Publisher: Wiley-VCH Verlag GmbH & Co. KGaA

Number or authors: 8

Volume: 36 **Number:** 9-10 **Pages, Initial:** 1130 **final:** 1141 **Year:** 2015 **Place of publication:** Weinheim (GERMANY) **ISBN:** --- **Legal Deposit:** ---

Key: Paper **Publication code:** 293279 **Order:** 007

Authors (signature): del Moral, B.; Álvarez-Azpeitia, J.M.; Oliva, A.M.; Colomer-Farrarons, J.; Castellarnau, M.; Miribel-Català, P.Ll.; Homs-Corbera, A.; Juárez, A.; Samitier, J.

Title: Dielectrophoretic concentrator enhancement based on dielectric poles for continuously flowing samples

Book: Special Issue: Dielectrophoresis 2015

Publisher: Wiley-VCH Verlag GmbH & Co. KGaA

Number or authors: 9

Volume: 36 **Number:** 13 **Pages, Initial:** 1405 **final:** 1413 **Year:** 2015 **Place of publication:** Weinheim (GERMANY) **ISBN:** --- **Legal Deposit:** ---

Key: Paper **Publication code:** 293280 **Order:** 008

Authors (signature): del Moral, B; Alvarez-Azpeitia, J.M.; Colomer-Farrarons, J.; Miribel-Catala, P.Ll.; Homs-Corbera, A.; Juarez, A.; Samitier, J.

Title: Towards Point-of-Use Dielectrophoretic Methods: A New Portable Multiphase Generator for Bacteria Concentration
Book: Micro and Nanosystems
Publisher: Bentham Science Publishers Ltd.
Number or authors: 7
Volume: 6(2) **Number:** --- **Pages, Initial:** 71 **final:** 78 **Year:** 2014 **Place of publication:** Sharjah (UNITED ARAB EMIRATES) **ISBN:** --- **Legal Deposit:** ---
Key: Paper **Publication code:** 293289 **Order:** 009

CONTRIBUTIONS TO CONGRESSES

Authors: Colomer-Fararrons, J.; Punter, J.; del Moral, B.; Miribel-Català, P.; Samitier, J.
Title: Bioelectronics: Discrete to full custom ASIC solutions for biomedical applications
Type of participation: Poster
Conference: 3rd IBEC Symposium on Bioengineering and Nanomedicine
Publication:
Number or authors: 5
Location: Barcelona (SPAIN) **Year:** 2010
Code: 306761 **Order:** 001

Authors: del Moral Zamora, B.; Colomer Farrarons, J.; Mir Llorente, M.; Homs Corbera, A.; Miribel Català, P.; Samitier Martí, J.
Title: Combined Impedance and Dielectrophoresis portable device for point-of-care analysis.
Type of participation: Presentation of communication
Conference: SPIE Microtechnologies. Conference 8068A Bioelectronics, Biomedical, and Bio-inspired
Publication: 8068A-31
Number or authors: 6
Location: Prague (CZECH REPUBLIC) **Year:** 2011
Code: 310755 **Order:** 002

Authors: del Moral Zamora, B.; Colomer Farrarons,J.; Alvarez Azpeitia, J.M.; Mir Llorente, M.; Homs Corbera, A.; Miribel Català, P.; Samitier Martí, J.
Title: Combined impedance and dielectrophoresis portable device for Point-of-Care analysis.
Type of participation: Poster
Conference: 4th IBEC Symposium. Bioengineering & Nanomedicine. 18 October 2011
Publication:
Number or authors: 7
Location: Barcelona (SPAIN) **Year:** 2011
Code: 331360 **Order:** 003

Authors: del Moral Zamora, B.; Álvarez Azpeitia, J.M.; Colomer Farrarons, J.; Miribel Català, P.L.; Homs Corbera, A.; Samitier Martí, J.
Title: Instrumentación portátil de bajo coste para Concentradores Dielectroforéticos de Escherichia Coli
Type of participation: Presentation of communication

Conference: XXX Congreso Anual de la Sociedad Española de Ingeniería Biomédica-CASEIB 2012

Publication: Instrumentación portátil de bajo coste para Concentradores Dielectroforéticos de Escherichia Coli

Number or authors: 6

Location: San Sebastián - Donostia (SPAIN) **Year:** 2012

Code: 348604   **Order:** 004

Authors: del Moral Zamora, B.; Álvarez Azpeitia, J.M.; Colomer-Farrarons, J.; Miribel-Català,P.Ll; Homs-Corbera,A.; Juárez, A.; Samitier, J.

Title: Towards Point-of-Use Dielectrophoretic Methods: A New Portable Multiphase Generator for Bacteria Concentration

Type of participation: Presentation of communication

Conference: XIII Mediterranean Conference on Medical and Biological Engineering and Computing 2013 (MEDICON 2013)

Publication:

Number or authors: 6

Location: Sevilla (SPAIN) **Year:** 2013

Code: 363036   **Order:** 005

RESUMEN EN CASTELLANO

El objetivo de esta tesis es el diseño de una instrumentación capaz de manipular y caracterizar células, a fin de realizar análisis más exhaustivos de elementos biológicos y acelerar procesos de detección de patógenos para aplicaciones de diagnóstico o de control de calidad de alimentos. El dispositivo se centra en dos tipos de técnicas eléctricas para la manipulación y detección de células: La dielectroforesis (DEP) y la medición de la bioimpedancia.

La DEP permite manipular material biológico por medio de campos eléctricos, aprovechando las propiedades eléctricas de la célula y el medio en que se encuentra. La manipulación es por tanto ajustable, mediante el control de estas propiedades, así como a través de la geometría de los electrodos usados, la frecuencia y el módulo de la tensión aplicada. Por otro lado, la bioimpedancia permite caracterizar material biológico mediante su comportamiento eléctrico en frecuencia. La medida se realiza a través de la aplicación de una corriente alterna controlada y la monitorización del efecto sobre el tejido mediante potencial eléctrico. Los dispositivos de bioimpedancia son fácilmente integrables con técnicas dielectroforéticas de manipulación, fusionando manipulación con detección.

En esta tesis, la combinación de estas técnicas permite la concentración de pequeños patógenos en grandes volúmenes de muestras y su posterior detección. Para ello, se crean diversos módulos de instrumentación electrónica. Algunos, están dedicados a generar señales alternas desfasadas a frecuencias óptimas para la manipulación de patógenos (módulo DEP). Otros, combinan módulos de generación, lectura y tratamiento digital, para la monitorización del comportamiento eléctrico de células (bioimpedancia). Los módulos diseñados son validados en un entorno real controlado para concentrar y detectar la bacteria *Escherichia Coli* en grandes volúmenes de agua. Como resultado, se obtiene una electrónica modular válida, autónoma, portátil y de bajo coste, capaz de disminuir tiempos de preparación y detección de muestras en laboratorio.

Para el correcto desarrollo del proyecto se definen una serie de objetivos que a su vez definen las diferentes etapas de éste y que devienen en los diferentes capítulos de esta memoria de tesis doctoral.

Se definen los siguientes objetivos:

a) Demostrar la viabilidad de un generador modular DEP para el control general de células, y en particular de bacterias. Investigar cuáles son las condiciones más óptimas para la manipulación, incluyendo no sólo a nivel de conductividad de medios y protocolo de experimentación, sino también a nivel de señal aplicada.

b) Encontrar la mejor opción, a nivel de chip microfluídico, para la preconcentración de bacterias en aplicaciones bioanalíticas. Detectar límites de tasa de flujo para mejorar los tiempos de preconcentrado en laboratorio.

c) Verificar la viabilidad del uso de un sistema adaptado para la medición por bioimpedancia por sistema de 4 electrodos tanto para medios fluidos, como tejidos.

d) Integrar en un mismo equipo los módulos anteriores para un fin común: diseñar un equipo completo, capaz de beneficiarse de la combinación de ambas técnicas para tener un sistema autónomo que permita manipular y medir células en entornos Lab-on-a-chip. Posteriormente demostrar la capacidad del dispositivo mediante prueba de concepto para el caso real de la concentración de *E. coli*.

En relación al punto a): Se exploraron las posibilidades de la dielectroforesis (DEP) y sus aplicaciones. Con el objetivo de manipular patógenos por medio de DEP, se realizaron diversos análisis a fin de obtener los posibles límites del dispositivo electrónico a diseñar, en términos de conductividad de la muestra y de características de la señal aplicada, tanto a nivel de potencia como frecuencia. Los primeros estudios, consideraron diferentes conductividades de muestra y rangos de

frecuencia, a fin de estimar la corriente necesaria a generar por el dispositivo.

Posteriormente, basándose en la literatura científica, se realizó un estudio de rangos de frecuencia empleados para la manipulación de la bacteria *E. coli*. Además, a fin de añadir más versatilidad al sistema al sistema de manipulación por DEP, se propuso generar señales en cuadratura para generar distintos gradientes de campo eléctrico. Además, esto proporcionaría capacidades de manipulación superiores en caso de utilizar otras células en el futuro y ampliaría el ámbito de aplicación del dispositivo.

Finalmente, se concibió un dispositivo electrónico, basado en un amplificador clase E modificado, con las características que se muestran a continuación:

Tabla 1. Principales características del dispositivo DEP

Tensión alimentación (V)	$10V_{DC}$
Carga mínima permitida	> 1 kΩ
Fases disponibles	4 (0º,90º,180º,270º)
Cantidad máxima permitida de electrodos por canal (Considerando una conductividad de 1,66S/m)	25 electrodos
Frecuencia de trabajo	1MHz
Rango de tensión disponible en la salida (Vpico)	1V- (V_{DC}-0.5) V
Corriente máxima disponible	1A

Para testear el prototipo electrónico, se diseñó un chip microfluídico, compuesto por un electrodo de oro interdigitado y una única cámara de PDMS. Se verificó el funcionamiento del dispositivo microfluidico, junto con el equipo electrónico, aplicándolos para un caso de concentración de *E. coli* a una tasa de flujo continúa. Como resultado, el dispositivo fue capaz de generar señales sinusoidales lo suficientemente estables para manipular *E. coli* por medio de DEP en el interior del chip microfluídico. Además, se verificó cual era la opción más óptima para concentrar bacterias por medio

de 5 casos de test (tabla 1) que obtenían la misma señal efectiva inyectada por medio de la aplicación de distintos gradientes de campo eléctrico.

Tabla 2. Casos experimentales propuestos

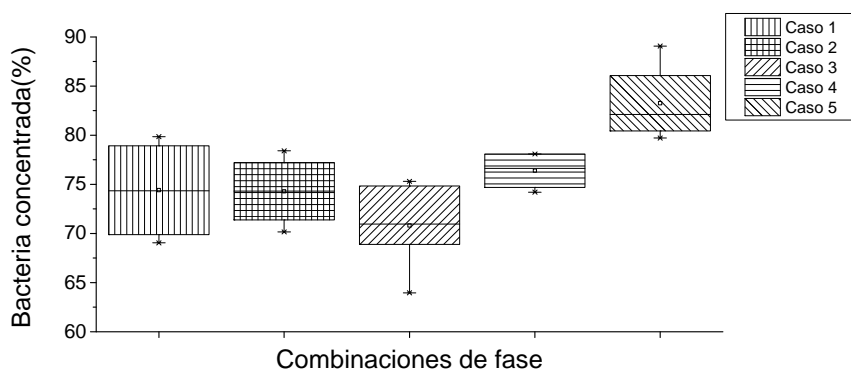| Casos experimentales	Señales aplicadas	Potencial resultante V_{RMS}	Voltaje aplicado $V_{pp} = 2V_m$
Caso 1- Una sola fase **(reference)**	E1: $\varphi_1 = 0^o$ E 2: GND	$V_m/\sqrt{2}$	10Vpp
Caso 2 90ºdesfase	E1: $\varphi_1 = 0^o$ E2: $\varphi_2 = 90$	V_m	7Vpp
Caso 3 270ºdesfase	E1: $\varphi_1 = 0^o$ E2: $\varphi_4 = 270^o$	V_m	7Vpp
Caso 4 180ºdesfase	E1: $\varphi_1 = 0^o$ E2: $\varphi_3 = 180^o$	$\sqrt{2}V_m$	5Vpp
Caso 5 180ºdesfase	E1: $\varphi_1 = 0^o$ E2: $\varphi_3 = 180^o$	$\sqrt{2}V_m$	10Vpp

Figura 1. Resultados experimentales en porcentaje de concentración de bacterias.

Del análisis de los resultados, se detectó que la mejor combinación para fines de concentración era el uso de señales en contra-fase. En este caso, aplicando 10Vpp por canal, y con una velocidad de flujo de 5 µl / min se

obtuvo una mediana del 83% de la eficiencia de concentración (Figura 1, caso 5).

Respecto a b): En los estudios de microbiología clásica a menudo resulta un reto purificar o pre-concentrar muestras como previo paso a procedimientos analíticos tales como disrupción celular o reacción en cadena de la polimerasa (PCR). Estos métodos no siempre se pueden llevar a cabo; especialmente si la muestra es escasa y los métodos clásicos no son lo suficientemente selectivos. Además, la mayoría de ellos requieren procedimientos de larga duración en el tiempo. Consecuentemente, en este punto centramos nuestra atención en demostrar la aplicabilidad de nuestro sistema al campo de la pre-concentración de muestras y en obtener los mejores resultados. Para ello, se realizó un estudio a fin de encontrar la mejor opción para aumentar los porcentajes de captura y mejorar las tasas de flujo aplicadas, por medio del análisis del chip microfluídico.

Habitualmente, para estos fines se utilizan dispositivos con un gran número de electrodos metálicos interdigitados colocados en un canal microfluídico; como el chip que usamos previamente para validar el dispositivo electrónico. Sin embargo, intuíamos que estos dispositivos sólo generaban DEP en el plano del electrodo, limitando sus capacidades. Por ello, se realizó un estudio a fin de verificar esta hipótesis. Para ello, se realizaron diversos experimentos de concentración de *E. coli* para distintas tasas de flujo. Los resultados obtenidos, verificaron que el hasta este punto actual dispositivo microfluídico, tenía un efecto de atrapamiento en 2D, capturando únicamente en el plano del electrodo y mermando su eficiencia a tasas de flujo elevadas.

Para solucionar este problema, se investigó en el uso de la incorporación de estructuras dieléctricas en el canal microfluídico (tecnología llamada iDEP). Estas estructuras son capaces de modificar el campo eléctrico aplicado, a fin de aumentar las áreas de captura eficaces. Se escogió por tanto incorporar pilares de PDMS al chip microfluídico, debido al bajo coste de la tecnología y sus rápidos métodos de fabricación. Posteriormente, se

realizaron nuevos experimentos a diferentes tasas de flujo, a fin de verificar el efecto de la inclusión de los pilares.

Los resultados del proceso experimental demostraron que este nuevo dispositivo era capaz de aumentar considerablemente la eficiencia de atrapamiento sin sacrificar la tasa de flujo aplicada. Un incremento promedio máximo de eficiencia de captura de 12,6% se obtuvo para caudales relativamente altos (20 µL/min). Además, la pérdida de bacterias se redujo en un promedio de 44,2% para 5 µL/min, 10 µL/min y 20 µL/min. La comparativa de resultados de los dispositivos microfluídicos analizados se muestra en la Figura 2.
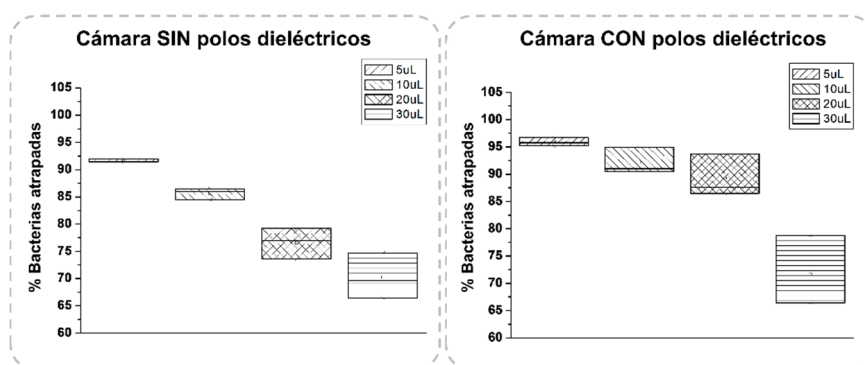

Figura 2. Comparativa de resultados para el dispositivo con cámara regular y el dispositivo con la inclusión de los polos dieléctricos.

Para comprobar visualmente el efecto de atrapamiento en 3D, se realizó un experimento adicional con fluorescencia, tanto en el dispositivo con cámara simple, cómo en la cámara con polos PDMS. En dicho experimento se pudo corroborar visualmente que la cámara sin pilares tenía limitada su capacidad de atrapamiento al plano del electrodo. No obstante en la cámara de pilares se corroboró un efecto de atrapamiento 3D, elevando por tanto el área efectiva de concentración de bacterias (Figura 3).
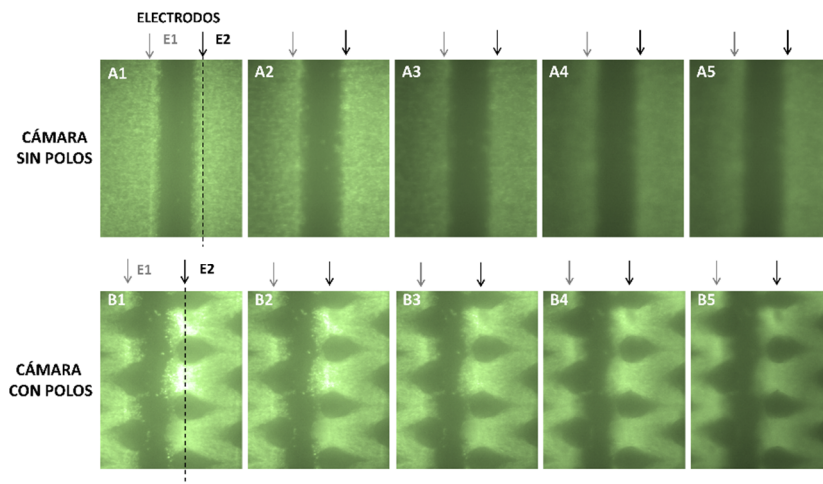
140

Figura 3. Experimento fluorescencia. Cada casilla representa un plano distinto en altura de la cámara del chip microfluídico. A1,B1 son planos más próximos a la parte superior de la cámara y A5,B5 son planos más próximos al electrodo. Las áreas brillantes indican que hay presencia de bacterias en dicho plano.

Finalmente, se realizó un tercer experimento a fin de concluir que el dispositivo con polos de PDMS es adecuado para ser utilizado como pre-concentrador de bacterias. Cuando las tasas de flujo son muy reducidas, las bacterias son irradiadas con un alto campo eléctrico por un largo periodo de tiempo. Por ello, se realizó un análisis proteómico a fin de verificar la viabilidad de la muestra. Los resultados verificaron que la expresión proteómica de las bacterias no se vio alterada por la larga exposición al campo eléctrico. Consecuentemente, las bacterias irradiadas eran válidas para posteriores análisis.

Respecto a c): En este punto se propuso mejorar el equipo de manipulación DEP mediante la inclusión de un módulo de detección de nivel de bacterias por bioimpedancia. En consecuencia, un nuevo módulo electrónico fue desarrollado.

En su etapa inicial, este módulo se definió para medir la bioimpedancia de

células, soluciones y tejidos en general. El módulo permitía realizar un barrido en frecuencia, con el fin de caracterizar el material biológico por medio de la bioimpedancia. Para la medida de bioimpedancia se decidió utilizar el método de 4 electrodos; cuya principal ventaja es la cancelación de la impedancia de los electrodos. Posteriormente se consideró la posibilidad de integrar el módulo de bioimpedancia con el equipo DEP.

El dispositivo electrónico diseñado estaba compuestos de dos módulos: Un módulo de inyección basado en una fuente de corriente Howland y un módulo de lectura basado en un amplificador de instrumentación. Las características del dispositivo se muestran en la siguiente tabla.

Tabla 3. Principales características del módulo de medición de bioimpedancias.

Tensión de alimentación	± 15 Vdc and +5V
Tensión minima de entarda	60mVpp
Tensión máxima de salida	8 Vpp
Rango de trabajo en frecuencia	68kHz-75kHz
Carga máxima permitida	2.5kΩ
Carga minima permitida	1Ω
Máxima capacidad de corriente en la salida	3,56mAp-p

Este primer dispositivo se testeó en una primera aproximación con diferentes soluciones y una matriz con sensores de pH, potasio y bioimpedancia, proporcionado por el equipo de Nanobioingenieria del IBEC. Primero, se realizó una medida del electrodo de referencia del sensor personalizado frente a un electrodo comercial, para observar si existían derivas en dicho electrodo que afectaran a la medida final. Los resultados demostraron la estabilidad de la referencia del sensor, cuya deriva era de +/- 0,001V.

Posteriormente, se probaron los sensores en diversas soluciones a distintos niveles de pH (desde 1.1 a 2.5pH) y potasio desde (10^{-1} M a 10^{-5}

M). El dispositivo fue capaz de medir las diferencias de bioimpedancia de las diferentes soluciones.

Finalmente, se utilizó el dispositivo en un proyecto europeo en colaboración con el equipo de Nanobioingeniería del IBEC. Para este caso, el dispositivo fue adaptado para leer las señales la matriz y sus sensores de pH y de potasio, así como impedancia. La matriz de sensores, junto con el dispositivo, se utilizó para medir la isquemia dentro del estómago de un cerdo. Por ello, se verificó la capacidad del sensor y el equipo para discriminar diferentes tipos de tejidos. Para ello, se realizó un último experimento con diferentes tejidos de cerdo inmersos en una solución de pH 1.9, equivalente a pH del estómago del cerdo, tratando de emular las condiciones del experimento in-vivo.

En la figura 3 se pueden observar los resultado del experimentos, donde tejidos magros y adiposos de cerdo son diferenciados por medio de este sistema. Además, los tejidos ayudaron a la adhesión de la membrana, ayudando a la estabilidad de la medida.
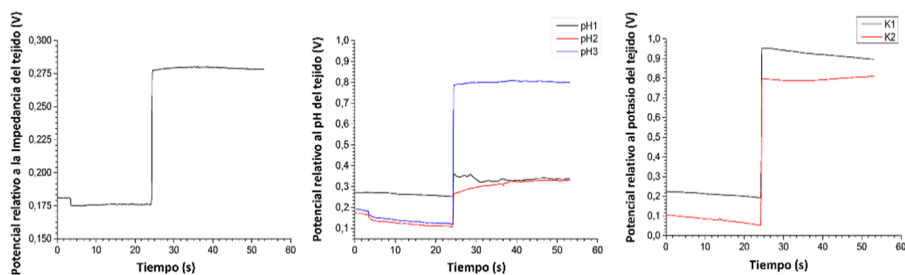

Figura 4. Diferencia entre tejido magro y adiposo de cerdo para los distintos sensores.

Respecto al punto d): En las etapas previas se crearon los distintos módulos que constituyen la base del sistema propuesto como objetivo final de la tesis. En esta etapa final se analizó la posibilidad de integrar el módulo bioimpedancia con el de generación DEP y su uso para entornos Lab-on-a-chip, y así mejorar los métodos de detección actuales por medio de la

combinación de la microfluídica, la bioimpedancia y la electrocinética. Con ello, se pretende reducir los procedimientos en los laboratorios. Los protocolos de detección de bacterias son caros a nivel de equipamiento y tiempo, ya que requieren de diversos dispositivos y de varios días para la obtención de resultados.

Para ello se adaptaron por completo los módulos diseñados, a fin de obtener un sistema de concentración de bacterias por medio de DEP, a tasas de flujo relativamente altas, que monitorice en tiempo real la evolución de la concentración por medio de la bioimpedancia. Además, para el diseño de la nueva electrónica autónoma, se tuvo en cuenta que ambos sistemas debían de combinarse en un mismo dispositivo microfluídico.

La electrónica fue embebida en un sistema sbRIO (propiedad de National Instruments), que permitía automatizar la aplicación de la DEP, para concentrar las bacterias y controlar la medición en tiempo real de la relación de la impedancia con la cantidad de bacterias concentradas. Se diseñó además, un nuevo dispositivo microfluídico, para facilitar la combinación de ambos sistemas en el mismo chip.
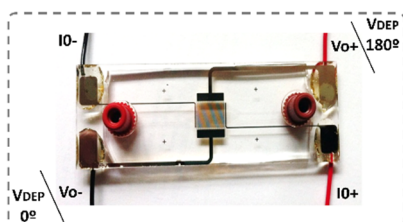

Figura 5. Dispositivo microfluidico diseñado para la combinación de la DEP y la bioimpedancia.

Posteriormente se verificó la viabilidad del sistema y su capacidad de concentrar y detectar en tiempo real las bacterias atrapadas en el interior del chip microfluídico.

144

Las pruebas se realizaron a tasas de flujo de hasta 10 µL/ min. Además, para la medición se tuvieron en cuenta los efectos de la variación de la conductividad del medio, problemática que no es habitualmente reportada en los estudios de impedancia sobre bacterias. Dicha variación, causada por la evolución temporal de la muestra de bacterias, torna el medio más conductivo, enmascarando la medida de impedancia. Por ello, se definió un protocolo de medida que asegurara una conductividad del medio estable durante la medición de la impedancia.

En una primera fase experimental, se realizó una espectroscopia de impedancias (IS) para detectar la frecuencia óptima para la detección de *E. coli* Los resultados de la IS mostraron mayor capacidad de discriminación de niveles de bacteria a 1,7 kHz. Posteriormente, se ejecutó un segundo experimento de concentración, evaluando la impedancia en tiempo real. Los resultados mostraron un error de precisión de menos de 2%, con una correlación de 0,988. Consecuentemente, la combinación de ambas técnicas es posible y útil para reducir largos procedimientos de pre-concentración y detección en laboratorios.
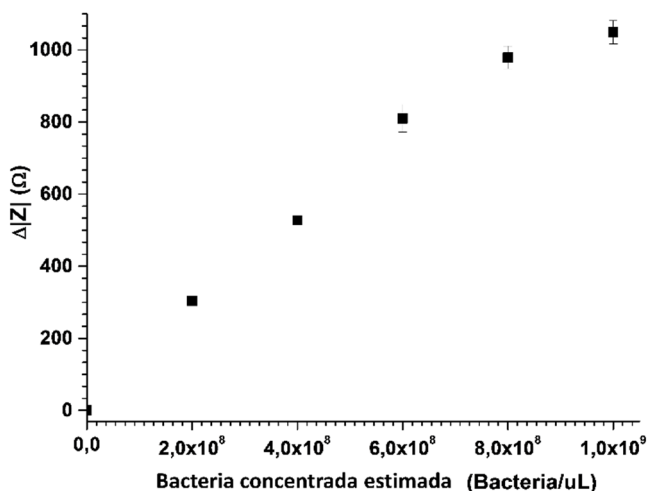

Figura 6. Estimación de la bacteria concentrada dentro del chip microfluídico, de acuerdo con los resultados de impedancia obtenidos.

Como conclusión, se ha realizado dispositivo final que consigue integrar la técnica DEP y la medida de bioimpedancia en un único dispositivo electrónico autónomo capaz de concentrar *E. coli* y medir la evolución del volumen de bacteria dentro del chip, en tiempo real.

Este estudio abre nuevas vías de investigación, como el desarrollo de nuevas electrónicas con microfluídica integrada para aumentar la portabilidad del dispositivo y así favorecer su uso en entornos *point-of-care* o en países en vías de desarrollo. O bien, para aprovechar la capacidad de selectividad de la DEP para realizar un discriminador de células, no sólo capaz de separar, sino también de medir las diferentes células recogidas.